A STRUCTURE/FUNCTION INVESTIGATION INTO BABOON CYTOCHROME P450 SIDE-CHAIN CLEAVAGE (CYP11A1)

Karl-Heinz Storbeck

Thesis

Presented for the

Degree Magister Scientiae

(Biochemistry)

in the

Faculty of Science

at the

University of Stellenbosch

Promoter: Dr AC Swart

Co-promoter: Prof P Swart

Department of Biochemistry, University of Stellenbosch

December 2005

Declaration:

I, the undersigned, hereby declare that the work contained in this thesis is my own original work and that I have not previously in its entirety or in part submitted it at any university for a degree.

Signature: .....….....

Date: .....

SUMMARY

This study describes:

1. The cloning of baboon cytochrome P450 side-chain cleavage (CYP11A1) cDNA by in vitro site-directed mutagenesis.
2. The identification and sequencing of three baboon CYP11A1 mutants: CYP11A1a, CYP11A1b and CYP11A1c.
3. The expression and characterisation of baboon and human CYP11A1 cDNA, CYP11A1a, CYP11A1b and CYP11A1c in nonsteroidogenic COS-1 cells. The K_m and V-values for the metabolism of 25-hydroxycholesterol were determined.
4. The construction of the first homology model of CYP11A1, using both mammalian (CYP2C5) and bacterial (CYP102) cytochromes P450 crystal structures as templates.
5. A structure/function study into the role of the amino acid residues Ile98, Lys103 and Thr291 in substrate binding and enzymatic activity.
6. The proposal of a topological model of the CYP11A1 active pocket as determined by substrate docking studies.

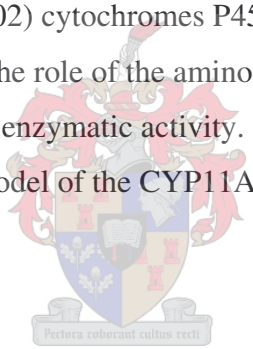

OPSOMMING

Hierdie studie beskryf:

1. Die kloneering van bobejaan sitokroom P450scc (CYP11A1) deur *in vitro* setel-gerigte mutagense.
2. Die identifisering en nukleotiedvolgordebepaling van drie CYP11A1 mutante: CYP11A1a, CYP11A1b and CYP11A1c.
3. Die *in vivo* ekspressie van bobejaan en mens CYP11A1 cDNA, en die CYP11A1a, CYP11A1b en CYP11A1c mutante. Die K_m en *V*-waardes vir 25-hydroxycholesterol is vervolgens bepaal.
4. Die konstruksie van die eerste homologie modelstruktuur van CYP11A1 gebaseer op die templaatstrukture van beide gekristaliseerde CYP101, ‘n bakteriële sitokroom P450, en CYP2C5, ‘n soorgduur sitokroom P450.
5. Die studie van die rol van aminosuurresidue, Ile98, Lys103 en Thr291 in die struktuur en funksie van CYP11A1 teen opsigte van substraat binding en ensiematiese aktiwiteit.
6. Die voorstelling van ‘n topologiese modelstruktuur van die aktiewe setel van CYP11A1 soos bepaal deur die substraatankering in die drie-dimensionelebindingsetel.

Dedicated to Patricia, whom I love with all my heart

ACKNOWLEDGEMENTS

I hereby wish to express my sincerest gratitude to the following persons and institutions:

Dr AC Swart, my promoter, for her excellent guidance, support and encouragement throughout this project, and for help with the preparation of this thesis.

Prof Swart, my co-promoter, for his enthusiastic leadership and for help with the preparation of this thesis.

Sandra Graham for sharing her modelling expertise with us.

Ralie Louw, **Natasja Brown** and **Norbert Kolar** for their technical assistance.

David Richfield for his technical assistance and for proof reading this manuscript.

The **NRF**, **University of Stellenbosch** and the **Wilhelm Frank Bursary Fund** for financial support.

All persons at the Department of Biochemistry who made my work there enjoyable.

Grant, **Des** and **Ilse** for their friendship and for making time spent in the lab enjoyable.

Mike and **Zita Berry** for their support and for making their home available to me.

My Dad, **Wolfgang**, for making Stellenbosch possible.

My Mom, **Sue**, for her love, support and encouragement.

Patricia for always supporting me and loving me just the way I am.

To the Creator of all things, the more I study the more I realise how amazing You are.

TABLE OF CONTENTS

ABBREVIATIONS

3βHSD	3β-hydroxysteroid dehydrogenase
ACAT1	acyl-CoA:cholesterol acyltransferase 1
ACE	angiotensin converting enzyme
ACTH	adrenocorticotrophic hormone
Adx	adrenodoxin
AdxR	adrenodoxin reductase
Apo	apolipoprotein
AR	androgen receptor
CAH	congenital adrenal hyperplasia
CBG	corticosteroid binding globulin
CE	cholesterol ester
CGRP	calcitonin gene-related peptide
CRH	corticotropin releasing hormone
CYP	cytochrome P450
CYP11A1	cytochrome P450 side-chain cleavage
CYP11B1	cytochrome P450 11β-hydroxylase
CYP11B2	cytochrome P450 aldosterone synthase
CYP17	cytochrome P450 17α-hydroxylase/17,20 lyase
CYP21B	cytochrome P450 21-hydroxylase
CYP101	cytochrome P450cam
CYP102	cytochrome P450BMP, the heme domain of the fusion protein BM-3
CYP107A1	cytochrome P450eryF
CYP108	cytochrome P450terp
DBD	DNA binding domain
DHEA	dehydroepiandrostenedione
DHEAS	DHEA-sulphate
ENaC	epithelial sodium channels
ER	estrogen receptor
FAD	flavinadenine dinucleotide
FMN	flavinmononucleotide
FSH	follicle stimulating hormone
GH	growth hormone
GHRH	growth hormone releasing hormone
GIH	growth hormone-inhibiting hormone
GR	glucocorticoid receptor
GRE	glucocorticoid-response element
GnRH	gonadotropin releasing hormone
HDL	high density lipoprotein
HPA-axis	hypothalamic-pituitary-adrenal axis
HSD	hydroxysteroid dehydrogenase
HSL	hormone sensitive lipase
LBD	ligand binding domain
LDL	low density lipoprotein
LH	luteinizing hormone

k_{cat}	catalytic rate constant
K_m	Michaelis constant
MR	mineralocorticoid receptor
NHR	nuclear hormone receptor
NPY	neuropeptides P
p37	37-kDa StAR
p30	30-kDa StAR
pp30	phosphorylated p30
pp37	phosphorylated p37
PAP	PBR-associated protein
PBR	peripheral benzodiazepine receptor
PDB	Protein Data Bank
PIH	prolactin-inhibiting hormone
PKA	cAMP-dependent protein kinase
POMC	pro-opiomelanocortin
RE	response element
RH	nonactivated substrates
RMSD	root mean square deviation
ROMK	inwardly rectifying potassium channel sodium channel (ROMK)
SF1	steroidogenic factor 1
SR-BI receptor	scavenger receptor class B type I receptor
SRS	substrate recognition site
SS	somatostatin
StAR	Steroid Acute Regulatory Protein
TRH	thyrotropin releasing hormone
TSH	thyrotrophin
U-CRE	upstream cAMP-response element
VIP	vasoactive intestinal peptide

CHAPTER 1
INTRODUCTION

Steroid hormones are essential for the maintenance of homeostasis in mammals. The adrenal gland secretes three types of steroid hormones, the mineralocorticoids, glucocorticoids and adrenal androgens. These hormones are responsible for the regulation of electrolyte concentration in the extracellular fluid; the regulation of carbohydrate, lipid and protein metabolism; and sexual development and reproduction, respectively [1]. All steroid hormones are derived from cholesterol and contain the basic parent cyclopentanoperhydrophenanthrene ring structure, which is modified by an array of enzymes, resulting in the unique bio-reactivity of each hormone [2]. In the adrenal gland, the biosynthesis of the steroid hormones from cholesterol involves two distinct groups of enzymes: the cytochromes P450 and the hydroxysteroid dehydrogenases [3]. Defects in enzymes catalysing the steroid producing reactions can result in well-documented clinical conditions such as congenital adrenal hyperplasia (CAH), Cushing's syndrome and adrenogenital syndrome. Conversely, the hypersecretory effects of adrenal steroids are exploited in the treatment of a number of disorders, including adrenal adenomas, allergy, arthritis and graft rejection [1].

This thesis aims to further our understanding of cytochrome P450 side-chain cleavage (CYP11A1), the first enzyme in the steroidogenic pathway, by structure/function analysis. As the catalytic cycle of the cytochromes P450 has not yet been fully elucidated, structure/function analysis serves as an important means of investigating the catalytic activity of these unique enzymes. This was accomplished by coupling kinetic studies and site directed mutagenesis to structural determinations. Although CYP11A1, like all other mammalian cytochromes P450, is a hydrophobic membrane bound protein not amenable to standard crystallisation techniques its three-dimensional structure can be predicted by homology modelling as was done in this study.

CYP11A1 is located in the inner mitochondrial membrane and catalyses the conversion of cholesterol to pregnenolone in three consecutive steps: a 20-hydroxylation, 22-hydroxylation and the cleavage of the C_{20}-C_{22} bond [4,5]. The electrons required for this reaction are provided by NADPH via a mitochondrial electron transfer system. As pregnenolone is the precursor to all steroid hormones, the regulation of CYP11A1 is essential in regulating adrenal steroidogenic output.

Chapter 2 presents an overview of the anatomy of the adrenal gland with reference to the morphological zonation in terms of the physiological importance of the mineralocorticoids, glucocorticoids and adrenal androgens and the expression of the relevant steroidogenic enzymes. The catalytic properties and mechanism of action of the enzymes catalysing the biosynthesis of these hormones, the cytochromes P450 and hydroxysteroid dehydrogenase enzymes are discussed. The complex regulation of adrenal steroidogenesis is addressed, highlighting the importance of the availability of cholesterol, the hypothalamic-pituitary-adrenal axis (HPA-axis) and the intra-adrenal regulatory mechanisms.

In chapter 3, the physiological importance and expression of CYP11A1 is addressed. The acute and chronic regulation of CYP11A1 is discussed in terms of the role played by the Steroid Acute Regulatory Protein (StAR) in governing the supply of the cholesterol substrate to the inner mitochondrial membrane and the transcriptional factors which come into play during CYP11A1 expression, respectively. The catalytic properties of the enzyme are presented in terms of reaction mechanism, the role of the redox partners and mitochondrial environment. Furthermore, an overview is given of the cloning of CYP11A1 from different species and the expression of the cloned enzymes in nonsteroidogenic COS cells.

Chapter 4 presents an overview of homology modelling, a technique used to predict the three-dimensional structure of proteins based on the observation that proteins with similar, but not identical, amino acid sequences have a tendency to adopt similar three-dimensional structures [6]. The common structural core shared by the cytochromes P450 [7], which make them ideal candidates for homology modelling, is presented. The five homology models of CYP11A1 constructed to date are presented and discussed in terms of the templates used and knowledge gained from these relevant studies. Furthermore, the orientation of cholesterol in the active pocket of CYP11A1, as predicted by previous groups, is discussed.

Total RNA and mRNA encoding baboon CYP11A1 was previously isolated in our laboratory. RNA from the adrenals of randomly selected Cape baboons was used to synthesise CYP11A1 cDNA through RT-PCR. The cDNA was subsequently subjected to a second round of PCR and ligated into a mammalian expression plasmid and three constructs; CYP11A1a, CYP11A1b and CYP11A1c were identified. Prior to the second round amplification the amplified cDNA was isolated and purified for direct sequence analyses.

In this study baboon CYP11A1 cDNA and the three constructs were characterised. The nucleotide sequences were determined and the baboon CYP11A1 cDNA sequence was submitted to GenBank (GenBank accession no. AY 702067). Sequence analyses revealed that while CYP11A1a and CYP11A1c had three amino acid substitutions each, CYP11A1b differed from CYP11A1 cDNA by a single substitution, K98I.

The constructs were coexpressed in nonsteroidogenic COS-1 cells with a human adrenodoxin construct the enzyme activity assayed using 25-hydroxycholesterol as substrate. CYP11A1b yielded a 2.8- and 2.5 fold greater K_m value than CYP11A1a and CYP11A1c, respectively, which was hypothesised to result from the single amino acid substitution, I98K. This was confirmed by constructing a homology model of CYP11A1b based on the solved crystal structures of the bacterial enzyme CYP102 and rabbit CYP2C5. Position 98 was found to be located in the B´-C loop, a domain associated with substrate binding [8]. These results were submitted to Endocrine Research and the published article is presented in chapter 5.

Baboon cDNA was subsequently constructed by mutating K98 in CYP11A1b to an isoleucine residue by site-directed mutagenesis. The K_m values of the cDNA and human CYP11A1 were determined in nonsteroidogenic COS-1 cells using 25-hydroxycholesterol as substrate. A K_m of 1.64 μM was obtained for baboon CYP11A1. Although eight amino acid differences occur between human and baboon CYP11A1, the K_m values obtained for these enzymes did not differ significantly.

A homology model of the baboon CYP11A1 cDNA was constructed based on the crystal structures of CYP102 and CYP2C5 and the eight differences between human and baboon CYP11A1 were found to be located on the surface of the enzyme, away from the active pocket. The role of residues 98 and 103 in the B´-C loop domain was subsequently examined by inserting the mutations I98Q and K103A into this domain by site-directed mutagenesis. The I98Q construct yielded a 1.7 fold increase in K_m, while the K103A construct yielded a 1.8 fold decrease in K_m. The constructed three-dimensional model revealed that both residues are essential in maintaining the structural integrity of the B´ through C helices, a structural region in the cytochromes P450 shown to be critical in determining substrate specificity and hydroxylation regioselectivity [7,9-11]. This data, used in conjunction with docking studies, permitted the proposal of a topological model of the CYP11A1 active pocket. The manuscript, which has been submitted for publication, is presented in chapter 6 in the format required by the journal.

In conclusion chapter 7 presents an overview of the results obtained in this study. Deductions pertaining to the structure/function of CYP11A1 are made by combing the kinetic analysis and homology modelling. The importance of the B´ through C helices is emphasised in terms of substrate binding and access. The results are compared to those previously published in the literature and a topological model for the active pocket of CYP11A1 is presented.

CHAPTER 2
ADRENAL STEROIDOGENESIS

2.1 The adrenal gland

2.1.1 Anatomy and morphology of the adrenal gland

Humans and most other mammals have two bilateral encapsulated adrenal (suprarenal) glands situated on the upper pole of each kidney [12]. In mammals the adrenal gland contains two functionally different types of endocrine tissue with different embryological origin: the outer adrenal cortex and the inner adrenal medulla, as shown in figure 2.1(A) [12,13]. The adrenomedullary chromaffin cells originate from neural crest precursor cells that migrate into the adrenal and subsequently differentiate into chromaffin cells [13]. Medullary chromaffin cells are organised into interlacing cords and are under the control of sympathetic preganglionic nerve stimulation of the splanchnic nerve [14]. The main secretory products of the chromaffin cells are the catecholamines: epinephrine and norepinephrine [12]. Chromaffin cells are characterised by dense-cored catecholamine-containing secretory vesicles [13]. The medullary cells are separated into two main cell types depending on their secretory product. These are: the epinephrine-secreting type, which have less dense granules; and the norepinephrine type, which have smaller, denser granules. Both cell types may also release smaller amounts of transmitters, neuropeptides and proteins together with the catecholamines [13].

The adrenal cortex is formed from the adrenal primordium during embryogenesis. The adrenal primordium consists of mesodermally derived fetal adrenal cells, which result from the condensation of celomic epithelium at the cranial end of the kidney [13]. The adrenal cortex secretes three classes of steroid hormones, namely mineralocorticoids, glucocorticoids and androgens. The steroid secreting cells of the adrenal cortex are characterised by large lipid droplets; numerous variably shaped mitochondria with tubulovesicular cristae; and a prolific system of smooth endoplasmic reticulum, as shown in figure 2.2 [12]. In most mammals including the baboon [15], the steroid secreting cortical cells are arranged into three distinct zones which differ in morphological features and steroid hormone production [12,13]. The three zones are, from the outer to the inner layer, the zona glomerulosa, the zona fasciculata and the

zona reticularis, as shown in figure 2.1(B) [12]. The cortical tissue constitutes 72% of the adrenal mass, of which the zona fasciculata constitutes 50%, the zona glomerulosa 15% and the zona reticularis 7% [16]. The zona glomerulosa often forms an incomplete layer and is the unique source of the mineralocorticoid aldosterone [12,13]. In this zone the secretory cells are arranged in irregular ovoid clusters separated by delicate trabeculae containing capillaries [12]. The cells of the zona glomerulosa are able to regenerate the zona fasciculata and reticularis when these layers are removed, suggesting an additional role of this zone in the production of new cortical cells [17]. The zona fasciculata produces the glucocorticoids cortisol and corticosterone, and trace amounts of the androgen dehydroepiandrostenedione (DHEA) [12,13]. The secretory cells of this zone are arranged in narrow radially arranged cords, often only one cell layer wide, separated by fine strands of supporting tissue containing capillaries [12]. The zona reticularis consists of an irregular network of branching cords and clusters of cells separated by numerous capillaries [12]. These secretory cells produce trace amounts of glucocorticoids and the androgens DHEA, DHEA sulphate and androstenedione [12,13]. It is the zonation of the steroidogenic enzymes, which will be discussed later in this chapter, that determines the steroidogenic output of each of the three adrenocortical zones.

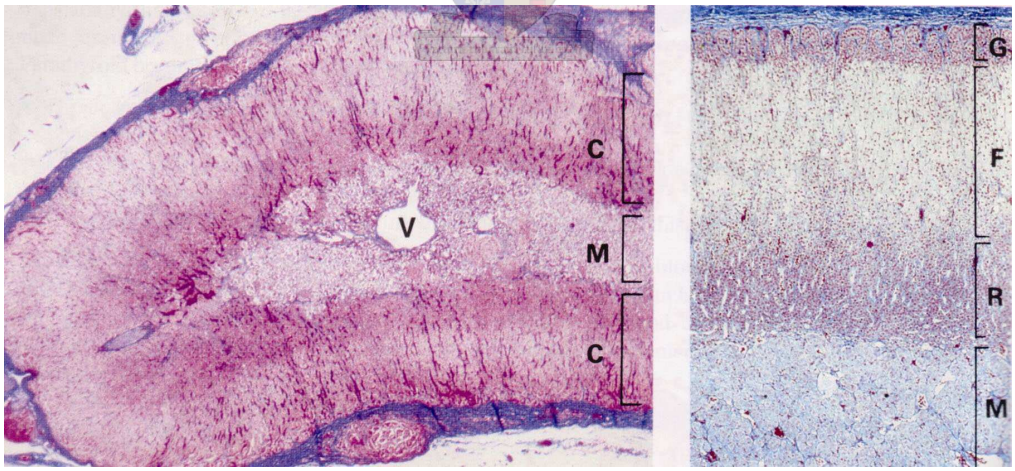

Figure 2.1. A: Cross section through the human adrenal gland. The adrenal cortex (C) is seen surrounded by a dense fibrous tissue capsule which supports the gland. A prominent vein (V) is characteristically located in the centre of the medulla (M). B: Cross section of the adrenal cortex and medulla (M). The three zones of the cortex, the zona glomerulosa (G), the zona fasciculata (F) and the zona reticularis (R) are clearly seen. Reproduced from [12].

The cortical and medullary cells are in direct contact with each other without separation by connective tissue or interstitium [12,13]. Although the adrenal is fundamentally arranged into the cortex and medulla, chromaffin cells are found in all three zones of the adult adrenal cortex, either radiating through the cortex from the medulla or distributed as islets or single cells. Furthermore, chromaffin cells may also spread and form larger nests in the subcapsular region [18-22]. Cortical cells are also found in the medulla as islets, either surrounded by chromaffin tissue or retaining some association with the rest of the cortex [13]. This intimate association and intermingling of the two cell types allows for extensive paracrine interaction, and is discussed later in this chapter.

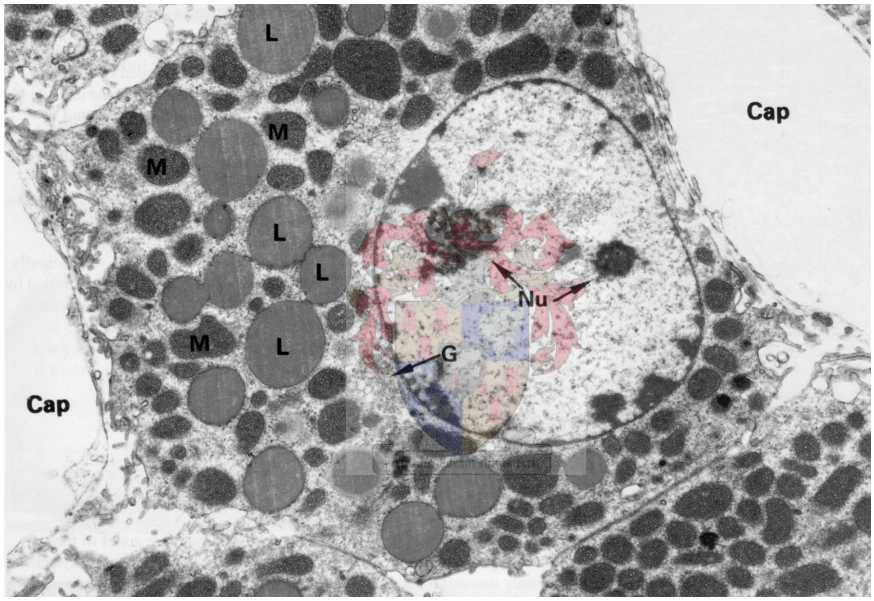

Figure 2.2 Typical steroid-secreting cell. A steroid cell is typically seen intimately associated with capillaries (Cap). Prominent nucleoli (Nu) are seen in the rounded nucleus, and a small Golgi apparatus (G) is seen close to the nucleus. The abundant cytoplasm contains many large lipid droplets (L), numerous variably shaped mitochondria (M) and an extensive network of smooth ER (not clearly visible at this magnification). Reproduced from [12].

2.1.2 Blood supply to the adrenal gland

The adrenal gland receives its blood supply from the superior, middle and inferior suprarenal arteries, which form a plexus just under the capsule of the gland. The cortex is supplied by an anastomising network of capillary sinusoids, which are supplied by branches of the subcapsular plexus known as short cortical arteries. These sinusoids

descend between the cords of steroid secreting cells in the zona fasciculata into a deep plexus in the zona reticularis before draining into small venules, which converge upon the central vein of the medulla. The central medullary veins contain bundles of smooth muscles between which the cortical venules enter. Contractions of these smooth muscle bundles restrict cortical blood flow as a regulatory mechanism. The medulla is supplied by long cortical arteries, which descend from the subcapsular plexus through the cortex and into a network of capillaries surrounding the medullary chromaffin cells. These capillaries also drain into the central vein of the medulla [12]. A schematic representation of the blood supply to the adrenal gland is shown in figure 2.3.

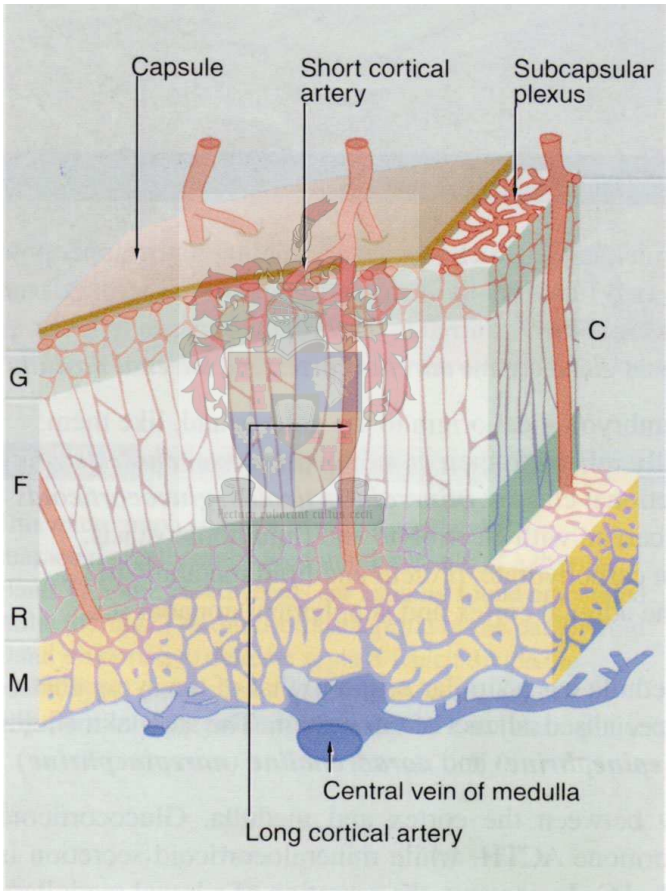

Figure 2.3. Schematic representation of the blood supply to the adrenal gland. C, Cortex; M, Medulla; G, zona glomerulosa; F, zona fasciculata; R, zona reticularis. Reproduced from [12].

2.2 Hormones of the adrenal cortex

2.2.1 Mechanisms of action

The steroid hormones produced by the adrenal cortex are all lipophilic and can transverse the plasma membrane. Although the primary effects of the steroid hormone stimulation occur via nuclear hormone receptor (NHR) mediated genomic effects, nongenomic effects mediated via receptors on the cell surface have been documented, but are beyond the scope of this discussion [23].

Once in the cell interior, the mineralocorticoids, glucocorticoids and androgens bind to their corresponding NHR's. All NHR's share common structural features, which include a central DNA binding domain (DBD) and a ligand binding domain (LBD) contained in the C-terminal half of the receptor [24]. The DBD is highly conserved, composed of two zinc fingers, and is responsible for targeting the receptor to a highly specific DNA sequence comprising a response element (RE) [24,25]. The N-terminal and C-terminal domains are variable and a variable length hinge region occurs between the DBD and the LBD. NHR's can exist as homo- or heterodimers with each partner binding to a specific RE sequence that exist as half-sites separated by variable length nucleotide spacers. Half-sites may occur as direct or inverted repeats depending on the NHR [24].

The mineralocorticoids, glucocorticoids and androgens, produced by the adrenal cortex, bind to specific NHR's, namely the mineralocorticoid receptor (MR), glucocorticoid receptor (GR) and the androgen receptor (AR), respectively [24]. The mechanisms of action of these three NHR's are similar and therefore only the best understood NHR of the three, the GR, will be discussed here. The GR is located in the cytoplasm of the target cell as part of a larger protein complex, in which it interacts with the heat shock protein HSP90. Upon ligand binding, the GR undergoes a conformational change, dissociates from the protein complex and translocates across the nuclear membrane. In the nucleus the GR binds as a dimer to a glucocorticoid-response element (GRE). This may induce the activation of a target gene by transactivation or the repression of the transcription of a target gene by transrepression. In the case of transrepression, the GRE is known as a negative GRE (nGRE) [24,25].

The functioning of the NHR's is not always as simple as described above. As a result of alternative splicing of the GR pre-mRNA primary transcripts, two protein

isoforms of the GR exist, namely GRα and GRβ. GRβ does not bind glucocorticoids and is an inhibitor of the glucocorticoid induced activity of GRα [26]. Furthermore, a number of regulatory proteins have been identified that form multicomponent assemblies with the NHR's and serve as either coactivators or corepressors. These coregulators can bind to the NHR's via specific amino acid sequence motifs in a ligand-dependent or ligand-independent manner and provide enzymatic or scaffolding functions. In addition, these proteins influence chromatin remodelling by histone acetylation/deacetylation, methylation, and also by other events that are beyond the scope of this discussion [27].

2.2.2 Mineralocorticoids

The mineralocorticoid aldosterone plays an essential role in the regulation of electrolyte concentration in the extracellular fluid. Aldosterone action results in the reabsorption of sodium from urine, sweat, saliva and gastric juices [28]. In the late part of the distal convoluted tubule, the connecting tubule and the cortical collecting duct of the kidney, sodium is transported through the epithelial cells into the interstitial fluid. Sodium diffuses through the epithelial sodium channels (ENaC) in the apical membrane and is then actively pumped out of the cell by the Na-K-ATPase, located in the basolateral membrane of these cells [25,29]. The potassium which enters the cell through the Na-K-ATPase may be secreted through the inwardly rectifying potassium channel (ROMK) in the apical membrane. The rate of sodium reabsorption is primarily determined by the activity of ENaC [29]. Aldosterone induces the expression of a serine-threonine kinase-1, which in turn results in the accumulation of ENaC in the apical membrane [25,29]. The activity of the Na-K-ATPase is also upregulated by the action of aldosterone [29]. Although there is some evidence that aldosterone-induced Spk1 can stimulate ROMK activity, it appears that potassium secretion through ROMK is primarily controlled by the concentration of potassium in the extracellular fluid mediated by various other signalling pathways still to be elucidated [29-31]. In addition to the regulation of sodium and potassium levels, aldosterone has also been shown to upregulate aquaporin-3 in the cortical collecting duct of the kidney, thereby facilitating the reabsorption of water together with sodium [32].

Sodium reabsorption is mediated by the binding of aldosterone to the MR. Interestingly the GR is expressed together with the MR in aldosterone target cells. The

MR has equal affinities for aldosterone and the glucocorticoids, but seems to be able to discriminate between glucocorticoids and mineralocorticoids. Furthermore, the plasma concentrations of glucocorticoids hormones are 100 to 1000-fold higher than those of aldosterone (0.1-1 nM). The high plasma glucocorticoids levels that could potentially bind the target cell MR's are reduced to about 10% by their binding to plasma albumin and corticosteroid binding globulin (CBG), whereas aldosterone circulates predominantly in a free form [25]. In addition, several aldosterone target cells, including those in the kidney, express 11β-hydroxysteroid dehydrogenase (11βHSD), which transforms cortisol and corticosterone into cortisone and 11-dehydrocorticosterone, respectively. This mechanism prevents the glucocorticoids from having a mineralocorticoid effect as these metabolites have weak or no affinity for the MR.

Regulation of aldosterone is primarily under the control of the renin-angiotensin system. Angiotensinogen is secreted by the liver and is cleaved in the bloodstream by renin, an enzyme secreted by the juxtaglomerular apparatuses in the kidney, to release angiotensin I. Angiotensin I is further cleaved to yield angiotensin II by angiotensin converting enzyme (ACE) found on the luminal surface of capillary endothelial cells in the lungs. Angiotensin II in turn stimulates the secretion of aldosterone from zona glomerulosa in the adrenal cortex. Angiotensinogen and ACE are present in the blood at relatively constant concentrations. The regulation of aldosterone secretion therefore lies in the secretion of renin. The juxtaglomerular apparatus acts as both a baroreceptor and a chemoreceptor, secreting renin when blood pressure or the concentration of sodium in the extracellular fluid decreases. In addition, an increased concentration of potassium in the extracellular fluid may also have a direct effect on aldosterone secretion by the adrenal cortex [1].

Adrenal insufficiency, resulting in insufficient aldosterone secretion, causes excessive sodium and water loss, which can lead to hypovolemia and fatal shock if untreated. An excess in aldosterone secretion results in potassium depletion and an increase in extracellular fluid volume due to sustained sodium and water reabsorption. When the extracellular fluid volume reaches a certain threshold, sodium excretion occurs in a phenomenon known as sodium escape. This escape phenomenon is believed to be mediated by the action of atrial natriuretic factor [33].

In addition to the role of aldosterone in sodium reabsorption, nongenomic effects of aldosterone have also been observed in the cardiovascular system and the central nervous system [34].

2.2.3 Glucocorticoids

The two glucocorticoids produced by the adrenal cortex are cortisol and corticosterone. Within different species, one of these glucocorticoids tends to dominate and is secreted at greater concentrations than the other. In humans and monkeys, cortisol is the dominant glucocorticoid [1] and all further discussion will deal with cortisol only. As mentioned previously, approximately 90% of the circulating cortisol is bound to plasma albumin and CBG [25]. Although the binding of cortisol to these proteins increases its half-life, it is only the free fraction of cortisol that is active and may bind to the GR.

The primary function of cortisol is the regulation of carbohydrate, lipid and protein metabolism [35]. At normal basal concentrations, cortisol has a permissive effect on the action of glucagon and epinephrine in stimulating gluconeogenesis and lipolysis during the postabsorptive state. During starvation and other physiological stress, the adrenal cortex is stimulated to secrete cortisol by the hypothalamic-pituitary-adrenal (HPA) axis, discussed later in this chapter. Increased plasma concentrations of cortisol result in: increased protein catabolism in the peripheral tissue; increased uptake of amino acids by the liver; increased gluconeogenesis; and decreased uptake of glucose by the muscle and adipose tissue. In addition to the increasing gluconeogenesis, cortisol also increases the release of glucose from the liver [1].

Since the action of cortisol is opposite to that of insulin, individuals with an abnormally high level of cortisol may develop symptoms that are similar to those seen in individuals with insulin deficiency. Conversely, cortisol deficiency can result in hypoglycaemia, serious enough to impair brain function during fasting [1].

At basal levels glucocorticoids suppress immune function to a certain extent and are important in preventing the onset of autoimmune diseases [36]. Binding of cortisol to GRα, resulting in transactivation, also has an inhibitory effect on certain transcription factors, such as nuclear factor kappa B, involved in immune function. This transrepression decreases the expression of many genes encoding inflammatory mediators [37]. The immunosuppressive and anti-inflammatory effects of glucocorticoids are significantly increased during periods of high glucocorticoid secretion that is brought about by stress. Cortisol also reduces the number of circulating lymphocytes and decreases both antibody production and the activity of helper T cells

and cytotoxic T cells. Glucocorticoid derivatives are therefore administered in high doses to reduce the inflammatory response to injury and infection; and in the treatment of allergy, arthritis and graft rejection [1].

It has been reported that high concentrations of cortisol may cause bone resorption by inhibiting osteoblasts and stimulating osteoclasts. High cortisol concentrations also inhibit the secretion of growth hormone (GH) by the anterior pituitary [1], and have disruptive effects on preovulatory events [38]. The number of circulating eosinophils [39] and basophils [40] are lowered by high cortisol levels, while the neutrophil [26], platelet [41] and red blood cell [42] counts are increased. Since cortisol also facilitates the vasoconstrictive effect of norepinephrine [1], adrenal insufficiency therefore prevents vascular compensation for hypovolemia. Other permissive effects of glucocorticoids include the pressor responses and the bronchodilatory effect of the catecholamines [37].

2.2.4 Adrenal androgens

Androgens synthesised in the gonads and adrenal are steroid hormones that bring about masculinity and promote protein anabolism and growth. The androgens produced by the adrenal cortex include androstenedione, DHEA, DHEA-sulphate (DHEAS) and testosterone [43]. Testosterone is the major male sex hormone and is secreted primarily by the testes [1]. The concentration of plasma testosterone derived from the adrenal is negligible and will be ignored for the purposes of this discussion. The adrenal androgens bind the AR with low affinity, having less than 20% of the potency of testosterone, and are therefore considered weak androgens [43]. Circulating DHEA and androstenedione are present at low levels in preadrenarchal children. Adrenarche, which is characterised by the activation of adrenal androgen production, results in sexual maturation. An increase in plasma concentrations typically occurs in children between the age of 6 and 8 years. Levels of DHEAS above 40–50 mg/dl are considered to be consistent with the advent of adrenarche [44]. The level of DHEA and DHEAS peak in the early twenties and are then higher than that of any other steroid hormone [43,45]. Their levels decline over the subsequent five decades. It has been suggested that this decline in adrenal androgens is linked to the loss of mental and physical capabilities in aging humans [45]. In prepubertal boys, increased androgen secretion can result in

precocious pseudopuberty, while pseudohermaphroditism and the adrenogenatil syndrome may arise in females [46].

The actions of DHEA, DHEAS and androstenedione may be mediated via the AR or estrogen receptor (ER), but binding can only occur after the enzymatic conversion of these steroids to the androgens, testosterone and dihydrotestosterone, or estradiol. DHEA can be converted to estrogen or testosterone in the appropriate tissues. Nongenomic effects have, however, also been observed for DHEA [47]. In certain tissue types androstenedione can be aromatised into estrone, an estrogen. In the plasma, up to 5% of the estrone is converted to estradiol. The plasma concentration of estradiol in males is significantly higher than that in postmenopausal woman. Estrogens in males are important in the regulation of gonadotropin feedback; brain function; bone maturation; and the regulation of bone resorption and lipid metabolism. DHEA and androstenedione are therefore an important source of estrogens in males and postmenopausal woman [48].

DHEA is involved in a number of functions including metabolism and vascular and immune function [49]. Studies have shown that DHEA can induce GH secretion by reducing the inhibitory action of somatostatin (SS), as well as by enhancing the somatotrope sensitivity to growth hormone releasing hormone (GHRH). Significant deficiencies of DHEA have been reported in patients suffering from various cancers, inflammatory diseases, type II diabetes, atherosclerosis, Alzheimer's disease and cardiovascular disorders [50]. Recently a study has shown that DHEA increases spine synapse density linking, the decrease in DHEA levels and mental acuity during aging [51]. This may explain the link between decreased DHEA levels and Alzheimer's disease [43].

2.3 Enzymes involved in adrenal steroidogenesis

The biosynthesis of the mineralocorticoids, glucocorticoids and adrenal androgens from cholesterol in the adrenal glad involves two distinct groups of enzymes: the cytochromes P450 and the hydroxysteroid dehydrogenases. The general biochemical properties of these enzyme groups will subsequently be discussed.

2.3.1 The cytochromes P450

The cytochromes P450 are a superfamily of heme-containing proteins found in bacteria, fungi, plants and vertebrates, including mammals [52]. Over 1200 individual cytochromes P450 have been reported to date [53]. Garfinkel [54] and Klingenberg [55] were the first to isolate this unusual cytochrome from mammalian liver microsomes in 1958 and the unique spectral properties of these cytochromes were first identified by Omura and Sato in 1962 [56]. The reduced cytochrome showed a distinct peak at 450 nm in the presence of carbon monoxide. This peak at 450 nm resulted in the name P450. Detergent treatment of P450 containing microsomes quantitatively converts the cytochrome to a soluble form with a peak at 420 nm, referred to as P420. Omura and Sato later showed that cytochromes P450 contain a protoporphyrin IX ring structure complexed with iron [57]. The heme iron is always penta- or hexacoordinated, with four of the ligands being contributed by the planar, tetradentate poryphyrin ring. The fifth or proximal ligand is a thiolate sulphur atom contributed by a cysteine residue from in the polypeptide chain. The sixth coordination position of the iron is believed to be occupied by water in the native, substrate free, ferric state. Upon reduction of the iron, the sixth position becomes the site of dioxygen binding [58].

The unique nature of these cytochromes allows them to catalyse the stereospecific hydroxylation of nonactivated substrates (RH) at physiological temperature, a reaction that, uncatalysed, requires extremely high temperatures to proceed. The general reaction is:

$$RH + O_2 + NADPH + H^+ \rightarrow ROH + H_2O + NADP^+$$

The cytochromes P450 function as monooxygenases in this reaction. They utilise reduced NADPH as the electron donor for the reduction of molecular oxygen, with the subsequent incorporation of one oxygen atom into the substrate as a hydroxyl group, while the other oxygen atom is reduced to water [3]. The reaction cycle of the cytochromes P450 has been the subject of many investigations and a general mechanism has been established, as shown in figure 2.4. The substrate binds to the active pocket with the iron in the ferric state. A single electron reduces the iron to the ferrous state, which allows for the binding of oxygen to form the ternary P450-oxygen-substrate complex. The addition of a second electron and two protons results in the

splitting of the molecular oxygen. One oxygen atom is lost to water, while the other remains bound to the ferric iron to form the activated oxygen intermediate. The activated oxygen is inserted into the substrate as a hydroxyl group to form the hydroxylated product. The product is released from the enzyme complex and the enzyme is regenerated into its native ferric form [58]. The presence of the ferrous dioxygen and an oxyferryl species was confirmed recently by Schlichting et al., using trapping techniques and cryocrystallography to investigate the catalytic pathway of cytochrome P450cam (CYP101) [59].

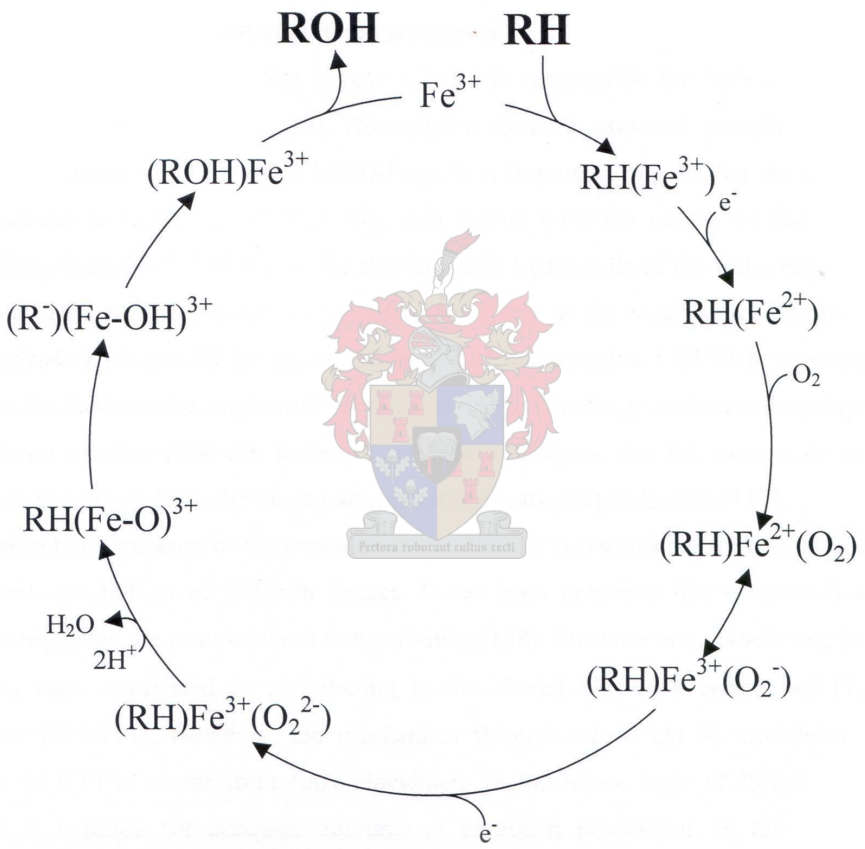

Figure 2.4. Proposed scheme for the mechanism of action of cytochrome P450 hydroxylation reactions. RH represents a substrate and ROH the corresponding hydroxylated product. Reproduced from [60].

The cytochromes P450 are vital for a number of physiological processes, which include the metabolism of xenobiotics [61] in the liver and the production of the steroid hormones in the gonads and adrenal cortex. Mammalian cytochromes P450 are all

associated with either the endoplasmic reticulum (microsomal) or the mitochondrial (mitochondrial) membranes. The microsomal and mitochondrial cytochromes P450 obtain the required electrons from NADPH via two different electron transfer systems. The mitochondrial system involves the transfer of the high potential electron to a flavoprotein, adrenodoxin reductase (AdxR), and subsequently to a nonheme iron-sulphur protein, adrenodoxin (Adx). Adx acts as an electron shuttle between AdxR and the mitochondrial cytochromes P450. This electron transfer system is discussed in detail in the following chapter. The microsomal electron transfer system involves a single protein, cytochrome P450 oxidoreductase, which contains two flavins. Electrons are transferred from NADPH to flavinadenine dinucleotide (FAD), and subsequently to flavinmononucleotide (FMN) and the microsomal cytochrome P450 [3]. A schematic representation of the microsomal electron transfer system is shown in figure 2.5.

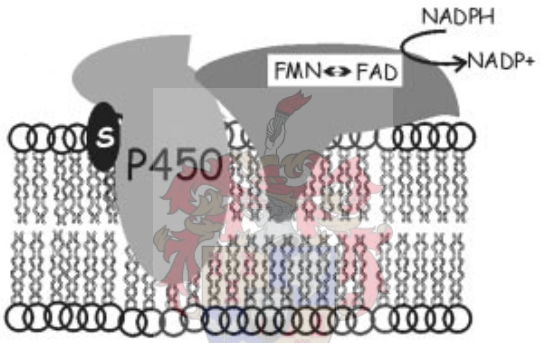

Figure 2.5. Schematic representation of the microsomal electron transfer system. S, substrate.

Three mitochondrial and two microsomal cytochromes P450 are involved in adrenal steroidogenesis. It is the zonation of these enzymes that determines the relative steroidogenic output of the different zones in the adrenal cortex.

2.3.2 The hydroxysteroid dehydrogenases

Two hydroxysteroid dehydrogenases (HSDs), 3β-hydroxysteroid dehydrogenase (3βHSD) and 17β-hydroxysteroid dehydrogenase (17βHSD), are involved in steroidogenesis and are members of the short-chain alcohol dehydrogenase reductase superfamily [62]. They are non-metallic enzymes that function as monomers or multimers, but are not known to form complexes with other proteins such as redox partners [2]. Only 3βHSD contributes significantly to adrenal steroidogenesis. Two

distinct isoforms of 3βHSD have been identified in humans, human 3βHSD I and II [3]. Both of these isoforms function as steroid dehydrogenase/isomerases and catalyse the conversion of Δ5-3β-hydroxysteroids to Δ4-3-ketosteroids. This conversion requires two sequential reactions. The first reaction is the dehydrogenation of the 3β-equatorial hydroxysteroid, and requires the coenzyme NAD^+, yielding a Δ5-3-keto intermediate and NADH. In the subsequent reaction, NADH activates the isomerisation of the Δ5-3-keto-steroid to yield the Δ4-3-ketosteroid, as shown in figure 2.6 for pregnenolone and DHEA. Both reactions are catalysed without the release of the intermediate or the coenzyme [63-65]. Unlike the reactions catalysed by the cytochromes P450, the reactions catalysed by the HSD's are reversible, and the reaction direction is dependent on the concentrations of the substrates, products and cofactors [2].

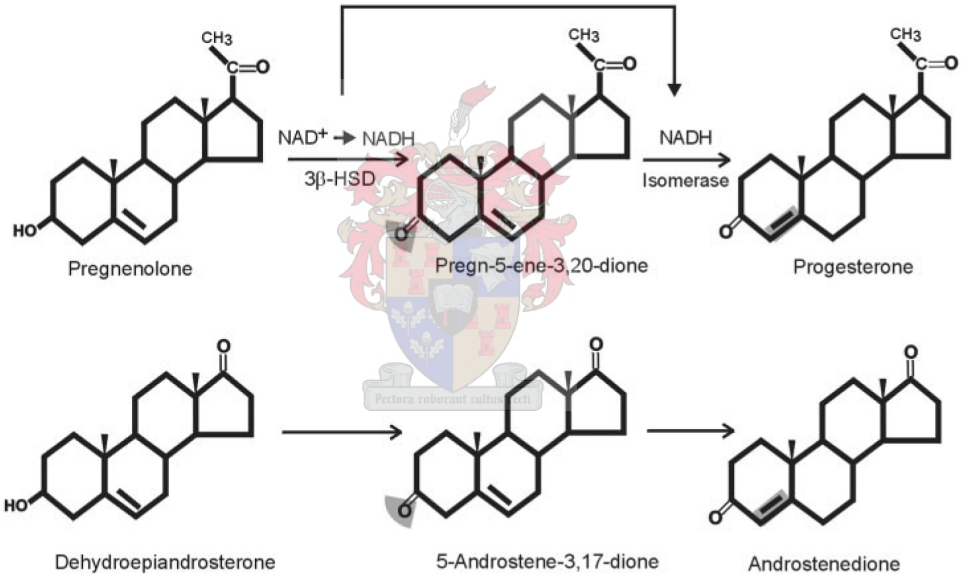

Figure 2.6. Enzymatic reaction catalysed by human 3βHSD. The enzyme catalyses the dehydrogenation of the 3β-hydroxyl group yielding a Δ5-3-keto intermediate and reduced NADP that activates the isomerisation of the Δ5-3-keto to yield the Δ4-3-ketosteroid, as shown here for the conversion of pregnenolone and DHEA to progesterone and androstenedione, respectively. Reproduced from [3].

The two isoforms of human 3βHSD are expressed in a tissue specific manner. Only 3βHSD II is expressed in the adrenal, ovary and testis, while 3βHSD I is expressed in the placenta, skin and breast tissue [66]. In rat adrenals and gonads, 3βHSD was detected mostly in the endoplasmic reticulum, but also in the cristae of the inner mitochondrial membrane [67]. In the human, 3βHSD is expressed in all three zones of

the adrenal cortex between 7 months and 8 years of age, followed by a decrease in the zona reticularis with increasing age [68].

2.3.3 Overview of the adrenal steroidogenic pathway

The steroid hormones produced by the adrenal cortex are all derivatives of cholesterol, containing the cyclopentanoperhydrophenanthrene nucleus shown in figure 2.7. Five cytochromes P450 and a single hydroxysteroid dehydrogenase, 3βHSD, catalyse the conversion of cholesterol to the adrenal steroid hormones. The cytochromes P450 involved are the mitochondrial enzymes: cytochrome P450 side-chain cleavage (CYP11A1), cytochrome P450 11β-hydroxylase (CYP11B1), aldosterone synthase (CYP11B2); and the microsomal enzymes: cytochrome P450 17α-hydroxylase/17,20 lyase (CYP17) and cytochrome P450 21-hydroxylase (CYP21B).

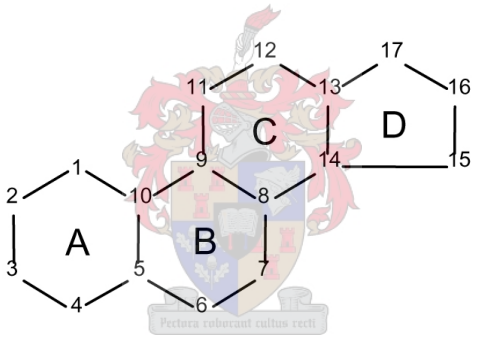

Figure 2.7. Cyclopentanoperhydrophenanthrene nucleus. Reproduced from [69]

CYP11A1 catalyses the conversion of cholesterol to pregnenolone, the first step in adrenal steroidogenesis. The pregnenolone produced in the mitochondria moves to the ER where it serves as a substrate for either CYP17 or 3βHSD. CYP17 hydroxylates pregnenolone at C17 to yield 17-hydroxypregnenolone, which can serve as a substrate for the lyase activity of CYP17 to produce DHEA. DHEA and 17-hydroxypregnenolone also act as substrate to 3βHSD. Pregnenolone, 17-hydroxypregnenolone and DHEA are all dehydrogenated at C3 and converted from the Δ5 to the Δ4 isoforms by 3βHSD. The resulting products are progesterone, 17-hydroxyprogesterone and androstenedione, respectively. Progesterone can be hydroxylated at C17 by CYP17 to form 17-hydroxyprogesterone. In addition, the lyase activity of CYP17 can cleave the C17-C20 bond of 17-hydroxyprogesterone to yield androstenedione. Progesterone and 17-

hydroxyprogesterone also act as substrates for CYP21, which hydroxylates these substrates at C21 to form deoxycorticosterone and deoxycortisol, respectively. These two intermediates move to the mitochondria where CYP11B1 catalyses their 11β-hydroxylation to yield corticosterone and cortisol, respectively. Deoxycorticosterone also serves as substrate for CYP11B2 which catalyses three sequential reactions. These reactions are: the 11β-hydroxylation of deoxycorticosterone, the hydroxylation of C18 and the oxidation of the C18 hydroxyl group to yield the C18 aldehyde group of aldosterone. A map of the adrenal steroidogenic pathways is shown in figure 2.8. [3].

It is essentially the distribution of the different steroidogenic enzymes in the three zones of the adrenal cortex that results in each zone's unique steroidogenic output. For example, the zona glomerulosa, which produces only aldosterone, expresses only CYP11A1, 3βHSD, CYP21 and CYP11B2. CYP17 and CYP11B1 are not expressed in this zone, while CYP11B2 is not expressed in either the zona fasciculata or the zona reticularis. The zona fasciculate, which produces mainly cortisol, and small amounts of DHEA and androstenedione, expresses CYP11A1, CYP17, 3βHSD, CYP21 and CYP11B1. Finally the zona reticularis, which produces primarily DHEA and androstenedione, and trace amounts of cortisol, express CYP11A1, CYP17, 3βHSD, and low levels of CYP21 and CYP11B1 [3].

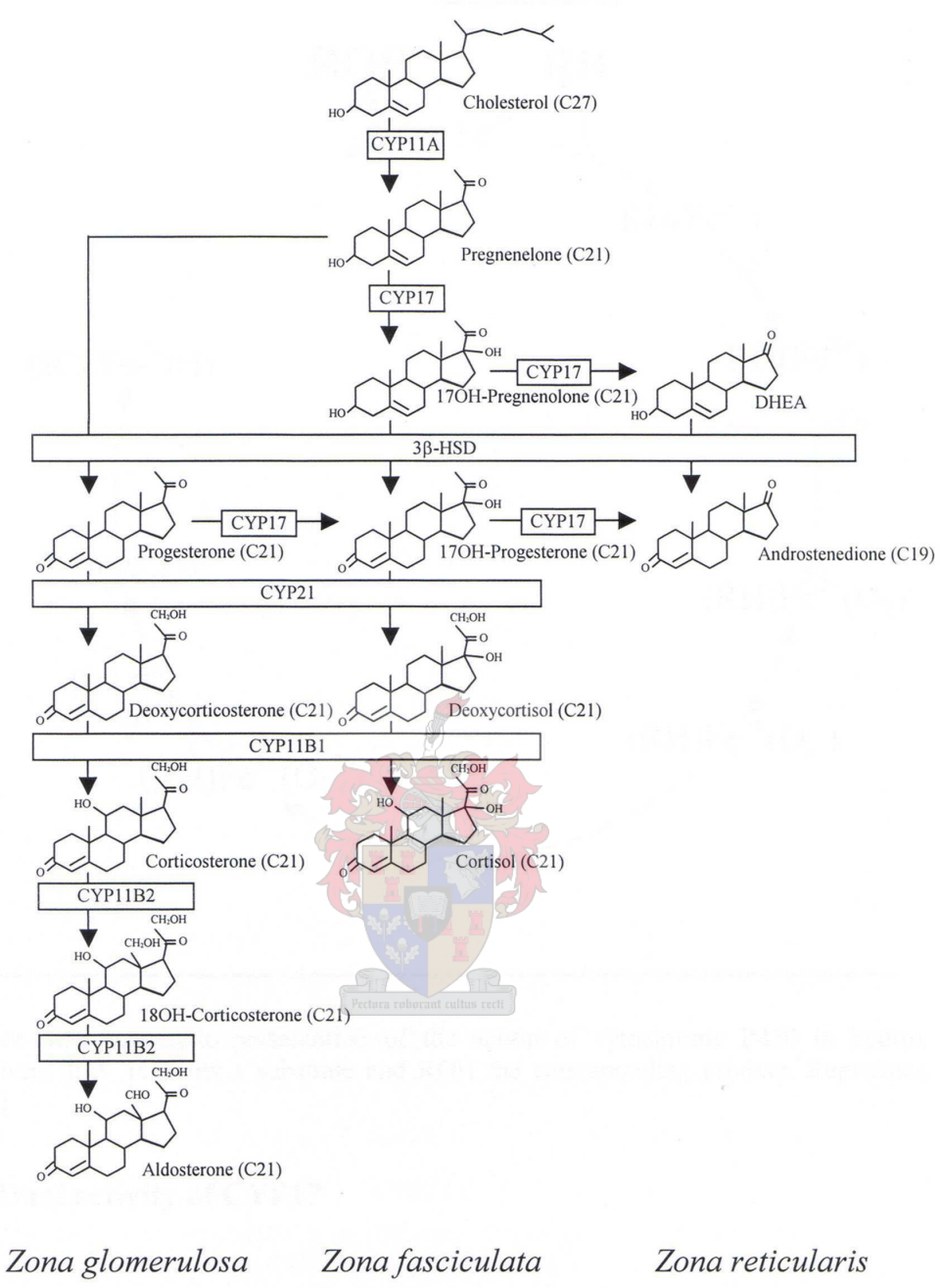

Figure 2.8 Overview of the adrenal steroidogenic pathway. Reproduced from [60].

2.4 The source of cholesterol for adrenal steroidogenesis

As previously mentioned, cholesterol is the precursor for all steroid hormones. Although all steroidogenic cells contain the necessary enzymes to synthesise endogenous cholesterol from acetate, the majority of cholesterol used in steroid biosynthesis is obtained via receptor-mediated uptake from circulating lipoproteins. Adrenocortical cells acquire cholesterol from both low density lipoprotein (LDL) and high density lipoprotein (HDL) cholesterol esters (CE) circulating in the blood [70].

LDL uptake is mediated by the LDL receptor. Binding of LDL to the LDL receptor results in the internalisation and degradation of the entire LDL molecule by lysosomal vesicles. CE's are hydrolysed in the lysosome by lysosomal acid lipase with the subsequent release of cholesterol [2,71]. Vesicles transport the majority of the released cholesterol to the endoplasmic reticulum [2]. Apolipoprotein E (apo E) E is present in high levels on adrenocortical cell membranes, and has been shown to facilitate cholesterol uptake by the LDL receptor [72]. Adrenocorticotrophic hormone (ACTH) promotes LDL mediated CE uptake in the adrenal [71].

Cholesterol uptake from HDL is mediated by the scavenger receptor class B, type I (SR-BI) receptor, also known as CLA-1 [73]. HDL CE uptake is a two step process. The first step involves the binding of the lipoprotein to the extracellular domain of SR-BI, while the second step involves the selective transfer of lipid to the plasma membrane. CE's are delivered to the plasma membrane without the uptake and degradation of the entire HDL particle, as occurs for LDL uptake [73,74]. SR-BI expression in the adrenocortical cell membrane results in the formation of microvilli and microvillar channels, the sites for cholesterol delivery. In addition, SR-BI appears to increase membrane fluidity by altering the lipid composition of the cell membrane [74]. The epitopes in HDL that recognise SR-BI are believed to be various phospholipids and apolipoproteins, specifically apoA-I [73,74]. CE delivered by SR-BI to the steroidogenic cell is hydrolysed extrasomally by a neutral CE hydrolase, hormone sensitive lipase (HSL) [75]. It would appear that HSL is also involved in the release of cholesterol from CE's stored in lipid droplets within the cytoplasm. The expression of SR-BI is hormonally regulated. Angiotensin II and ACTH promote SR-BI-mediated HDL selective CE uptake in the zona glomerulosa and zona fasciculata, respectively [74]. However, depletion of adrenal cholesterol stores can promote SR-BI-mediated HDL uptake in the absence of hormone stimulation [76].

Studies have shown that in humans, and other animals that carry their plasma cholesterol mainly in LDL, cholesterol for adrenal steroidogenesis is derived primarily from LDL uptake via the LDL receptor. Conversely, in animals such as rodents most of the cholesterol is bound to HDL, therefore cholesterol for adrenal steroidogenesis is derived primarily from SR-BI-mediated HDL uptake [70,71].

Esterification of cellular cholesterol with fatty acids is catalysed in the endoplasmic reticulum by acyl-CoA:cholesterol acyltransferase 1(ACAT1). CE's accumulate in the endoplasmic reticulum and bud off as lipid droplets.

2.5 The hypothalamic-pituitary-adrenal axis

The hypothalamus, anterior pituitary and adrenal cortex constitute a controlling loop known as the HPA-axis [77]. Interplay between these organs through the endocrine, paracrine and autocrine action of their hormones is essential in the maintenance of homeostasis in response to physiological and environmental stimuli. Stimulation of the HPA axis results in increased hormone secretion from all three zones of the adrenal cortex. The HPA axis is therefore vital for adrenocortical regulation, although other adrenocortical regulatory mechanisms occur, such as the renin-angiotensin system (section 2.2.2) and other intra-adrenal regulatory mechanisms. The HPA axis will therefore be discussed here in some detail.

2.5.1 The hypothalamus

The hypothalamus is a complex structure of the brain forming part of the diencephalon. It is central to a complex neural network that enables it to control the homeostasis of an organism. The hypothalamus is connected to a number of different centres in the central nervous system via many different afferent and efferent neural pathways. These include afferent pathways from the brain stem, hippocampus, limbic lobe, midbrain, thalamus and the medulla and efferent pathways to the hippocampus, limbic lobe, medial eminence, pituitary stalk and posterior pituitary [78]. The hypothalamus receives an array of chemical and electrical stimuli allowing it to sense the homeostatic state of the organism. In response it generates chemical and electrical signals, which in turn stimulate the anterior and posterior pituitary to release the appropriate hormones necessary for the maintenance of homeostasis. This discussion

will focus only on the regulation the hypothalamus exerts on adrenal steroidogenesis via the anterior pituitary. A schematic representation of the human hypothalamus and pituitary gland is shown in figure 2.9.

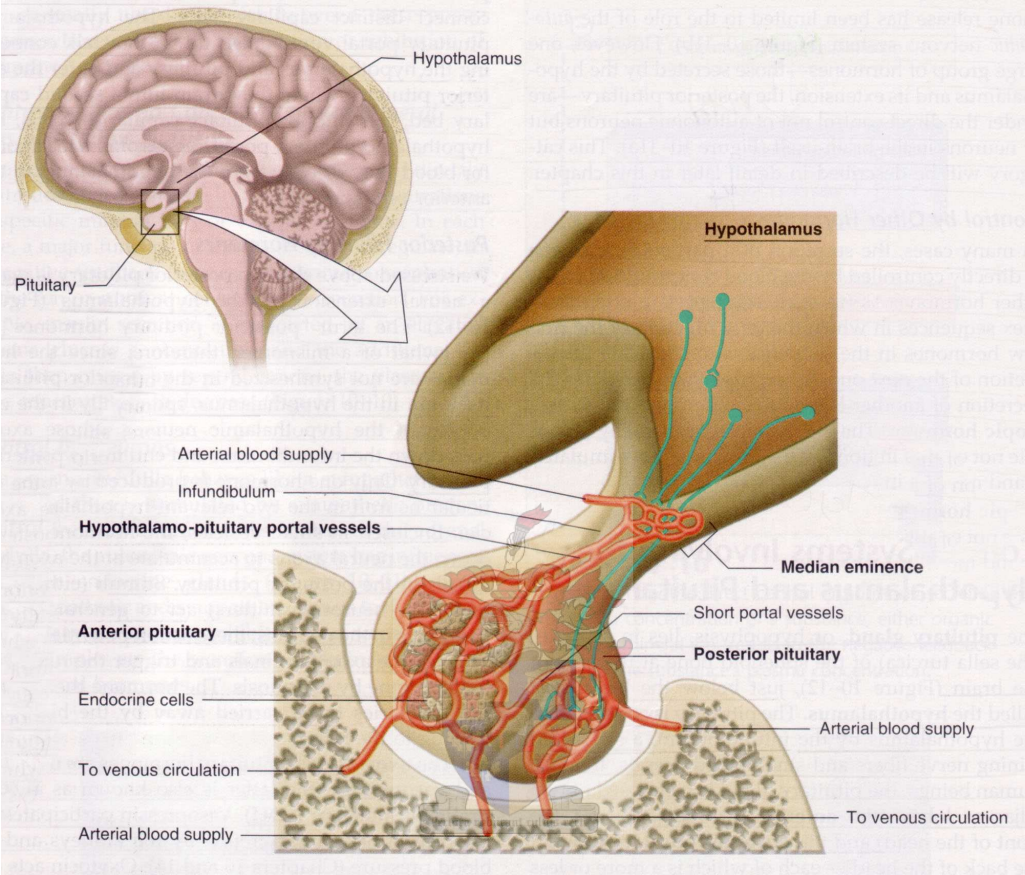

Figure 2.9. Human hypothalamus and pituitary. Reproduced from [1].

2.5.2 The pituitary

The pituitary gland, or hypophysis, lies in a pocket of the sphenoid bone, known as the sella turcica, at the base of the brain just below the hypothalamus. A stalk known as the infundibulum connects pituitary to the hypothalamus. The infundibulum contains nerve fibres and small blood vessels. The pituitary is comprised of two adjacent lobes, the anterior pituitary and the posterior pituitary, which have distinct embryological origins, functions and control mechanisms [1,12].

The posterior pituitary, also known as the neurohypophysis or pars nervosa, is derived from the downgrowth of nervous tissue from the hypothalamus to which it

remains joined by the infundibulum. Axons of the supraoptic and paraventricular hypothalamic nuclei pass down the infundibulum and end in the posterior pituitary.

The anterior pituitary arises as an epithelial upgrowth from the roof of the primitive oral cavity, known as Rathke's pouch. This specialised glandular epithelium is wrapped around the anterior aspect of the posterior pituitary and is also known as the adenohypophysis. A vestigial cleft may divide the major part of the anterior pituitary from a thin zone of tissue lying adjacent to the posterior pituitary, known as the pars intermedia. An extension of the adenohypophysis, which surrounds the neural stalk, is known as the pars tuberalis [12]. The anterior pituitary is not connected to the hypothalamus by a neural network, but by a special vascular system. Capillaries of the primary plexus at the base of the hypothalamus, the median eminence, recombine to form the hypothalamo-pituitary portal vessels. These portal vessels pass down the infundibulum and enter the anterior pituitary where they form a second capillary bed, the anterior pituitary capillaries. This blood vessel system is known as the hypothalamo-pituitary portal system, which ensures that blood from the hypothalamus flows directly to the anterior pituitary [1].

The posterior pituitary secretes two hormones, vasopressin, also known as antidiuretic hormone, and oxytocin. Vasopressin is synthesised in the cell bodies of the supraoptic nucleus, while oxytocin is synthesised in the cell bodies of the paraventricular nucleus of the hypothalamus. Both hormones travel down their respective axons through the infundibulum to the posterior pituitary, where they are stored in small vesicles. The release of these hormones by exocytosis is controlled triggered by the depolarisation of the axons [1,12]. Vasopressin and oxytocin are released into the posterior pituitary capillaries, which drain directly into the main blood stream. Vasopressin increases the permeability of the collecting ducts in the kidney, facilitating the re-uptake of water. Oxytocin acts on the smooth muscles of the breast and uterus to increase contraction [1].

Anterior pituitary function is regulated by six hypophysiotrophic hormones which are secreted by various neurons from the hypothalamus that terminate in the median eminence and deliver their hormones to the primary plexus. These hormones are: corticotropin releasing hormone (CRH); thyrotropin releasing hormone (TRH); GHRH; growth hormone-inhibiting hormone (GIH) or SS; gonadotropin releasing hormone (GnRH); and prolactin-inhibiting hormone (PIH), also called dopamine. These hypophysiotrophic hormones reach the anterior pituitary by the hypothalamo-pituitary

portal system and control the production and secretion of trophic hormones in the anterior pituitary before reaching the main blood stream.

The anterior pituitary hormones are produced by five different secretory cell types: the somatotrophs, mammotrophs, corticotrophs, thyrotrophs and gonadotrophs. Somatotrophs are responsible for GH secretion and make up more than 50% of the cells in the anterior pituitary. They are stimulated by GHRH and inhibited by GIH. GH facilitates growth and regulates protein, carbohydrate and lipid metabolism. Mammotrophs secrete prolactin and comprise up to 20 % of the anterior pituitary. Prolactin secretion is inhibited by PIH. Prolactin stimulates breast growth and milk synthesis in females and may be permissive to certain reproductive functions in the males. Corticotrophs constitute about 20% of the anterior pituitary and secrete ACTH in response to CRH. ACTH is a polypeptide that is cleaved from a larger polypeptide known as pro-opiomelanocortin (POMC). Lipotropins, which are involved in lipid metabolism, and endorphins, which are endogenous opioids, are also derived from POMC and can be secreted in small amounts together with ACTH. ACTH primarily stimulates the release of the glucocorticoids, but also mineralocorticoids and androgens (with the exception of DHEAS), from the adrenal cortex. Thyrotrophs make up to 5 % of the anterior pituitary and secrete thyrotrophin (TSH) in response to TRH. TSH, in turn, stimulates the release of thyroid hormone from the thyroid gland. Gonadotrophs constitute the remaining 5% of the anterior pituitary and secrete follicle stimulating hormone (FSH) and luteinizing hormone (LH) in response to GnRH. Both FSH and LH facilitate gamete production and stimulate the release of androgens and estrogens from the gonads [1, 12].

2.5.3 The adrenal

ACTH is the principal hormone from the anterior pituitary that stimulates adrenal steroidogenesis. Although, β-lipoprotein, secreted with ACTH, has been shown to augment the action of ACTH. As discussed previously, ACTH stimulates the delivery of cholesterol to the adrenocortical cells by the upregulation of SR-BI and the LDL receptor [71,74]. Furthermore, ACTH promotes the delivery of cholesterol to the inner mitochondrial membrane, the site of CYP11A1, as will be discussed in chapter 3. Therefore, by increasing the availability of cholesterol, ACTH stimulation results in an increase in the steroidogenic output of all three zones of the adrenal cortex. These

effects are, however, limited. Only the production and secretion of the glucocorticoids are significantly increased by ACTH, as ACTH results in an increased expression of CYP11A1, CYP17, CYP11B1 and CYP21 in the zona fasciculata. The expression of CYP11B2 in the zona glomerulosa is not affected by ACTH, but controlled primarily by the renin-angiotensin system [3].

2.5.3.1 Mechanism of ACTH action

ACTH primarily stimulates the secretion of the glucocorticoids, but also the mineralocorticoids and androgens from the adrenocortical cells, upon binding to the ACTH receptor. The ACTH receptor is mainly expressed in the adrenal cortex and is a member of the superfamily of G-protein coupled receptors with seven transmembrane domains. The ACTH receptor belongs to the melanocortin receptor subfamily, which is characterised by: short N-terminal extracellular domains; short intracellular C-terminal domains; and short fourth and fifth transmembrane domains [79]. This transmembrane hormone receptor is associated with a trimeric signal-transducing G protein on the cytoplasmic side of the cellular membrane. The trimeric G-protein consists of α, β and γ subunits. When no ligand is bound to the ACTH receptor, the α subunit is bound to GDP and complexed with the β and γ subunits. Binding of ACTH to the receptor causes a conformational change resulting in the displacement of GDP by GTP in the α subunit. The α subunit dissociates from the β and γ subunits and subsequently associates with adenylate cyclase, which is bound to the inner cell membrane. Adenylate cyclase is activated by the binding of the α subunit and catalyses the conversion of ATP to cAMP. The α subunit has intrinsic GTPase activity and once the bound GTP is hydrolysed to GDP, the α subunit dissociates from adenylate cyclase and relocates to the β and γ subunits. This activation cycle continues while ACTH is bound to the receptor and is shown in figure 2.10. The displacement of GDP by GTP in the α subunit upon ACTH binding causes a decrease in receptor affinity for ACTH that may result in the dissociation of ligand from the receptor [80].

The cAMP produced by adenylate cyclase acts as a second messenger by inducing changes in various metabolic pathways by first binding to and activating cAMP-dependent protein kinase (PKA). Activated PKA can phosphorylate a number of enzymes at specific serine and threonine residues, resulting in a change in their catalytic

activity. The action of cAMP is terminated by its eventual conversion to noncyclic AMP by phosphodiesterase [1].

In the adrenocortical cells, the ACTH induced cAMP and PKA result in a number of effects, which lead to increased steroidogenesis and the secretion of the steroid hormones. These effects are discussed in terms of cholesterol availability and the acute and chronic regulation of CYP11A1 during the following chapter.

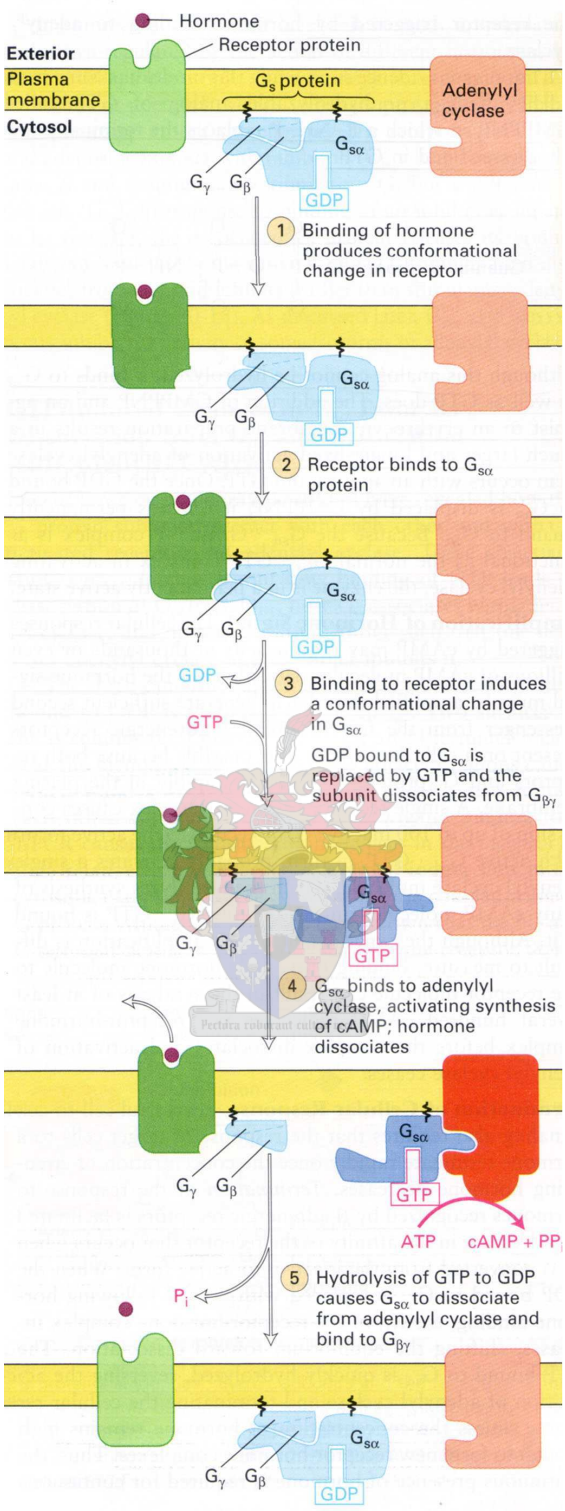

Figure 2.10. Graphic presentation of the ACTH receptor activation cycle. Reproduced from [80].

2.5.3.2 The HPA negative feedback loop

An important facet of ACTH secretion is the control exerted by the glucocorticoids themselves. The glucocorticoids produced by the zona fasciculata and zona reticularis, in response to ACTH stimulation, have a negative feedback effect on the hypothalamus and pituitary. Rising glucocorticoid levels suppress the release of CRH and ACTH by the hypothalamus and anterior pituitary, respectively. This effect is achieved through negative feedback acting on both the release and synthesis of ACTH and CRH. In the anterior pituitary the glucocorticoids inhibit the transcription of POMC [81]. In addition, ACTH itself downregulates CRH secretion from the hypothalamus, forming a short negative feedback loop [77]. Feedback inhibition is principally mediated by the GR. The negative feedback loops are illustrated in figure 2.11. The circadian rhythm of basal ACTH secretion is characterised by highest levels upon waking, with a decline in these levels throughout the day, reaching their minimum in the evening. The negative feedback of basal activity in the HPA axis is also subject to circadian rhythms, as it requires less glucocorticoid at the trough than at the peak of diurnal rhythm [82].

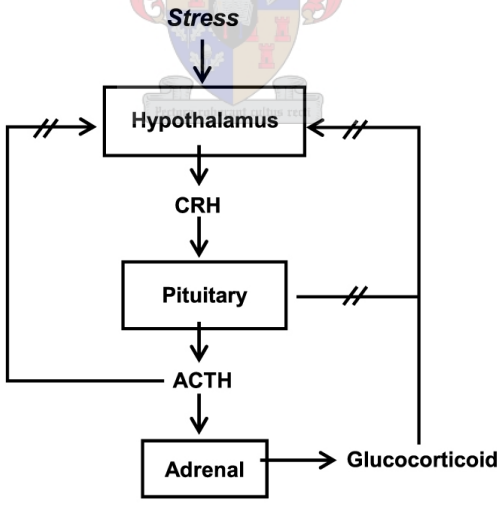

Figure 2.11. Schematic representation of HPA axis regulation. Reproduced from [77].

2.6 Intra-adrenal regulatory mechanisms

2.6.1 Interaction between the adrenal medulla and cortex

Although adrenal steroidogenesis is primarily regulated by the HPA axis and the renin-angiotensin system [12], other regulatory mechanisms have been shown to exist. Diurnal variation in adrenal steroidogenesis persists in CRH knockout mice [83], and steroidogenesis can be stimulated independently of the HPA axis in isolated perfused adrenal glands with intact splanchnic innervation [84].

As mentioned earlier in this chapter, the adrenal is fundamentally arranged into the cortex and medulla. Medullary chromaffin cells are, however, found dispersed in all three zones of the adult adrenal cortex. The catecholamines epinephrine and norepinephrine are secreted by chromaffin cells in response to stimulation by the splanchnic nerve [13]. These catecholamines stimulate the secretion of cortisol, aldosterone and androstenedione in isolated perfused adrenal glands [84]. Splanchnic nerve stimulation also enhances the adrenocortical secretion of glucocorticoids in response to ACTH stimulation [85]. Sectioning of the splanchnic nerve decreases the adrenal response to ACTH [86]. Furthermore, the catecholamines have a long term effect on steroidogenesis in isolated adrenocortical cells, involving the transcriptional upregulation of steroidogenic enzymes [87].

In addition to the catecholamines, chromaffin cells produce, store and secrete many other neuropeptides, which stimulate and inhibit adrenocortical function. Pituitary adenylate-cyclase activating peptide, vasoactive intestinal peptide (VIP), substance P, adrenomedullin and neuropeptides P (NPY) have been shown to be stimulatory, while atrial natriuretic peptide, SS, dynorphin and enkephalins have been shown to be inhibitory to adrenocortical function. Atrial natriuretic peptide and SS preferentially reduce the release of mineralocorticoids by the zona glomerulosa [13]. The importance of these neuropeptides as paracrine agents has been demonstrated in coculture systems of bovine adrenomedullary chromaffin cells with bovine adrenocortical cells, as shown in figure 2.12.

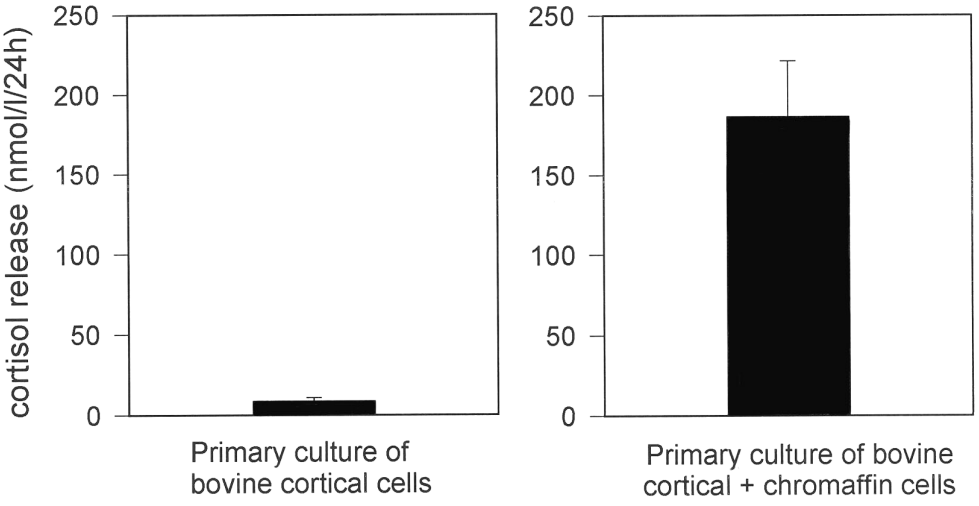

Figure 2.12. Cortisol release from primary cell cultures of bovine cortical cells alone (left) and mixed with bovine chromaffin cells (right). Reproduced from [13].

Different populations of chromaffin cells exist in the medulla, varying in their neuropeptide composition and effect on adrenocortical steroidogenesis. Independent mechanisms, characterised by different second messenger pathways, exist and differentially regulate the release of neuropeptides from the different populations of chromaffin cells [88]. Humoral and immune factors, from either intra-adrenal or extra-adrenal origin, can act to stimulate the release of neuropeptides from the chromaffin cells. For example, interleukin-1α and tumor necrosis factor-α differentially regulate Met-enkephalin, VIP, neurotensin and substance P biosynthesis in chromaffin cells [89]. These cytokines are also produced locally by adrenocortical cells and may complete an adrenal regulatory circuit. The cortex may release cytokines, which influence the composition of the neuropeptides secreted by the chromaffin cells, subsequently influencing adrenocortical steroidogenesis [13].

Although the adrenal cortex contains many adrenomedullary chromaffin cells, only a small percentage of the adrenocortical cells lie in direct contact with chromaffin cells. Gap junctions, which allow small, water-soluble molecules to pass directly from the cytoplasm of one cell to the next, are found in all three zones of the adrenal cortex. [90]. Furthermore, gap junctions are induced rapidly after ACTH stimulation, suggesting a specific response to hormonal stimulation. The presence of gap junctions would permit paracrine signals from a chromaffin cell to pass from one adrenocortical cell to the next.

2.6.2 Innervation of the adrenal cortex

The neural regulation of adrenal steroidogenesis is complex and not well understood. Although the classic view of adrenal anatomy is that the nerve supply to the adrenal medulla passes directly through the cortex without branching or synapsing, it is now generally accepted that the adrenal cortex receives a rich nerve supply [13,91]. Nerve endings terminating in the adrenal cortex originate from two different sources – some have their cell bodies outside the adrenal gland and reach the cortex together with blood vessels, while others originate from cell bodies in the medulla and may be regulated by splanchnic nerve activity [92]. A large number of neurotransmitters, including catecholamines and acetylcholine, have been identified in nerves innervating the adrenal cortex. Intrinsic adrenal peptidergic nerves containing VIP, calcitonin gene-related peptide (CGRP), substance P and neuropeptide Y have also been described [93-95].

There is some evidence for the regulation of adrenocortical function in the absence of splanchnic nerve stimulation. For example, VIP release in the adrenal is stimulated either by a high potassium [92] or low sodium diet [96]. The intrinsic neuropeptides may therefore regulate adrenocortical function in response to the electrolyte balance of the animal [13]. The neural control of the adrenal cortex is therefore at least partly derived from the splanchnic nerve, but may also regulate adrenocortical function by monitoring the physiological status of the animal. The role of adrenocortical innervation is probably best seen as fine tuning the steroidogenic function of the adrenal cortex [13].

2.6.3 Regulation of adrenal blood flow

The blood supply to the adrenal gland is extensive and was previously addressed in section 2.1.2. The rate of blood flow through the adrenal gland is regulated by a number of different neural and hormonal mechanisms. Adrenal blood flow is stimulated by depolarisation of the splanchnic nerves and may be mediated by a number of neuropeptides [85,97]: VIP, Met-enkephalin and CGRP cause vasodilation; while NPY causes vasoconstriction. Still other neuropeptides, including substance P, neurotensin and Leu-enkephalin have no significant vascular effects [98,99].

It is well known that ACTH stimulates increased adrenal blood flow. ACTH administration to isolated perfused rat adrenals results in an overall increase in flow rate through decreased vascular resistance within the gland [100]. The vascular effects of ACTH are believed to be mediated by neurotransmitters, histamine and 5-HT, which are released by mast cells in response to ACTH. Mast cells are present in the adrenal capsule, particularly in regions where the adrenal arteries enter the capsule [101, 102].

It has been proposed that increased blood flow to the adrenal gland causes an increase in the rate of presentation of ACTH to the adrenocortical cells, which in turn results in an increased steroidogenic output by the cells [103]. However, in isolated perfused rat adrenal, there is an increase in glucocorticoid secretion in the absence of ACTH when flow is increased mechanically or by the use of vasodilators. This effect is unique to the intact gland and it has been postulated that it may be mediated by an element present in the intact gland that is lost when the cells are dispersed [100]. Therefore, this effect could be modulated by a compound released from the vascular epithelium.

The vascularisation of the adrenal cortex creates an optimal environment for the vascular endothelial cells to exert paracrine actions on the adrenocortical cells, as almost every adrenocortical cell is directly adjacent to a vascular endothelial cell. Secretory products of the vascular epithelium, nitric oxide, endothelin-1 and adrenomedullin, have all been implicated in the local regulation of adrenal blood flow [13]. In addition to its effect on adrenal vascular regulation, endothelin-1 has been shown to stimulate aldosterone secretion in several species, including the human [104]. Nitric oxide has been implicated in maintaining basal levels of adrenal steroidogenesis, as basal levels of steroid output are significantly lower in the absence of endogenous nitric oxide synthesis [105]. Adrenomedullin modulates aldosterone secretion, but there is some disagreement in the literature as to whether it stimulates or inhibits aldosterone secretion [13].

The regulation of adrenal blood flow is therefore complex, and there is a close relationship between vascular events and steroid secretion, which seems to be mediated by the vascular epithelium in a paracrine manner.

2.6.4 The intraadrenal CRH/ACTH system

As was previously discussed in section 2.5, adrenocortical function is regulated primarily by the HPA axis. CRH and ACTH, the key regulatory hormones in the HPA axis, are not only produced by the hypothalamus and anterior pituitary, but also by the adrenal gland itself. Evidence has been provided showing that the intra-adrenal CRH/ACTH system influences adrenocortical steroidogenesis independently of the HPA axis [13].

High doses of CRH had a trophic effect on the adrenal cortex of hypophysectomized rats [106]. CRH also enhanced adrenal responsiveness to ACTH stimulation in a dose dependent manner [107] and was found to stimulate cortisol secretion in healthy humans [108]. The perfusion rate in isolated perfused adrenal glands was increased by CRH and ACTH together, while neither CRH nor ACTH alone had an effect on the perfusion rate, suggesting that the CRH-enhanced adrenal response to ACTH may result from a synergistic action on adrenal blood flow [107].

CRH-enhanced glucocorticoid secretion by rat adrenal slices requires the presence of chromaffin cells, suggesting the involvement of the medulla in the intra-adrenal CRH/ACTH system. This stimulatory effect of CRH was blocked by corticotropin-inhibiting peptide, indicating the involvement of ACTH and that the adrenal medulla is the source of extrapituitary ACTH. Furthermore, chromaffin cells were shown to secrete ACTH in response to high concentrations of CRH [109,110]. Secretion of CRH by chromaffin cells was found to be stimulated by a number of physiological stimuli, including potassium induced depolarisation, splanchnic nerve stimulation and numerous neuropeptides [13].

Similarly to the HPA axis, regulation of the intraadrenal CRH/ACTH system is achieved by negative feedback through ACTH and the glucocorticoids [13]. This system is believed to be of great importance in regulating adrenocortical function.

It may be concluded that the regulation of adrenal steroidogenesis is a highly complex system, which includes: the zonation of the adrenal cortex; the blood flow to the adrenal cortex; the availability of cholesterol for steroidogenesis; the HPA axis; and intra-adrenal regulatory mechanisms. However, the conversion of cholesterol to pregnenolone, the universal precursor to all steroid hormones, is the first committed step to steroidogenic biosynthesis in the adrenal cortex. The regulation of this reaction, which is catalysed by CYP11A1, is therefore critical to adrenal steroidogenesis. The

following chapter will therefore discuss the regulation of this key enzyme in the steroidogenic pathway. The physiological importance, reaction mechanism and characterisation of CYP11A1 will also be discussed.

CHAPTER 3

AN INTRODUCTION TO CYTOCHROME P450 SIDE-CHAIN CLEAVAGE (CYP11A1)

3.1 Regulation of CYP11A1

As discussed in the previous chapter, ACTH stimulates the adrenal cortex to secrete primarily glucocorticoids, but also mineralocorticoids and androgens. Both acute and chronic regulatory effects result from ACTH stimulation. Acute effects occur within a matter of minutes, while chronic effects occur after a few hours, involving increased gene transcription and translation of the appropriate steroidogenic enzymes [111-114].

The conversion of cholesterol to pregnenolone by CYP11A1 is the first step in steroidogenesis. As pregnenolone is the precursor to all steroid hormones, the regulation of CYP11A1 is essencial to the regulation of all steroidogenesis. This section will therefore focus on the acute and chronic regulation of CYP11A1.

3.1.1 Acute regulation of CYP11A1

It is the availability of the cholesterol substrate that forms the critical point in the regulation of CYP11A1 activity. As discussed previously in chapter 2, the adrenal cortex is a highly vascular tissue and contains significantly high levels of lipoprotein receptors, readily providing it access to dietary cholesterol [114]. This allows the adrenocortical cells to maintain CE stores in lipid droplets which are abundant in the cytoplasm of adrenocortical cells [12]. In the adrenal cortex, steroidogenesis is acutely regulated by ACTH stimulation, which acts by elevating cAMP levels and activating PKA [12]. Increased cholesterol metabolism is observed in adrenocortical cells within 3 minutes of ACTH treatment and peaks after 10-15 minutes. Defects in either PKA or G protein coupling, preventing cAMP formation, abolish this response. In the adrenal cortex: cAMP elevates the expression of the LDL receptor and SR-BI; promotes cholesterol delivery from the plasma membrane and the late endosomes to the mitochondria; and stimulates cholesterol esterase activity, while inhibiting ACAT1. These events favour the release of cholesterol from stored CE's and its accumulation in the outer mitochondrial membrane [114]. Another response to ACTH stimulation is the

cAMP-dependent dephosphorylation of the cytoskeleton-associated protein paxillin, which is a component of the focal adhesion complex [115]. The dephosphorylation of paxillin is proposed to be involved in a change in cytoskeleton organisation that results in the pronounced rounding of steroidogenic cells within 5 minutes of ACTH stimulation [113-115]. The reorganisation of the cytoskeleton causes the clustering of the steroidogenic organelles bringing the mitochondria in close contact with CE pools [116]. Inhibitors that block paxillin dephosphorylation also inhibit the acute regulation of CYP11A1 activity [115].

ACTH also stimulates endothelin production and acute stimulation of blood flow to the adrenal and enhances the extracellular access of cholesterol and oxygen, the co-substrate of all cytochromes P450, to CYP11A1 [12]. The proposed routes through which cholesterol can reach the mitochondria are shown in figure 3.1.

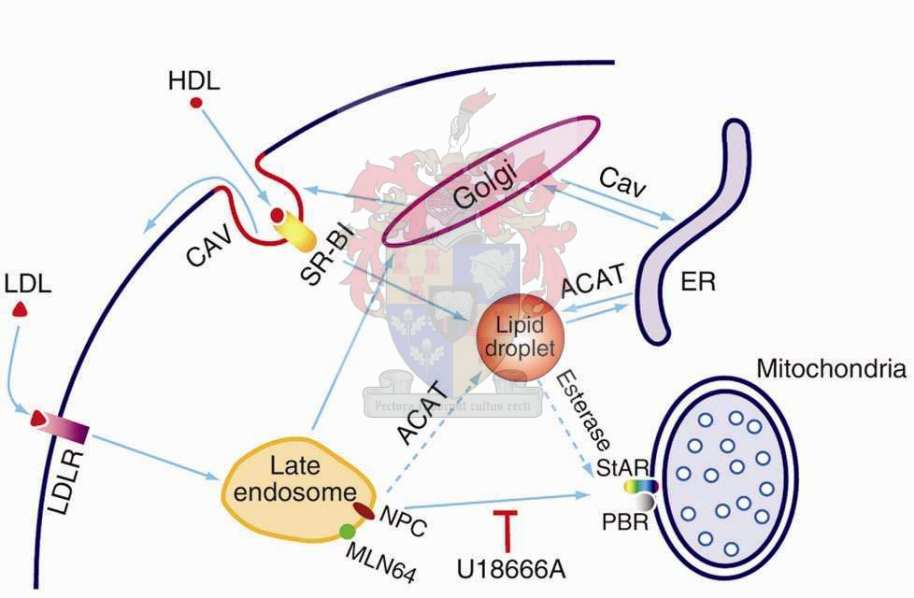

Figure 3.1. Mechanisms of cholesterol transport to the mitochondria. Cholesterol is taken up from both LDL receptors and apoA/HDL receptors (SR-BI) in caveolin-rich domains (CAV). Late endosomes mediate the transfer to the mitochondria via the activities of NPC-1 (inhibited by U18666A) and possibly the StAR-like protein MLN64. Acyl-CoA:cholesterol acyltransferase (ACAT) converts free cholesterol to the CE's that are stored in the lipid droplets. Reproduced from [114].

3.1.1.1 The role of StAR

Once delivered to the mitochondria, the only remaining barrier for the delivery of cholesterol to the inner mitochondrial membrane and CYP11A1 is the aqueous space between the outer and inner mitochondrial membranes [113]. As the aqueous diffusion

of cholesterol is slow and CYP11A1 metabolises relatively soluble hydroxycholesterols in the absence of ACTH stimulation, it was proposed that the acute effects of cAMP and PKA are mediated by StAR, which is required for the transfer of cholesterol from the outer to the inner mitochondrial membrane [111-114,117-119]. StAR is expressed as a 37-kDa preprotein known as p37 and contains a 68 amino acid mitochondrial targeting presequence, which is cleaved upon mitochondrial uptake to yield the 30-kDa mature protein known as p30. ACTH stimulation results in PKA-dependent phosphorylation of the p37 protein to yield phosphorylated p30 protein (pp30) upon mitochondrial processing [114]. Some steroidogenic cells are regulated by hormones other than ACTH and require other pathways to activate StAR. For example, glomerulosa cells, which produce the mineralocorticoid aldosterone, are regulated by renin-angiotensin system [111]. Angiotensin II activates the PKC pathway and increases intracellular levels of calcium. StAR responds to the increased calcium levels as it contains consensus sequences for PKA and calmodulin-dependent kinase [120].

The mechanism of action of StAR is not yet fully understood. There has been some debate as to whether the phosphorylated p37 protein (pp37) or pp30 is the active form of StAR, and if StAR acts on the outer or inner mitochondrial membrane. Early models suggested that cholesterol transfer from the outer to the inner mitochondrial membrane occurs during the processing and import of StAR, which results in contact sites being formed between the two membranes, and that pp30 StAR, which is associated with the inner mitochondrial membrane or the mitochondrial matrix, is inactive [113]. However, deletion of the N-terminal targeting sequence, which directs the StAR to TOM20, the receptor in the outer mitochondrial membrane where it is cleaved and imported to the inner mitochondrial membrane, does not diminish the steroidogenic enhancing activity of StAR in COS-1 cells [121,122]. In addition, chimeric StAR bound TOM20 effectively activated cholesterol metabolism in isolated basal steroidogenic MA10 mitochondria [121]. Tuckey et al. have shown that StAR can mediate the transfer of cholesterol between synthetic membranes without other protein components found in mitochondria [123]. This evidence suggests that StAR functions at the outer mitochondrial membrane and remains active in the absence of its N-terminal mitochondrial targeting sequence.

Recently a more complex model has been proposed and shows that the activity of StAR, necessary for high cholesterol trafficking, may involve StAR processing as well as other protein factors. Jefcoate et al. have questioned the relevance of the models used

to determine StAR activity, as COS-1 cells are insensitive to changes in the level of StAR expression and process p37 to pp30 at a much slower rate than adrenal cells [114]. During peak cholesterol metabolism in steroidogenic MA10 cells, p37 is scarcely detectable. Furthermore, inhibitors of mitochondrial proteases and protein uptake, which block pp30 formation, prevent the activation of cholesterol metabolism in MA10 cells. However, cholesterol metabolism is unaffected when sufficient pp30 was generated, demonstrating the importance of pp30 in cholesterol transport [124]. It is estimated that each molecule of pp30 mediates the transfer of 400 cholesterol molecules per minute, while Tuckey et al. showed a stoichiometry of 2.8 molecules of cholesterol per molecule of StAR [123] This suggests that p37 may well have activity at the outer mitochondrial membrane, but that it is the processed pp30 form that is crucial for cholesterol uptake for steroidogenesis in the inner mitochondrial membrane. The conversion of newly synthesised p37 to pp30 reaches steady state between formation and processing within 5 minutes. This is consistent with the time frame for acute regulation of CYP11A1 activity by ACTH. Although cAMP has no measurable effect on these rates, maximal stimulation may ensure near-complete conversion by the phosphorylation of extramitochondrial p37 to pp37 [114]. Although StAR transcription is also elevated in response to cAMP, it has been suggested that newly synthesised StAR arises from the translation of pre-existing stable mRNA in the cytoplasm and not from transcription. [112,114].

StAR is believed to partially denature as it moves through the mitochondrial membranes and then refold after cleavage in the matrix to generate pp30 [114]. Assisted by HSP70, which continuously acts on StAR as it enters the mitochondrial matrix, StAR adopts a molten globule structure and associates with the inner mitochondrial membrane [125]. In nonsteroidogenic cells, cholesterol is largely excluded from the inner mitochondrial membrane as it can be detrimental to the activity of mitochondrial proteins involved in cellular respiration [114]. The inner mitochondrial membrane of adrenal cells is extensive and vesiculated, with limited direct contact with the outer mitochondrial membrane [12,114]. This implies a further role of StAR in the distribution on cholesterol to locations that are well removed from the outer mitochondrial membrane. Here StAR facilitates the transfer of cholesterol from the cholesterol rich domains in the outer mitochondrial membrane to the inner mitochondrial membrane, including regions that are far removed from the outer membrane and possible matrix vesicles which contain CYP11A1 [114].

3.1.1.2 The role of the peripheral benzodiazepine receptor in StAR activity

The peripheral benzodiazepine receptor (PBR), which is located in the outer mitochondrial membrane of most mitochondria and is elevated in steroidogenic cells, has been implicated in mitochondrial cholesterol uptake and linked to the activity of StAR [113,114]. PBR is associated with a member of the porin protein family in the outer mitochondrial membrane. When PBR is activated by the adrenal acyl-CoA-binding protein and other agonists, the structure of the porin is altered and a number of mitochondrial functions are affected [114]. PBR stimulation has also been linked to an increase in cholesterol metabolism in steroidogenic cells, while PBR antagonists inhibit mitochondrial cholesterol transport in the presence of cAMP [126]. Furthermore, cholesterol metabolism is severely impaired in cells where PBR has been deleted, but can be restored by transfection of the cells with PBR constructs [114].

In steroidogenic cells, PBR-associated protein 7 (PAP7) has been shown to bind both PBR and PKA, forming a multiprotein complex leading to the phosphorylation of p37, possibly mediating the interaction between PBR and StAR [114,127]. In MA10 cells the suppression of PAP7, using antisense technology, prevents the cAMP-dependent stimulation of steroidogenesis [114]. PAP7 is therefore believed to link PKA to PBR and facilitate the phosphorylation of StAR during its mitochondrial uptake. Interestingly, upon agonist binding to PBR, the cholesterol in the outer mitochondrial membrane aggregates around PBR providing high local concentrations of cholesterol in areas of the outer mitochondrial membrane directly opposite the site of StAR uptake in the inner mitochondrial membrane. The proposed model for the role of PBR and PAP7 in the mitochondrial import of StAR is shown in figure 3.2.

Fatty acyl-CoA's formed during the hydrolysis of CE's are able to bind to the acyl-CoA-binding protein, which is responsible for activating PBR, resulting in the interaction of fatty acyl-CoA near StAR [126]. This may promote the translocation of the fatty acyl-CoA's to the inner mitochondrial membrane [114]. A mitochondrial thioesterase hydrolyses acyl-CoA to release fatty acids and may be an essential mechanism to maintain membrane fluidity in the presence of high levels of cholesterol [128]. These free fatty acids may promote the interaction of cholesterol with StAR and CYP11A1 and are discussed later in this chapter.

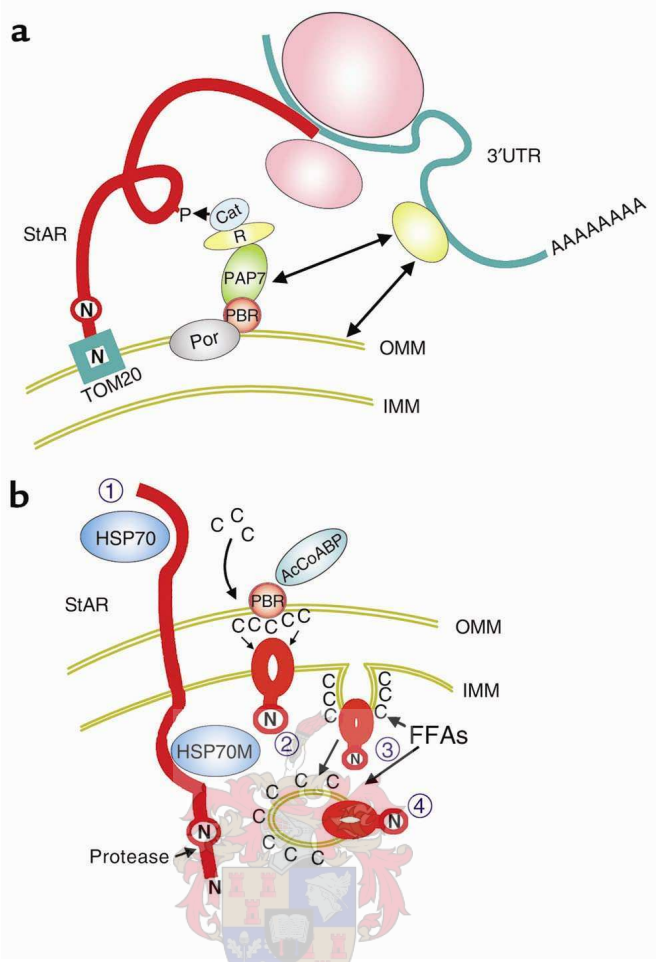

Figure 3.2. Model for cholesterol transfer into the mitochondrion mediated by StAR. 'N' indicates the N-terminal of p37, while the circled 'N' indicates the N-terminal of p30. (A) The N-terminal of newly synthesized p37 becomes associated with the outer mitochondrial membrane surface protein TOM20. Phosphorylation of p37 by the catalytic unit of PKA (Cat) is facilitated by the interaction of the regulatory subunit (R) with the adaptor protein PAP7. PAP7 binds in turn to PBR in the outer mitochondrial membrane, which is partnered with porin (Por). Possible interactions between the StAR 3'-untranslated region (3'UTR) and the outer mitochondrial membrane proteins may also target StAR to the mitochondrion. (B) In step 1 following the phosphorylation of p37 and interaction with TOM20, pp37 is denatured with the help of the cytosolic HSP70 complex and transported across the outer and inner mitochondrial membranes. This process is assisted by HSP70 protein complexes in the mitochondrial matrix (HSP70M). A mitochondrial protease cleaves pp37 to yield pp30, which is then integrated into the inner mitochondrial membrane. In step 2, cholesterol (C) is transferred to pp30 from domains in the outer membrane formed by PBR, which is activated by acyl-CoA-binding protein (AcCoABP). In step 3, activated inner membrane domains accept the transfer of free fatty acids (FFA) and cholesterol from the cholesterol rich domains in the outer membrane. AcCoABP may also facilitate the transfer of acyl-CoA to the inner mitochondrial membrane, where mitochondrial thioesterase hydrolyses acyl-CoA to FFA. In step 4, pp30 may facilitate the relocation of cholesterol to regions in the inner mitochondrial membrane that are far removed from the outer membrane, as well as possible matrix vesicles. Reproduced from [114].

3.1.2 Chronic regulation of CYP11A1

The chronic effects of CYP11A1 regulation take place after several hours in response to cAMP, which stimulates the expression of the CYP11A1 gene [77]. Expression of CYP11A1 reaches a plateau 6 hours after cAMP stimulation in adrenocortical Y1 cells and placental JEG-3 cells. Furthermore, this cAMP induction was sensitive to cycloheximide in JEG-3 cells, but not in Y1 cells, suggesting a cell type-selective mechanism of cAMP regulation of the expression of CYP11A1 as shown by Guo et al. [129]. *Cis*-acting elements conferring cAMP responsiveness, via interactions with specific transcription factors, have been identified in the CYP11A1 promoter [77]. The transcription factor, steroidogenic factor 1/Ad4-binding protein (SF1/Ad4BP, also known as NR5A1) [130,131], is critical in mediating the cAMP response in all studied species of CYP11A1 [77]. SF1 belongs to the orphan nuclear receptor family and binds variants of an AGGTCA sequence motif found in the proximal promoter of all steroidogenic cytochromes P450 [132]. In humans the expression of CYP11A1 is controlled by SF1 interacting with adjacent factors like CRE and Sp1 [133-136]. The human CYP11A1 promoter contains: two adrenal-specific enhancers in -1900/-1840; an upstream cAMP-response element (U-CRS) at -1640/-1540; a negative controlling region at -600/-350; and a basal promoter within 120bp from the transcriptional start, as shown in figure 3.3 [77,134,137]. The proximal basal promoter contains 3 *cis*-acting elements, which include Sp1, SF1 and a TATA box [138,133]. While the basal promoter is functional in both Y1 and JEG-3 cells, the U-CRS is only functional in adrenocortical Y1 cells [129,134], indicative of the important role played by the U-CRS in the regulation of adrenal-specific CPY11A1 expression [77].

The U-CRS contains three protein-binding sites C1, U and C2, and specific protein-DNA complexes formed on this region are significantly enhanced by cAMP stimulation [139,140]. Furthermore, it has been shown that U binds to the steroidogenic transcription factor SF1 and that C1 and C2 bind to AP-1 proteins. Mutations directed to U and/or C1/C2 demonstrated that the SF1 site is the main site for cAMP induction, but that the cooperation of all three elements is important for maximal cAMP response in Y1 cells [77].

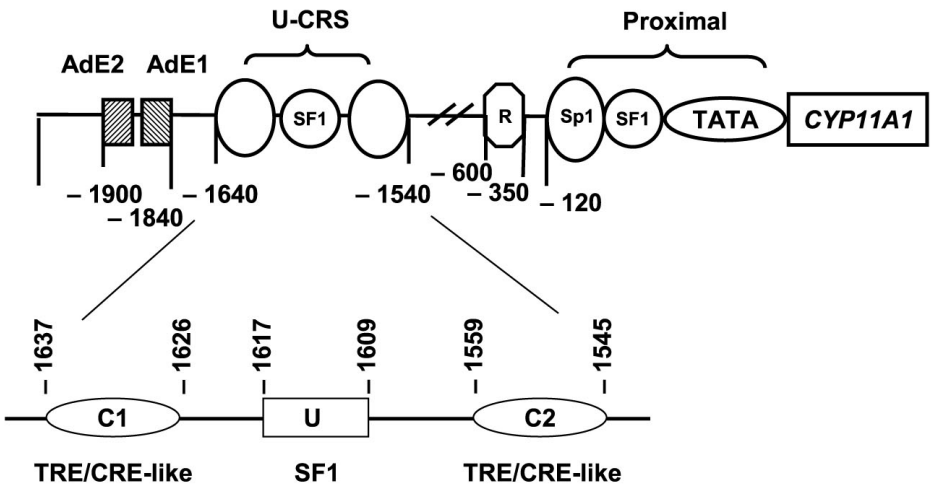

Figure 3.3. Map of *cis*-elements located within the human CYP11A1 promoter region. The proximal promoter containing Sp1, SF1 and TATA sites is within 120 bp upstream of the transcription start site. Two adrenal-specific enhancers lie within -1900/-1840, an upstream cAMP-response element (U-CRS) is located within -1640/-1540, and a negative controlling region is found at -600/-350. Reproduced from [77].

SF1 is an essential transcription factor in adrenal and gonadal expression of all steroidogenic enzymes [141]. To elucidate the role of the two SF1 sites in the human CYP11A1 promoter, Hu et al. mutated the sites individually, mtP (proximal, in the basal promoter), mtU (upstream, in U-CRS) and together (mt2X). The mutated promoters were fused to the LacZ reporter gene and transgenic mice created. The transgenic lines from both mtP and mtU had reduced reporter gene expression in the adrenal compared to those from the wild-type promoter [142]. No reporter activity was detected in the transgenic mice carrying the double mutant mt2X. One of the mtU lines, U4, retained appreciable amounts of reporter activity, but reporter gene expression was not stimulated by ACTH in the adrenal, demonstrating that the SP1 binding site in U-CRS is important for hormonal stimulation, while the SP1 binding site in the basal promoter is essential for basal transcription [77,142]. These results revealed that SF1 is important in both basal transcription as well as hormone-stimulated transcription [77]. Although SF1 phosphorylation has not been correlated with the cAMP response, the mutation of the AF-2 activation domain of SF1 suppresses the PKA-dependent transactivation of gene expression [143]. SF1 is known to interact with proteins such as c-Jun – resulting in enhanced transcription and possibly participating in the cAMP response through its interaction with the AP1 proteins that are also activated in response to cAMP [77,142].

A proposed DNA-protein-protein-DNA complex combined with the TATA-binding RNA polymerase complex II that initiates CYP11A1 transcription is shown in figure 3.4.

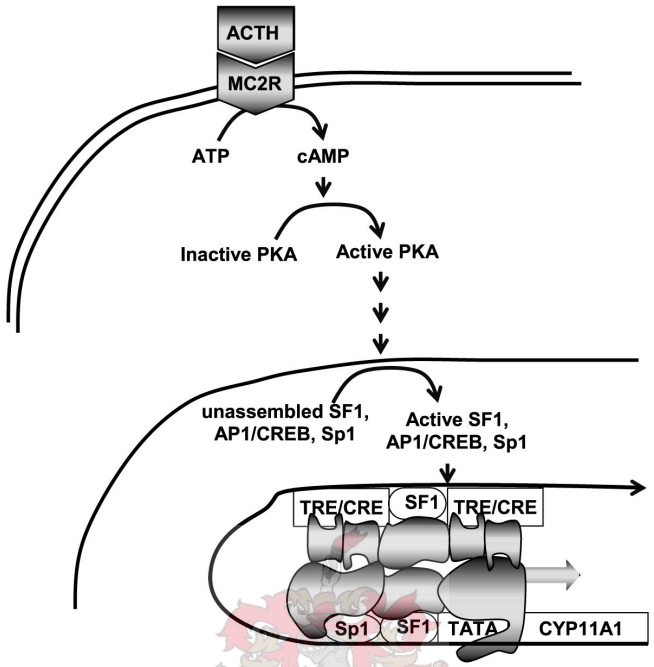

Figure 3.4. Regulation of the CYP11A1 promoter by the cAMP-PKA signalling pathway. Tropic hormones like ACTH bind to the appropriate G-protein coupled receptors such as MC2R and induce the production of cAMP. cAMP activates PKA and this signal activates several transcriptional factors such as SF1, AP1/CREB and Sp1 via several unclear steps. These activated transcriptional factors in turn bind their respective DNA-binding sites on the promoter region. A possible DNA-protein-protein-DNA complex that includes the TATA-binding RNA polymerase complex II is created and results in CYP11A1 transcription. Reproduced from [77].

3.2 The expression and physiological importance of CYP11A1 in steroidogenic tissue

3.2.1 CYP11A1 expression in steroidogenic tissue

CYP11A1 is expressed at all the major sites of steroidogenesis, namely the adrenal cortex, ovary, testis, and placenta [3]. CYP11A1 is expressed in all three zones

of the adrenal cortex [144,145]. In the ovary, CYP11A1 is expressed in the theca interna and the granulosa cells of ovulatory follicles [146]; while in the testis CYP11A1 is only expressed in the Leydig cells [147]. The synciotrophoblast cell is the site of CYP11A1 expression in the primate placenta [148]. In addition, CYP11A1 has been detected in the central and peripheral nervous system [149], skin [150] and heart [151,152].

Studies of the expression of steroidogenic enzymes in human fetal adrenal glands and gonads showed that between week 20 and 21, CYP11A1 is most abundant in the adrenal, followed by the testis and minor expression in the fetal ovaries [153]. Human adrenal glands express CYP11A1 between week 14 and 22 of gestation only in the fetal and transitional zones of the adrenal cortex. Expression in the definitive zone is only detectable after 23 weeks [154,155]. Expression of CYP11A1 occurs in all three zones of monkey adrenal cortex during late gestation [155]. Testicular expression of CYP11A1 shows a decrease from a maximum in week 15 to significantly lower levels by week 26 [153]. At the beginning of pubertal development, testicular expression of CYP11A1 decreases as the fetal population of Leydig cells disappears and the adult Leydig cell population develops in the human [156].

3.2.2 Physiological importance of CYP11A1

In humans expression of CYP11A1 is essential to normal physiological development due to its catalytic importance in the biosynthesis of all steroid hormones. Congenital lipoid adrenal hyperplasia (lipoid CAH) is a severe endocrine disorder that is characterised by a deficiency of all cholesterol derived hormones and leads to the accumulation of lipoids and cholesterol esters in steroidogenic tissue [157,158]. Lipoid CAH was previously misnamed 20,22 desmolase deficiency and thought to be caused by mutations in CYP11A1 [159,160]. This was strongly supported by Yang et al. who showed that rabbits that are homozygous for CYP11A1 gene deletions have a phenotype corresponding closely to lipoid CAH [161]. Lipoid CAH has subsequently been found to be caused primarily by mutations in StAR and not by deficiencies in CYP11A1 [162,163]. Since progesterone is required for the maintenance of mammalian pregnancy, [164] and CYP11A1 is the only enzyme able to convert cholesterol to pregnenolone, a progesterone precursor, a deficiency in CYP11A1 activity would result in uterine contractions with ensuing spontaneous abortions [165]. In the human, the maternal corpus luteum secretes progesterone during the first trimester; followed by a

luteoplacental shift to the production of progesterone by the syncytiotrophoblasts of the placenta, which are of fetal origin [166,167]. Fetuses carrying mutations in StAR, causing lipoid CAH, reach term as the placenta does not express StAR and produces progesterone by a StAR-independent process which possibly involves the StAR-like protein MLN-64 [165]. In the rabbit, the corpus luteum secretes progesterone throughout pregnancy, [167] which permits rabbits homozygous for CYP11A1 gene deletions to reach term without the placenta producing progesterone [165].

To date, only three patients have been diagnosed with lipoid CAH resulting from deficiencies in CYP11A1. Late-onset lipoid CAH, adrenal insufficiency and male to female sex reversal due to a heterozygous mutation for CYP11A1 was reported in a single case study. One CYP11A1 gene contained a six base pair in-frame insertion which impaired CYP11A1 activity [168]. In the second case study, compound heterozygous mutations in CYP11A1 resulted in late-onset lipoid CAH and severe adrenal insufficiency. One mutation found in this patient preserved partial enzyme activity and the patient was therefore able to synthesise low levels of steroids, resulting in a normal phenotype until adrenal insufficiency was diagnosed at seven months of age [169]. Recently, a third case study was reported, defying the paradigm that pregnancies with severe disruptions of CYP11A1 are incompatible with a full term in humans. A child carrying a homozygous single nucleotide deletion in CYP11A1 resulting in a premature termination codon at position 288 was born prematurely to healthy parents both heterozygous for this mutation. Lipoid CAH, severe adrenal insufficiency and male to female sex reversal were present from the first day of life. It was postulated that the maternal steroids contributed to the survival of the child. Although it could not be determined whether two previous miscarriages reported by the mother were due to affected pregnancies with homozygous CYP11A1 mutations, this single case study demonstrated that, in rare cases, homozygous disruption of CYP11A1 may be compatible with survival. Furthermore, it can be concluded that CYP11A1 deficiencies are inherited in an autosomal recessive fashion and heterozygous carriers can be healthy and fertile [170].

Partial defects in CYP11A1 have been shown to result in pseudohermaphroditism in genetic males and the lack of secondary sexual characteristics in genetic females [141]. Polymorphisms in the CYP11A1 locus have been linked to polycystic ovary syndrome, also known as Stein-Leventhal syndrome and hyperandrogenemia [171].

3.3 Catalytic activity of CYP11A1

As previously mentioned, CYP11A1 catalyses the first step in steroidogenesis, namely the conversion of cholesterol to pregnenolone [172]. This reaction consists of three consecutive monooxygenations, with each reaction requiring one molecule of oxygen and one molecule of NADPH [5,173,174], as shown in figure 3.5. Cholesterol is hydroxylated at the C22 position to yield 22(R)-hydroxycholesterol, which is subsequently hydroxylated at C20 yielding 20α,22(R)-dihydroxycholesterol, followed by cleavage between C22 and C20 during the final step, to yield pregnenolone and isocaproaldehyde [4,5]. Isocaproaldehyde is subsequently oxidised to isocaproic acid [175]. The accumulation of the intermediates is prevented by thermodynamic stabilisation of the enzyme-intermediate complex, as the CYP11A1 has a far greater affinity for 22(R)-hydroxycholesterol and 20α,22(R)-dihydroxycholesterol than it has for cholesterol [176].

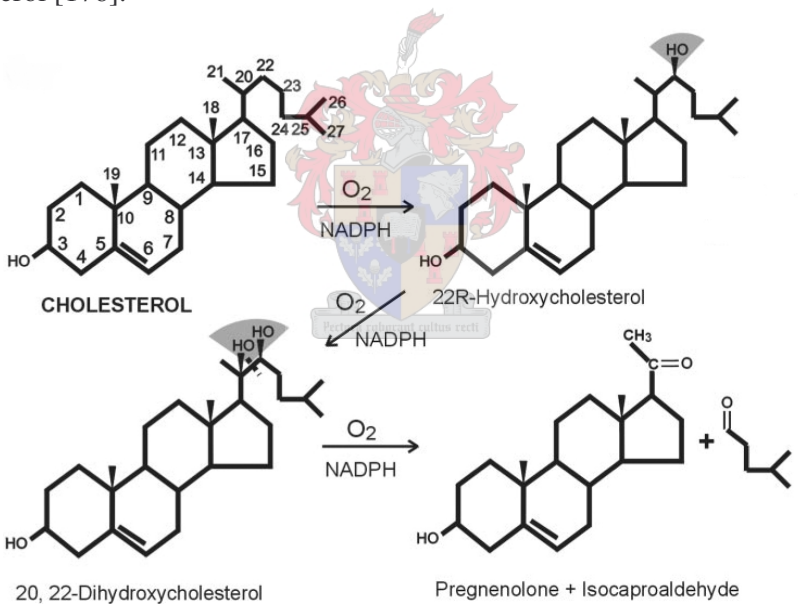

Figure 3.5. The three sequential oxidation reactions catalysed by CYP11A1 to yield pregnenolone from cholesterol. Each oxidation reaction requires one molecule of molecular oxygen and one molecule of NADPH. Reproduced from [3].

3.4 Electron transfer system

CYP11A1 is associated with the inner mitochondrial membrane on the matrix side [3]. The six electrons required for the side-chain cleavage of cholesterol are provided by NADPH via a mitochondrial electron transfer system, as shown in figure 3.6. This

system consists of: AdxR, a FAD-containing reductase; and Adx, a soluble, low molecular weight iron sulphur (Fe_2-S_2) ferredoxin-type electron transfer protein. AdxR is reduced by NADPH, which in turn reduces Adx. Adx acts as an electron shuttle between AdxR and CYP11A1 and other mitochondrial cytochromes P450 [177,178].

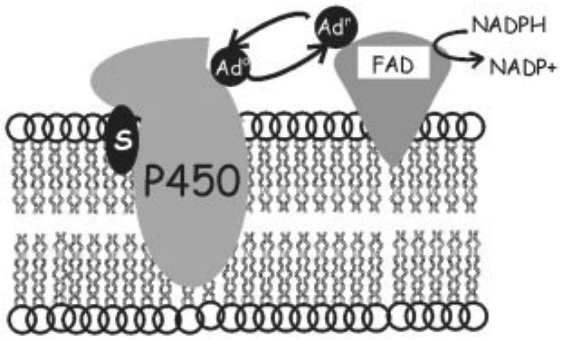

Figure 3.6. Schematic representation of the mitochondrial electron transport system. FAD, Flavin adenine dinucleotide; Ad^r, reduced adrenodoxin; Ad^o, oxidised adrenodoxin; S, substrate. Reproduced from [3].

Physical chemistry [179-183], site directed mutagenesis [184-187] and homology modelling studies have demonstrated that Adx interacts with CYP11A1 by electrostatic interactions. More specifically, negatively charged acidic residues in Adx interact with positively charged basic residues in CYP11A1 [3,177,178]. Using a homology model of CYP11A1 docked with the crystallised Adx molecule in combination with site-directed mutagenesis, Usanov et al. identified four salt bridges between bovine CYP11A1 and Adx: K267, K403, K405 and R426 of CYP11A1 with E47, D76 D72 and E73 of Adx, respectively. In their model, the loop domain around the iron-sulphur complex (FeS) of Adx is associated with the heme binding domain in CYP11A1, readily allowing electron transfer from Adx to CYP11A1 [178,188]. The binding of Adx to CYP11A1 via electrostatic interactions is well supported by Lambeth et al. who previously showed that CYP11A1 activity is minimal at low ionic strength, optimal at physiological ionic strength, and decreases at higher ionic strength. Adx was proposed to interact with CYP11A1 or AdxR via charge-charge interactions. At low ionic strength the stability of these interactions limited the ability of Adx to act as an electron shuttle. At high ionic strength a 'shielding' effect was proposed that limits the interaction of Adx with its redox partners, thereby limiting CYP11A1 activity [189].

While the conversion of cholesterol to pregnenolone is proposed to be the 'rate-limiting' step in steroidogenesis, the transfer of electrons to CYP11A1 by its redox

partners appears to be a limiting factor in CYP11A1 activity. Schiffler et al. were able to show that a S112W mutant of truncated Adx resulted in a 100-fold increase in the conversion of cholesterol to pregnenolone by CYP11A1 [190]. Tuckey et al. have shown that the limiting component for CYP11A1 activity in the human placenta is the concentration of AdxR in the mitochondria. Limited AdxR concentrations limit the reduction of the Adx pool to 30%. In addition to this limitation on CYP11A1 activity, it was found that oxidised Adx acts as a competitive inhibitor of CYP11A1, resulting in a further decrease in CYP11A1 activity [191]. In the human adrenal, three mitochondrial steroidogenic cytochromes P450, CYP11A1, CYP11B1 and CYP11B2, require electrons from the same electron transfer system. Cau and Bernhardt have shown that in addition to Adx levels limiting mitochondrial cytochrome P450 activities, these enzymes also compete for reduced Adx in COS-1 cells [192].

3.5 The role of the mitochondrial environment

In addition to CYP11A1 requiring a mitochondrion-specific electron transfer system, studies have shown that the enzyme requires the physiological milieu of the mitochondrion for activity. In steroidogenic cells, CYP11A1, AdxR and Adx are expressed as higher molecular weight precursors with amphipathic N-terminal presequences that target the enzymes to areas on the mitochondrial surface where the inner and outer membranes are in close proximity. These preproteins are subsequently translocated to the inner mitochondrial membrane, and the leader sequences are cleaved by specific peptidases found in the mitochondrial matrix, yielding the mature forms of CYP11A1, AdxR and Adx [193-196]. It has been shown that the mitochondria from bovine adrenal cortex and corpus luteum can to process the immature form of CYP11A1, while the mitochondria from bovine heart, liver and kidney cannot [195]. However, nonsteroidogenic COS-1 cells, which contain a mitochondrial cytochrome P450, are able to process CYP11A1 [197]. This suggests that only the mitochondria of steroidogenic tissues, or of those tissues expressing other mitochondrial cytochromes P450, have the necessary machinery required to process and include CYP11A1 into the mitochondrial membrane. Harikrishna et al. were able to engineer CYP11A1, AdxR and Adx into a single fusion protein which exhibited enhanced enzymatic activity when targeted to the mitochondria in COS-1 cells [198]. Using this fusion protein with different targeting sequences and soluble 22-hydroxycholesterol as substrate, Black et

al. showed that the fusion protein was active when targeted to the mitochondria but inactive when targeted to the ER. This demonstrates that CYP11A1 activity requires the mitochondrial environment in addition to the specific mitochondrial electron transfer system [199]. Lambeth et al. showed that phosphatidylcholine and cardiolipin, a mitochondrion-specific lipid, are both effective activators of CYP11A1 activity. The increase in activity is believed to be due to specific phospholipid effects which promote cholesterol binding to CYP11A1 [200,201]. Furthermore, Schwarz et al. have shown that nonbilayer lipids such as phosphatidylcholines with saturated branched fatty acyl chains in the 2-position of the main chains have a significant stimulatory effect on the activity of CYP11A1 [202]. It may therefore be concluded that the lipid composition of the mitochondrial membrane is an essential requirement for the optimal functioning of CYP11A1.

3.6 Characterisation of CYP11A1

3.6.1 Cloning of CYP11A1

CYP11A1 was first cloned from bovine adrenal cortex mRNA in 1984 by Morohashi et al. The nucleotide sequence encoded 520 amino acid residues, with the predicted residues showing an excellent agreement with the composition determined from the 60 kDa purified protein. In addition, the first 39 amino acids of the N-terminal were shown to be a mitochondrial targeting presequence [193]. Human CYP11A1 was cloned in 1986 by Chung et al. and encodes a predicted 521 amino acid protein. The human cDNA and protein sequences are 82% and 72% homologous to that of the bovine sequences [203]. The presence of a 39 amino acid mitochondrial targeting presequence was predicted and later confirmed by Woods et al. [194,203]. Human CYP11A1 is encoded by a single gene located on chromosome 15q23-q24 [203]. The gene is 20 kb, consists of nine exons and contains an unusual exon/intron junctional sequence that begins with GC in the sixth intron [204].

Due to its physiological importance, CYP11A1 has been cloned from numerous species including human [203], cow [193], rat [205], mouse [206], hamster [207], rabbit [161], chicken [208], pig [209], goat [210], sheep [210] and zebra fish [211]. Sequence alignments of deduced amino acid residues of CYP11A1 from various species have predicted steroid- and heme-binding domains with some success [193,207,208,210].

From these alignments, however, neither the three-dimensional structure of the enzyme nor the residues that constitute the active pocket have been accurately predicted. However, much insight into the structure/function relationship of CYP11A1 and its interaction with Adx has been obtained by the expression of the cloned enzyme using various expression systems, including the expression of CYP11A1 in nonsteroidogenic COS-1 cells.

3.6.2 Expression of CYP11A1 in COS cells

COS-1 cells are nonsteroidogenic kidney cells derived from an African Green monkey and contain a mitochondrial cytochrome P450, CYP27B1. After successfully expressing active CYP17, a microsomal steroidogenic cytochrome P450, in COS-1 cells, Zuber et al. were the first to propose that they could support mitochondrial steroidogenesis [197].

This group transfected COS-1 cells with bovine CYP11A1 and showed that CYP11A1 was successfully processed by the mitochondria and was enzymatically active when incubated with 22(R)-hydroxycholesterol, which is able to bypass the action of StAR [113,197]. CYP11A1 activity was supported by the endogenous COS-1 renodoxin reductase and renodoxin proteins that normally support the activity of CYP27B1 in kidney mitochondria. Pregnenolone production was significantly higher when COS-1 cells were cotransfected with both bovine CYP11A1 and bovine Adx, with the concentration of pregnenolone produced increasing as the concentration of Adx increased, as shown in table 3.1 [197].

Table 3.1. Pregnenolone produced from 22(R)-hydroxycholesterol at 2 nmol/ml in COS-1 cells cotransfected with bovine CYP11A1 and bovine Adx after 24 hours. Reproduced from [197].

Adx (µg of plasmid DNA)	CYP11A1 (µg of plasmid DNA)	Pregnenolone (pmol/ml)
0	0	21
0	10	153
0.1	10	230
1	10	470
10	10	550

Cotransfections of COS-1 cells with plasmids expressing human CYP11A1 and AdxR yield no more CYP11A1 activity than transfections with CYP11A1 alone. Additionally, cotransfections with human CYP11A1, Adx and AdxR do not yield more activity than cotransfections with just CYP11A1 and Adx, indicating that Adx is a limiting factor of CYP11A1 activity [198]. CYP11A1 activity supported by endogenous renodoxin is limited due to either the limited amount of endogenous renodoxin present in COS-1 cells, or to the interaction of CYP11A1 with renodoxin not being as efficient as with Adx, even though the two are structurally closely related. Transfections of COS-1 cells with bovine CYP11A1, Adx and CYP17, demonstrated that the pregnenolone produced in the mitochondria of COS-1 cells by CYP11A1 can translocate to the endoplasmic reticulum were it is further metabolised by CYP17 to 17α-hydroxypregnenolone and dehydroepiandrosterone [197].

Zuber et al. therefore demonstrated that nonsteroidogenic COS-1 cells are suitable for the expression of both mitochondrial and microsomal steroidogenic cytochromes P450. As the apparent K_m value of a complex enzyme like CYP11A1 is influenced by a number of factors such as the membrane environment, redox partner type and availability, and the substrate used, the K_m values obtained in different heterologous expression systems cannot be directly compared to one another. However, when CYP11A1 constructs are expressed in the same cellular environment, such as COS-1 cells, under the same conditions, the data obtained becomes directly comparable. Much insight into the structure/function relationship of CYP11A1 can therefore be gained by combining site-directed mutagenesis with the expression of the recombinant enzymes in nonsteroidogenic COS-1 cells [197]. This has made the expression of recombinant steroidogenic cytochromes P450 in COS-1 cells very popular and it is our chosen expression system. This system for elucidating structure/function relationships becomes even more powerful when combined with homology modelling, which is discussed in the next chapter.

To date CYP11A1 has been cloned from numerous species, expressed in nonsteroidogenic COS-1 cells and studied by site-directed mutagenesis and other methods. Most studies have, however, focused on the regulation of the enzyme and on its interaction with Adx. Little is known about the interaction of cholesterol with the CYP11A1 active pocket. The next chapter focuses on the crystallisation and homology modelling of the cytochromes P450. Special attention is given to the generalised structure of the cytochrome P450 active pocket and the current three-dimensional

models of CYP11A1. Finally an overview is given of the current predictions of the CYP11A1 active pocket.

CHAPTER 4
HOMOLOGY MODELLING OF CYP11A1

4.1 Homology modelling of the mammalian cytochromes P450

The mammalian cytochromes P450 have been the subject of numerous studies, due to their physiological importance. However, even with the abundance of data gathered by such studies, deductions regarding the structure/function relationship of these enzymes remain difficult to make in the absence of crystal structures. The mammalian cytochromes P450 are all membrane bound and are not amenable to crystallisation due to their extreme hydrophobic nature. Since limited structural information is available, methods of predicting the three-dimensional structure of these proteins are extremely useful [212].

Homology or comparative modelling is a technique used to predict the three-dimensional structure of proteins based on the observation that proteins with similar, but not identical, amino acid sequences have a tendency to adopt similar three-dimensional structures [6]. Homology modelling predicts the three-dimensional structure of a protein based only on its amino acid sequence and its alignment with the solved crystal structures of proteins with similar sequences. Although the three-dimensional structures obtained by modelling are less accurate than those derived experimentally, they are invaluable as they provide a testable hypothesis in the absence of experimental data [212].

While unrelated proteins may share similar amino acid sequences (similarity), the cytochromes P450 are homologous as they share an evolutionary similarity known as homology, making them particularly amenable to homology modelling. This comparative technique has been used to predict the structures of several mammalian cytochromes P450 [212], including all of the adrenal steroidogenic cytochromes P450 [213]. Homology models of the cytochromes P450 have contributed greatly to the study of the structure/function relationship of these enzymes: enabling the identification of key residues by designing site-directed mutants; investigations into redox partner interactions; and the prediction of ligand binding and product formation.

The construction of a homology modelling consists of four basic steps, namely: template selection, target template alignment, model building and evaluation [212,214].

These steps will be discussed, focusing on the modelling of the mammalian cytochromes P450.

4.1.1 Template selection in homology modelling

Homology modelling is a predictive technique in which a protein of known amino acid sequence (target) is modelled against the crystal structure of a protein with a similar amino acid sequence (template). The choice of template is therefore critical to the accuracy of the model.

Until recently structural models of the mammalian cytochromes P450 were based on the crystal structures of one or more of the bacterial cytochromes P450. The bacterial cytochromes P450 are amenable to crystallisation as they are soluble and not associated with membranes. The bacterial cytochromes P450 most commonly used as templates for homology modelling include, CYP101 isolated from *Pseudomonas putida* [9,10], P450BMP (CYP102, the heme domain of the fusion protein BM-3) from *Bacillus megaterium* [215], P450terp (CYP108) from *Pseudomonas saccharophiai* [216] and P450eryF (CYP107A1) from *Saccharopolyspora erythraea* [217]. However, the amino acid sequence homology between the mammalian and the bacterial cytochromes P450 is as low as 20%, complicating the accurate alignment between the target and template amino acid sequences [212].

The first mammalian cytochrome P450 structure to be solved, rabbit CYP2C5, was engineered as a soluble protein which could readily be displaced from membranes by modifying the N-terminal sequence. In addition to removing the transmembrane domain, four amino acid residue changes (N202H, I207L, S209G and S210T) were made in the G helix minimising protein aggregation [218]. This breakthrough which lead to the elucidation of the crystal structure of CYP2C5 [219,220] was subsequently followed by the determination of the crystal structures of more mammalian cytochromes P450. To date these include, human CYP2C9 [221,222], human CYP2C8 [223], rabbit CYP2B4 [224, 225] and human CYP3A4 [226,227].

The inclusion of the abovementioned mammalian cytochromes P450 as templates has improved the reliability of homology models of other mammalian cytochromes P450 due to their increased sequence homology to these target proteins. Kemp et al. demonstrated this by comparing the amino acid sequence of CYP2D6 against the available sequences of crystal structures in the Protein Data Bank (PDB) [228] using

BLAST [229] as is shown in table 4.1 [212]. The effect of incorporating the crystal structures of the mammalian cytochromes P450 as structural templates was demonstrated by Kirton et al., who created four different homology models of human CYP2D6. One model based on the structures of the bacterial cytochromes P450, CYP101, CYP102, CYP108 and CYP107A1; another on CYP2C5, the only mammalian cytochrome P450 structure available at the time; and two based on alternative amino acid sequence alignments of 2D6 with all five of these structures. Analysis of the models showed that the inclusion of CYP2C5 as a template had a profound effect on the modelling process, altering the general topology of the active pocket [230].

Table 4.1. Amino acid sequence of CYP2D6 run against the sequences of structures in the PDB [228] using BLAST [229]. Reproduced from [212].

Protein	%identity	Blast score
CYP2C8	41	705
CYP2C9	40	690
CYP2C5	40	678
CYP2B4	41	615
CYP101	17	306
CYP102	18	229
CYP108	20	199
CYP107A1	15	197

4.1.2 Target template alignment in homology modelling

The correct alignment of the target amino acid sequence to that of the templates is critical to the accuracy of the final model. Frequent alignment errors are detrimental as they have a large influence on model accuracy [231]. Alignment errors become more significant when the amino acid sequence similarity of the target and templates is less than 30%, as is often the case with the cytochromes P450 [232,233]. At 30% sequence identity it is estimated that approximately 20% of the amino acid residues are misaligned on average [234]. Even residues that are misaligned by a single position are often modelled with an error larger than the spacing between two consecutive Cα

positions (3.8 Å) [231]. Alignment errors are the single most important limitation on homology modelling, due to their frequency and impact [235].

Although alignments may be generated by several automated programs, most published cytochrome P450 homology alignments are generated by hand. Related proteins contain domains with conserved structure, normally within the inner core, which stabilise the overall structure and are critical to catalysis. These highly conserved domains are therefore aligned first. Secondary structures such as helices and sheets are also conserved within a protein family, while loops are variable. Secondary structure predictions are therefore used to optimise amino acid alignments. The placement of variable domains, which may include insertions or deletions, are optimised considering the context of the template structure [214].

4.1.3 Model building

Several programmes allowing the construction of three-dimensional homology models are available. These include programmes such as SWISSMODEL [236], COMPOSER [237,238] and Modeller [239], which use one of two modelling approaches, namely molecular replacement (SWISSMODEL, COMPOSER) or consensus homology modelling (Modeller) [212].

In molecular replacement modelling the coordinates for each of the structurally conserved domains and secondary structures are assigned directly to the model from the template with the highest homology in this domain. Loops are constructed either by searching the PDB for loops of the predefined length or *de novo* by using random tweak algorithms, after which the N- and C- termini are modelled. The model is then refined by sequential minimisation of the structural elements. A refinement order of the N-terminal, loops, C-terminal and structurally conserved domains, and finally a minimisation of the whole structure is followed [240].

During consensus homology modelling the backbone of a model is generated using the coordinates of all of the template structures based on spatial restraints. Each residue in the structurally conserved domains of the target has a list of equivalent residues from the templates. For each reference residue in the target, the equivalent atoms are found in the templates, and the maximum, minimum and average interatomic distances calculated. The programme predicts the best fit for the target residues using

these values together with experimentally determined values, after which the model is minimised to obtain the most stable structure.

Minimisation is accomplished by the systematic alteration of molecular geometry to derive the coordinates where the model has lowest potential energy and is most stable. Minimisations are accomplished by the use of molecular force fields. A molecular force field is a collection of functions and constants which allow for the computation of potential energy as a function of molecular geometry. All molecular force fields describe the potential energy of a molecule as a function of molecular geometry, and are a function of four key terms as is illustrated schematically in figure 4.1. The four fundamental terms are: bond stretching; angle bending; bond rotation; and non-bonded interactions, which include van der Waals forces and electrostatic interactions [241]. All molecular force field constants and reference geometrical parameters are derived empirically from experimental data [240].

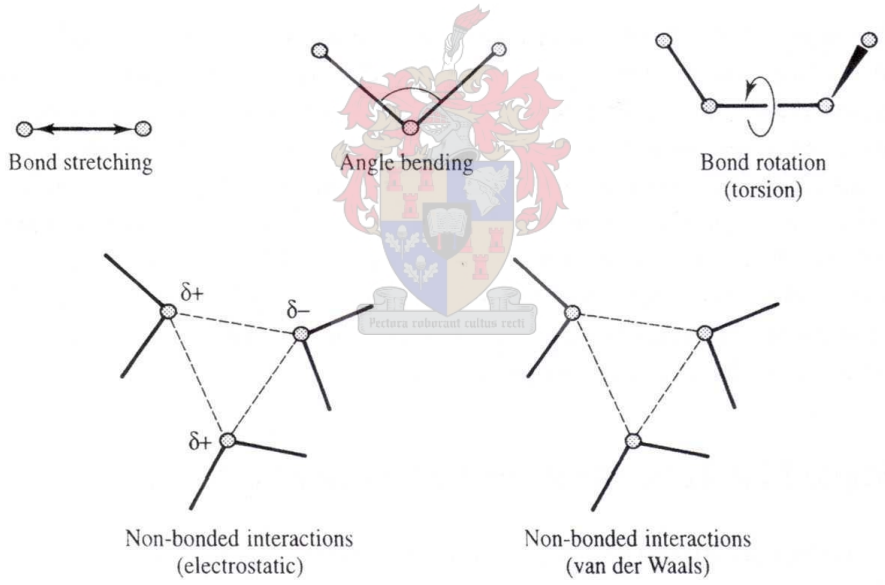

Figure 4.1. Schematic representation of the four key terms in a molecular mechanics force field: bond stretching, angle bending, bond rotation and non-bonded interactions. Reproduced from [241]

During an energy minimisation, the potential energy of the model is calculated using a molecular force field and can be represented by a point of a curve. When represented graphically the energy profile or 'energy surface' of a given model has numerous peaks and troughs. Minimisation algorithms are used to locate the conformation with the lowest potential energy known as the global energy minimum.

However, most algorithms are only able to locate the minimum that is nearest to the starting point, as is shown in figure 4.2, and to locate the global energy minimum numerous starting points must be generated and minimised [241].

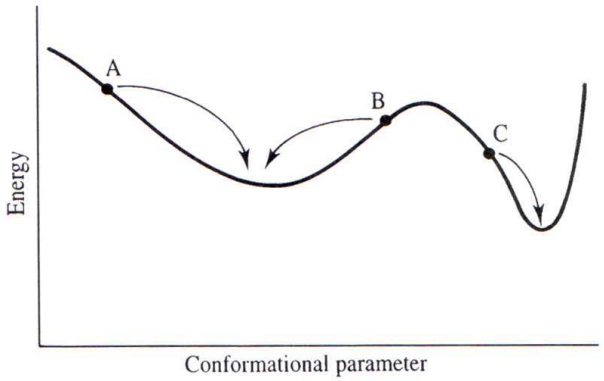

Figure 4.2. Schematic one-dimensional energy surface and the minima that would be obtained starting from points A, B and C. Reproduced from [241]

Derivatives are often used during energy minimisations. When drawn graphically, the gradient is equal to the first derivative of the potential energy for a given model. During a minimisation a small change is made to the geometry of the model, δr, in response to the forces acting on it. The potential energy is recalculated and the energy difference, δE, between the two points is used to determine the gradient, δE/δr, as is shown in figure 4.3. The direction of the gradient indicates where the minimum lies, and the magnitude indicates the steepness of the local slope. The geometry is altered again to obtain the next structure closer to the minimum. This procedure is continued until a negligible change in energy results from a change in geometry, ideally when the derivative is equal to zero.

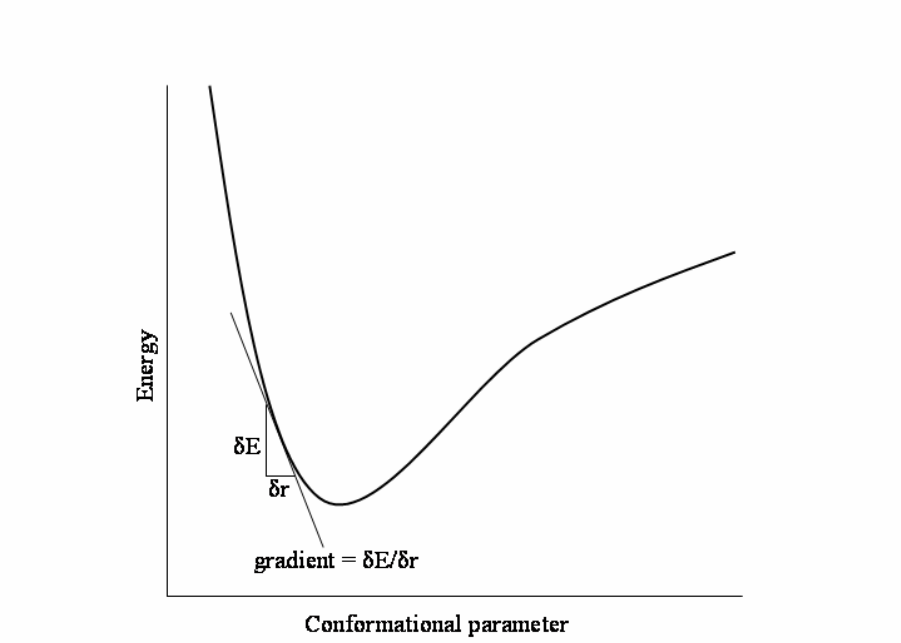

Figure 4.3. Schematic one-dimensional energy surface showing the derivative or gradient δE/δr obtained by altering the geometry of a hypothetical model by a small amount δr. Redrawn from [240].

Two minimising algorithms, steepest descent and conjugate gradient, are commonly used during energy minimisations of homology models. In steepest descent, the gradient is calculated and followed "downhill" until it reaches a point where the gradient increases. At that point a new gradient direction, orthogonal to the previous direction, is calculated and followed. The process is continued until the minimum energy is reached, as shown for the function $x^2 + 2y2$ in figure 4.4. Steepest descent rapidly corrects bad initial geometries, but have poor convergence properties as the derivatives become increasingly small nearing the minimum [240].

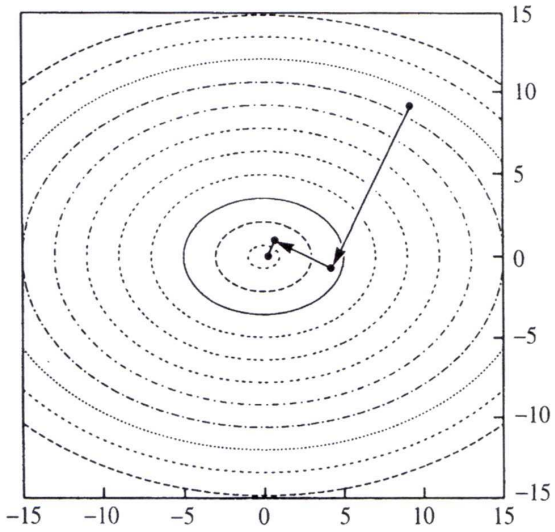

Figure 4.4. Application of the steepest descent algorithm to the function $x^2 + 2y^2$. Reproduced from [241].

In conjugant gradient, the data gained from previous gradients is used, making the search direction a linear combination of a current gradient and that of the previous one. Unlike gradients generated using steepest descent, these gradients are not always orthogonal to the previous direction. Conjugate gradient is more efficient than steepest descent as it converges rapidly as is shown for the function $x^2 + 2y^2$ in figure 4.5 [240].

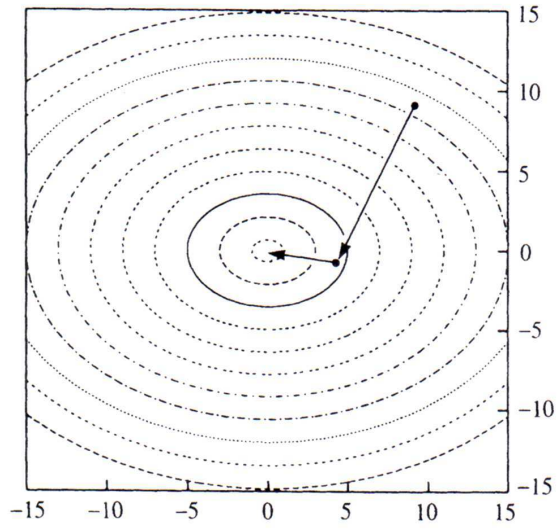

Figure 4.5. Application of the conjugate gradient algorithm to the function $x^2 + 2y^2$. Reproduced from [241].

During molecular replacement modelling, steepest descent is often used first, followed by conjugate gradient, as this combination gives good initial geometries and converges rapidly [240]. For consensus homology modelling, programmes such as Modeller use a combination of conjugate gradient and stimulated annealing [242]. During stimulated annealing, energy is introduced into the model by heating after which the model is allowed to cool slowly to produce a stable conformation [240].

4.1.4 Evaluation

The quality of a model can be assessed by structural and functional evaluations. Structural evaluations check whether the model structure resembles the known structures of correctly folded proteins, while functional evaluation involves the experimental validation of the model.

Structural evaluation methods check bond angles and distances, backbone and side chain conformations and detect bad steric contacts and misfolded regions [240]. Programs used to assess the stereochemical quality of models include: PROVE [243]; WhatIf [244]; Verify 3D [245]; and PROCHECK [246], which can be accessed online at: http://deposit.pdb.org/cgi-bin/validate/aditsession-driver. It has also been shown that the root mean square deviation (RMSD) between the main chain atoms of the model and the most homologous template is a reliable method for validation [235]. Furthermore, it is useful to evaluate the templates by the same methods used to evaluate the model. Comparative values between the templates and the model indicate a valid model. However, it should be noted that it is unreasonable to expect the model to perform better than any of the templates it was based on [212].

Finally, functional evaluations can verify the validity of a model experimentally. The model can either be compared to existing data or predictions can be made from the model and verified experimentally [240].

4.2 The structural core of the cytochromes P450

The cytochromes P450 can be divided into four classes. The class I cytochromes P450 require both an iron sulphur protein (ferredoxin) and a FAD-containing NAD(P)H-ferredoxin reductase for catalysis, while the class II enzymes require a single FAD/FMN containing NADPH-P450 reductase. Class III and IV cytochromes P450 do not require an electron transfer partner as they are able to accept electrons directly from NADPH [7,247], and NADH [247], respectively. The class I cytochromes P450s consist of the mitochondrial cytochromes P450 found in vertebrates, insects, nematodes, and the soluble bacterial cytochromes such as CYP101 and CYP108. The class II cytochromes P450 include a variety of eukaryotic cytochromes P450 found in the endoplasmic reticulum and the soluble bacterial cytochromes, such as fatty acid monooxygenase, CYP102. Class III cytochromes P450, such as allene oxide synthase (CYP74) and thromboxane synthase (CYP5), have been identified in a number of different subcellular locations in animals and plants [7,247], while the class IV cytochromes P450 have only been identified in fungi [247].

Studies have shown that despite the low degree of homology, all classes of the cytochromes P450 share a common structural fold [7]. After the crystal structure of CYP101 was solved [9,10], Goto aligned the sequences of CYP101 with a number of cytochrome P450 CYP2 proteins. Optimisations were carried out by aligning the predicted secondary structures of the CYP2 proteins to the secondary structures of CYP101. The CYP2 secondary structure profiles correlated very well with that of CYP101, suggesting similar three-dimensional structures. Based on the alignment and the regions of CYP101 that make contact with the substrate camphor, Goto predicted six substrate recognition sites (SRS) for the CYP2 enzymes. The predicted SRS were substantiated by the observation that in the nucleotide sequences missence (amino acid-replacing) mutations are more frequent within the SRS than outside of these sites [8]. Furthermore, the SRS corresponded well to those determined experimentally for CYP2 proteins. Today the six SRS are generally accepted for all cytochromes P450 – SRS1 is located between in the B´-C loop; SRS2 is located at the C-terminal end of the F helix extending into the F-G loop; SRS3 begins in the F-G loop and extends into the G helix; SRS4 is located in the N-terminal region of the I helix; SRS5 is located in the loop between K helix β-sheet β1-4; and SRS6 is located in the loop between the two β-sheet β-4 sheets [8,222].

After the crystal structure of the third bacterial cytochrome P450, CYP108, was solved, Haseman et al. proposed that the cytochrome P450 architectures are remarkably more conserved than their primary sequences indicate. Comparisons of the crystal structures of CYP101, CYP102 and CYP108 showed that the cytochromes P450 are composed of two domains: an α-helical domain accounting for approximately 70% of the protein structures and a β-sheet domain accounting for approximately 22% of the protein structures. The α-helical domain contains: the helices B´, C, D, E, F, G, H, I, J, J´, K, and L and the β-sheets β3, β4, β5. The β-sheet domain contains: the helices A, B and K´ and the β-sheets β1 and β2 [248]. A conserved "core structure" was identified when the crystal structures of the three available cytochromes P450 were superimposed by overlaying the heme groups. This core structure includes of a four α-helix bundle consisting of the parallel helices D, I**,** and L, and the anti-parallel helix E; helices J and K; β-sheets β1 and β2**;** the heme-binding region; and the "meander," a 14 or 15 amino acid residue stretch immediately carboxy-terminal to the K´ helix. These conserved structures are believed to play a role in protein folding and heme binding [7,248,249]. The structural core of CYP102 is shown in figure 4.6. Alignments of the three bacterial cytochromes P450 with several mammalian cytochromes P450 identified three residues that are absolutely conserved. These include the cysteine residue in the heme binding domain that serves as the fifth coordinating ligand to the heme iron, and a glutamate and arginine residue in the K helix, one helical turn apart, forming a salt bridge directed into the meander. Highly conserved residues located in the I helix of most cytochromes P450 include a threonine residue pointing into the active pocket [7], and an acidic residue (glutamate or aspartate). Both are believed to be involved in oxygen activation [7,250,251] and lie in the highly conserved sequence (A/G)GX(E/D)T near the middle of the I helix (SRS4), directly over pyrole ring B of the heme, forming a slight bend in the I helix [7].

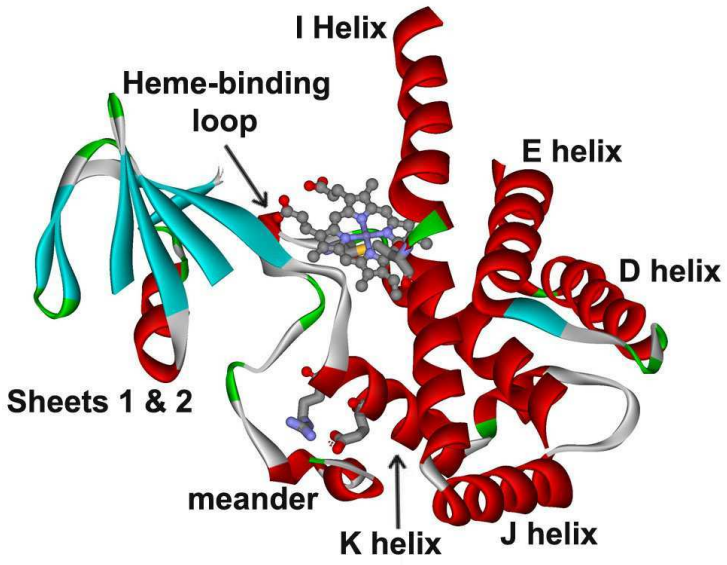

Figure 4.6. Structural core of CYP102. The conserved glutamate and arginine residues are shown in the K helix and the conserved threonine residue is shown in the middle of the I helix. The sulphur (yellow) of the conserved cysteine residue is just visible directly below the heme iron in the active pocket. The coordinates of CYP102 were downloaded from the PDB.

The core structure of the cytochromes P450 were confirmed subsequent to the crystallisation of another bacterial cytochrome P450, CYP107A1, and mammalian enzyme CYP2C5. Overlays of the four bacterial proteins, CYP101, CYP102, CYP108 and CYP107A1, and the mammalian enzyme CYP2C5 revealed the structural similarity of these enzymes even though they differ in terms of solubility, amino acid sequence homology, redox partners and substrate specificity. The overlays showed that >50% of each enzymes backbone occurs within a RMSD of 2Å and that at least 90% of the backbone occurs within a RMSD of 5Å, as is shown in figure 4.7 [247].

While the structural core may be essential to the final structure and hydroxylase activity of the cytochromes P450, it is the regions of greatest structural differences that have been proposed to be involved in substrate recognition and binding, membrane binding and interaction with redox partners. The diversity of substrates catalysed by the cytochromes P450 is well demonstrated when comparing bacterial enzymes CYP101 and CYP102. The substrate for CYP101 is camphor, a small bicyclic monoterpene, while the substrates of CYP102 are long-chain fatty acids and eicosanoids. It is therefore not surprising to find differences in the topology of the structural elements involved in substrate recognition, binding and orientation [7].

Figure 4.7. Structural overlay of four bacterial cytochrome P450 crystal structures, CYP101, CYP102, CYP107A1 and CYP108, and one mammalian cytochrome P450, CYP2C5. Green indicates the Cα backbone trace of CYP102, blue includes the Cα backbone trace of CYP102 contained within a RMSD of 5Å in all five cytochrome P450 crystal structures and red indicates the Cα backbone trace of CYP102 contained within a RMSD of 2Å in all five cytochrome P450 crystal structures. Reproduced from [247].

Two of the most variable domains amongst the cytochromes P450 include the F and G helices together with the F-G loop and the B´-C loop. The antiparallel F and G helices vary structurally between CYP101, CYP102 and CYP108, in both length and position relative to the core structure. The F-G loop has the highest crystallographic B factors of all domains indicating flexibility within the F-G loop as it does not occupy a single conformation in the crystal structures [10,215,216]. The F-G loop together with β sheets, β1 and β2, is believed to act as the 'mouth' of the substrate access channel formed by the F, G, B´ helices, the B-B´ and B´-C loops and the β1 sheet. The crystal structure of CYP101 showed its substrate, camphor, bound in the buried active pocket, isolated from the surrounding solvent. The substrate-free form of CYP101 was found to be virtually identical to the substrate-bound structure. However, the substrate free form of CYP102 exhibits an open channel to the active pocket [252]. When the long-chain fatty acids and eicosanoids substrates bind, the carboxyl group of the substrate remains near the entrance of the channel. Movement of the F-G loop causes the rest of the channel to collapse around the hydrocarbon tail [253,254]. An open conformation of CYP101 was identified when crystallised with large tethered compounds bound [255].

Open conformations in the absence of substrate have also been described in the crystal structures of the prokaryotic cytochromes P450 oxyb [256] and CYP154C1 [257] and more recently in the mammalian enzyme CYP2B4 [224,225]. In CYP2C5 movement of the F and G helices has been shown to facilitate the binding of structurally diverse substrates [219,220]. The flexibility of the F-G loop therefore appears to be critical in allowing structurally diverse compounds access to the buried active pockets in the cytochromes P450.

Amongst the cytochromes P450, the B´-C loop varies greatly in three-dimensional topology. The loop snakes in and out of the active pocket and forms the SRS1 [7]. Specific residues within the B′-C loop have been shown to play an essential role in substrate specificity and hydroxylation regioselectivity in both bacterial [7] and mammalian cytochromes P450 [7,8,258,259]. The B´-C loop, like the F-G loop, has been shown to be flexible. In CYP2C5 movement of the B´-C loop was observed when larger substrates were bound [220]. Flexibility of the B´-C loop may therefore alter substrate affinity by changing the shape of the active pocket [7].

4.3 Homology modelling of CYP11A1

Five homology models of CYP11A1 have been reported to date. The first model, which used CYP101 as the template, was published in 1992 by Vijayakumar and Salerno [260]. This is the only homology model of CYP11A1 currently available in the PDB. The second model employed CYP102 as the template and was published in 1996 by Lewis et al. Comparing their model to that of Vijayakumar and Salerno, Lewis et al. showed that the two models shared close structural similarities. However, variations resulting from differences between the two alignments were observed [213]. The model of Lewis et al. supported the results obtained by Tsujita and Ichikawa, which showed that a twenty amino acid residue sequence near the N-terminal of CYP11A1 is able to bind cholesterol [261]. The model suggests that this represents a likely recognition site for the substrate to enter the access channel. This result is supported by other studies with cytochromes P450 showing that the respective substrates are initially recognised at the surface of the enzymes before moving through the access channel to the active pocket [7,215,216,248].

The third model of CYP11A1 was published in 2002 by Usanov et al. The C-terminal domain of the model was constructed using CYP102 as the template. Helices A

and A´ were, however, constructed using the backbone of CYP108, as there was a greater similarity between CYP108 and CYP11A1 in the length of these helices. Helices B through B´ were constructed by hand as this region is highly variable in all cytochromes P450 [178]. CYP2C5 does not have a B´ helix, but displays a loop or coil in this region [219,220]. The B´ helix in CYP11A1 was predicted by the amphipathic nature of the residues and length of the sequence, and was constructed to optimise charge-charge interactions. Similarly, the F and G helices were constructed by hand and positioned across the top of the structure to optimise charge-charge interactions. Numerous differences were noted when comparing their model to that of Vijayakumar and Salerno. The most noticeable being the absence of the J´ helix in the model of based on CYP101. The J´ helix was first identified in the crystal structure of CYP102 [215] and is believed to be present in all mammalian cytochromes P450 [178]. In addition, the model constructed by Lewis et al. contains a J´ helix as it was based on the crystal structure of CYP102 [213]. Other differences between the model of Usanov et al. and that of Vijayakumar and Salerno are the length and orientation of the F and G helices. Usanov et al. docked their model of CYP11A1 with the crystallised Adx molecule, and in combination with site-directed mutagenesis, they were able to identify four salt bridges essential for the interaction of CYP11A1 and Adx [178].

The first homology model of CYP11A1 created using a mammalian cytochrome P450 as the structural template was published in 2003 by Headlam et al. [262]. The model was based on the crystal structure of CYP2C5. The alignment of CYP2C5 with CYP11A1 was optimised by secondary structure predictions. Helices A and A´ were constructed using CYP108 as the template, as was done by Usanov et al. [178], due to the poor homology between the N-termini of the two cytochrome P450. A B´ helix was predicted in the secondary structure of CYP11A1 and was incorporated in the model, although the CYP2C5 template did not contain a B´ helix. Furthermore, the F-G loop of CYP2C5 was not incorporated in the model as it was shorter than the loop predicted for CYP11A1. Instead a loop of similar length was selected from the loop database in the Swiss Model automated server and used as a template for the F-G loop. Using site-directed mutagenesis, together with their model, Headlam et al. were able to show that hydrophobic aromatic residues in the F-G loop of CYP11A1 can integrate into a membrane. This group suggested that the F-G loop may be the primary site of interaction between the mitochondrial cytochromes P450 and the inner mitochondrial membrane since the mitochondrial cytochromes P450 lack a transmembrane anchor at

the N-terminal [262], present in the microsomal enzymes [263]. This finding suggests that the mouth of the access channel formed by the F-G loop is in direct contact with the inner mitochondrial membrane. As CYP11A1 is not embedded within the hydrophobic membrane environment [264,265] this orientation would provide easy access for cholesterol in the membrane to the active pocket of CYP11A1 via the hydrophobic access channel. Furthermore, the association of the mouth of the access channel with the membrane environment has been proposed for other cytochromes P450 such as CYP19, which also contains a high concentration of aromatic residues in the F-G loop [7,249]. Conversely, the soluble bacterial cytochromes P450 such as CYP102 have several charged residues in this region [7].

The most recent model of CYP11A1 to date was published in 2004 by Sivozhelezov et al. [266]. This group used CYP2B4 as the template and based their alignment on that of Headlam et al. [262]. All of the previously mentioned models were based on crystal structures in which the access channel is in a closed state. However, the CYP2B4 crystal structure shows an open state with a large cleft extending to the active pocket [224]. As expected the model of CYP11A1, based on the crystal structure of CYP2B4, showed significant differences in the region of the access channel, with the overall structural fold of the enzyme was being maintained. This model permitted Sivozhelezov et al. to make predictions concerning residues affecting the electrochemical gradient of CYP11A1 [266].

Therefore, as can be seen by the abovementioned studies, in the absence of a crystal structure homology modelling of CYP11A1 used in conjunction with other techniques, such as site-directed mutagenesis, continues to be a valuable asset in understanding the structure/function relationship of this essential enzyme.

4.4 The orientation of cholesterol in the active pocket of CYP11A1

An important aspect to understanding the structure/function relationship of CYP11A1 is the elucidation of the orientation of the substrate and intermediates in the active pocket. In the absence of a crystal structure, predictions have been made using site-directed mutagenesis, kinetic studies, chemical modifications and docking studies.

Catalytic and binding studies have indicated that an amino acid residue in the active pocket of CYP11A1 hydrogen bonds to the 3β-hydroxyl group of cholesterol and one or more residues hydrogen bond to the 20α-hydroxyl and 22(R)-hydroxyl groups of

the reaction intermediates [176,267-269]. Heyl et al. showed that since epicholesterol (3α-hydroxyl) and 3-ketocholesterol show no detectable binding to CYP11A1 the 3β-hydroxyl group of cholesterol must exhibit the correct stereochemistry. It was also proposed that hydrogen binding to the 3β-hydroxyl group of cholesterol involves the oxygen and not the hydrogen of the 3β-hydroxyl as binding occurred using both short chain ethers and esters. Furthermore, the derivatives of cholesterol, 22(R)-hydroxyl- and/or a 20α-hydroxycholesterol, were shown to bind significantly tighter to CYP11A1 than cholesterol or 25-hydroxycholesterol. Interestingly, the stereoisomer 22(S)-hydroxycholesterol was found to bind very poorly to the enzyme, demonstrating the importance of the 22(R)-hydroxyl group in the binding of the 22(R)-hydroxycholesterol intermediate. Results indicated that the 22(R)-hydrogen of cholesterol is located in line with the heme iron approximately perpendicular to the heme plane (2.5-3.5Å from the iron). Heyl et al. hypothesised that after the initial sterically favoured 22(R)-hydroxylation, a hydrogen bond is formed with a residue in the active pocket that shifts the intermediate to favour the 20α-hydroxylation [268].

Pikuleva et al. proposed the first topological model for the active pocket of CYP11A1, using site-directed mutagenesis and arylhydrazine probes. This group observed that the region above pyrole ring A of the heme is open, while the regions directly above pyrole rings B, C and D are densely occupied by amino acid side chains. An open region was also detected above the amino acid side residues which lie directly above pyrole ring D. Binding studies lead the group to suggest that the side chain of cholesterol occupies the space above pyrole ring D, interacting with Y94, while the rest of the steroid occupies the open region directly above pyrole ring A. A less likely orientation was also suggested, where the sterol binds high over pyrole ring D with the side chain extending down toward the iron and into the open region above pyrole ring A. However, this group was unable to determine whether the observed topological change proposed for the region above pyrole ring D, resulting from the double mutation Y93S/ Y94S, was caused by the residues being located in that area or resulted from a structural adjustment at a more distant site. [270].

Tuckey et al. have demonstrated that cholesterol fatty acid esters with acyl chain lengths of up to four carbons are able to undergo side-chain cleavage, suggesting that the substrate binding site in the region of the 3β-hydroxyl group is larger than previously believed [269].

Lewis et al. are the only group to use their homology model of CYP11A1 to predict the orientation of cholesterol in the active pocket using docking strategies. Their results suggest that the 3β-hydroxyl group of cholesterol forms a hydrogen bond with T354, while the 3β-hydroxyl group of the intermediary substrate 22(R)-hydroxycholesterol hydrogen bonds with S352 [213].

Using site directed mutagenesis together with kinetic studies Woods et al. predicted that I462 lies in close proximity to the side chain binding site of cholesterol. Mutation of I462 to leucine resulted in a decrease in the catalytic rate constant (k_{cat}) for cholesterol, an increased K_m for 22(R)-hydroxycholesterol, but no change in the kinetic constants for 20α-hydroxycholesterol [194].

Although numerous predictions have been made for the orientation of cholesterol no clear picture exist. It is apparent that residues in the active pocket of CYP11A1 interact with the 3β-hydroxyl group as well as the 20α-hydroxyl and 22(R)-hydroxyl groups of cholesterol and the reaction intermediates via hydrogen bonds [176,267-269]. Pikuleva et al. predicted that W94 interacts with the side chain of cholesterol [270], while Woods et al. proposed that the side chain lies in close proximity to I462 [194]. Lewis et al. have hypothesised that T354 and S352 hydrogen bond with the 3β-hydroxyl groups of cholesterol and the 22(R)-hydroxycholesterol intermediate, respectively, while Tuckey et al. have shown that substrate binding site in the region 3β-hydroxyl group is larger than previously believed [269].

In the absence of a crystal structure, homology models have greatly contributed to our understanding of CYP11A1. They have been instrumental in identifying the substrate recognition site [213]; amino acid residues essential for the interaction with Adx [178]; membrane binding domains [262]; and residues that affect the electrochemical gradient of CYP11A1 [266]. However, to date homology models of CYP11A1 have not been used to validate predictions pertaining to the orientation of cholesterol in the active pocket.

Applying the lessons learnt from previous models of CYP11A1, homology modelling of baboon CYP11A1, a species closely related to the human, may therefore help to further elucidate the structure/function relationship of this key enzyme. Furthermore, such a model may be useful in evaluating the predictions made for the orientation of cholesterol in the active pocket.

CHAPTER 5

THE INFLUENCE OF THE AMINO ACID SUBSTITUTION I98K ON THE CATALYTIC ACTIVITY OF BABOON CYTOCHROME P450 SIDE-CHAIN CLEAVAGE (CYP11A1)

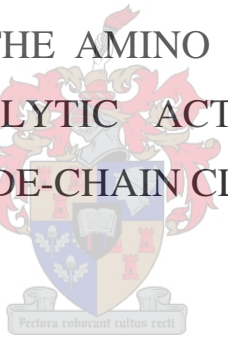

ENDOCRINE RESEARCH
Vol. 30, No. 4, pp. 761–767, 2004

The Influence of the Amino Acid Substitution I98K on the Catalytic Activity of Baboon Cytochrome P450 Side-Chain Cleavage (*CYP11A1*)

K.-H. Storbeck,[1] P. Swart,[1] S. Graham,[2] and A. C. Swart[1,*]

[1]Department of Biochemistry, University of Stellenbosch, Stellenbosch, South Africa
[2]Department of Biochemistry, University of Texas Southwestern Medical Center, Dallas, Texas, USA

ABSTRACT

Cytochrome P450 side-chain cleavage (*CYP11A1*) catalyzes the first and ''rate-limiting'' step in steroidogenesis, the conversion of cholesterol to pregnenolone. In an effort to gain further insight into the structure/function relationship of this key enzyme, *CYP11A1* was characterized in the Cape baboon (Papio ursinus), a species closely related to humans. Baboon cDNA was isolated from adrenal tissue and direct sequence analysis showed mature baboon and human *CYP11A1* share 98% deduced amino acid homology. The cDNA was subsequently amplified and two recombinant constructs, *CYP11A1a* and *CYP11A1b*, were cloned. Sequence analyses of the constructs revealed four amino acid substitutions. The constructs were expressed in nonsteroidogenic mammalian COS-1 cells with 25-hydroxycholesterol as substrate. Apparent K_m values of 1.62 and 4.53 μM were determined for *CYP11A1a* and *CYP11A1b*, respectively. Homology modeling revealed that the lower substrate affinity of *CYP11B1b* could be attributed to an I98K substitution, which lies between the B and C helices, providing further evidence for the importance of this domain in the catalytic activity of *CYP11A1*.

Key Words: P450 side-chain cleavage; Baboon.

*Correspondence: A. C. Swart, Department of Biochemistry, University of Stellenbosch, Stellenbosch 7602, South Africa; E-mail: acswart@sun.ac.za.

DOI: 10.1081/ERC-200044031
0743-5800 (Print); 1532-4206 (Online)

INTRODUCTION

Cytochrome P450 side-chain cleavage (*CYP11A1*) catalyzes the conversion of cholesterol to pregnenolone, the first step in steroidogenesis. This reaction consists of three consecutive monooxygenations: a 20-hydroxylation, 22-hydroxylation, and the cleavage of the $C_{20}-C_{22}$ bond to produce pregnenolone and isocaproic aldehyde. Electrons required to activate molecular oxygen for each monooxygenation are provided by NADPH via adrenodoxin reductase (AR) and adrenodoxin (Adx), with Adx acting as a shuttle between AR and *CYP11A1*. Only a single gene encoding human *CYP11A1* has been identified (1). A lack of homology between human *CYP11A1* and that of species investigated thus far has complicated deductions pertaining to the structure/function relationship of the enzyme. Therefore, the characterization of baboon *CYP11A1*, a species more closely related to humans, could possibly contribute towards a greater understanding of this facet of *CYP11A1* enzymology.

Human *CYP11A1* contains a 39 amino acid N-terminal presequence, which targets the enzyme to the inner mitochondrial membrane and is cleaved upon mitochondrial uptake (2). Predicted steroid- and heme-binding domains in the C-terminal have been shown to be well conserved between species (3). Amino acids essential in protein–protein interactions with Adx have been identified by site directed mutagenesis and molecular modeling (4). The role of the N-terminal in the catalytic activity of *CYP11A1* has not yet been investigated as previous studies have focused on amino acid alignments of homologous domains. The B and C helices located in the N-terminal region of the structurally known cytochromes P450 play an essential role in substrate selectivity (5,6). Recently, N-terminal amino acids of human aldosterone synthase (*CYP11B2*), also a mitochondrial cytochrome P450, have been shown to contribute to substrate recognition and conversion (7). In this paper we report the nucleotide sequence of baboon *CYP11A1* and the effect of an amino acid substitution in the N-terminal region on the catalytic activity of the recombinant enzyme.

MATERIALS AND METHODS

Preparation and Sequencing of Baboon *CYP11A1* cDNA

Baboon *CYP11A1* cDNA was prepared by RT-PCR from total RNA extracted from adrenal cortex tissue as previously described. The cDNA was amplified using high fidelity DNA polymerase (Roche) and the PCR products sequenced. Forward and reverse primers used in amplification reactions were complementary to the 5′ and 3′ ends of human *CYP11A1* (GenBank accession no. M 14565). Prior to ligation into the pTargeT™ mammalian expression vector system (Promega), the cDNA was amplified using Taq polymerase (Thermoprime, DNA polymerase, Advanced Biotechnologies) as previously described and clones were selected and sequenced (8).

Functional Expression of Baboon *CYP11A1* in COS-1 Cells

Baboon *CYP11A1* plasmid constructs (5 μg/ml) were cotransfected with a (5 μg/ml) pCI-neo/human Adx construct into COS-1 cells, using the DEAE-Dextran method

(9). Enzyme activity was assayed by following the conversion of 25-hydroxycholesterol to pregnenolone using [^{3}H]25-hydroxycholesterol (Sigma). Steroid metabolites were extracted with dichloromethane as previously described (9). On the completion of each experiment, the cells were washed with and collected in 0.1 M phosphate buffer, pH 7.4. The cells were homogenized with a small glass homogenizer and the protein content of the homogenate determined by the Pierce BCA method according to the manufacturers instructions.

Chromatography was preformed on a Waters (Milford, MA) high performance liquid chromatograph attached to a WISP^{TM} automatic injector (Waters) and a Flo-One liquid scintillation spectrophotometer (Radiomatic, Tampa, FL). The ratio of scintillant to column element was 3:1. Metabolites of 25-hydroxycholesterol were isocratically separated on a Novapak® C18 column with acetonitrile/isopropanol (50/50) at a flow rate of 1 ml · min^{-1} for 10 min.

Molecular Modeling of Baboon *CYP11A1*

A model of the three-dimensional structure of baboon *CYP11A1* was constructed using an Indigo2 Silicon Graphics workstation and Insight II (version 98) from MSI (4). The model was soaked in a layer of water and the pH set to 7.4. Energy minimizations were preformed until the derivative was less than 0.1. The heme and its thiolate ligand were held fixed during all minimizations.

RESULTS

Baboon *CYP11A1* Sequence Analyses

Amplification of baboon mRNA yielded a single 1566 bp product, which was subjected to a second round of amplification using high fidelity polymerase and subsequently subjected to direct sequence analysis. The nucleotide sequence of Baboon *CYP11A1* (GenBank accession no. AY 702067) encodes a predicted 521 amino acid protein, 97% homologous to human *CYP11A1* (1). The putative presequence is 85% homologous to the human mitochondrial targeting sequence, containing several basic and hydroxylated residues, as well as hydrophobic stretches, conforming to the general rule for this domain (10,11). While the mature enzyme shares 98% amino acid homology with mature human *CYP11A1* the predicted steroid

Table 1. Corresponding amino acids of baboon *CYP11A1* cDNA and constructs *CYP11A1a* and *CYP11A1b*.

Position	Baboon *CYP11A1* cDNA	*CYP11A1a*	*CYP11A1b*
98	Ile	Ile	Lys
141	Ser	Asn	Ser
157	Gly	Trp	Gly
199	Tyr	His	Tyr

Amino acids numbers represent that of mature *CYP11A1* without the 39 amino acid presequence.

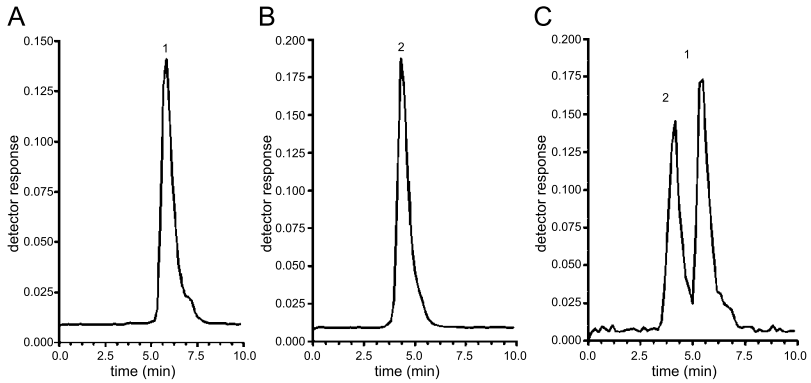

Figure 1. HPLC analysis of 25-hydroxycholesterol (A), pregnenolone (B), and products of 25-hydroxycholesterol metabolism by baboon *CYP11A1* (C). Peaks on the chromatogram are: 1, 25-hydroxycholesterol (5.8 min); and 2, pregnenolone (4.3 min).

binding domain, heme-binding domain and residues involved in protein–protein interactions with Adx are 100% homologous (3,4).

Sequence analysis of the *CYP11A1a* and *CYP11A1b* constructs revealed four amino acid substitutions as shown in Table 1.

CYP11A1 Activity in COS-1 Cells Transfected with Cloned Baboon *CYP11A1*

The constructs were cotransfected into COS-1 cells with human Adx and the enzymatic activity of the constructs was measured by the conversion of 25-hydroxycholesterol to pregnenolone. The activity of *CYP11A1* is normally dependent

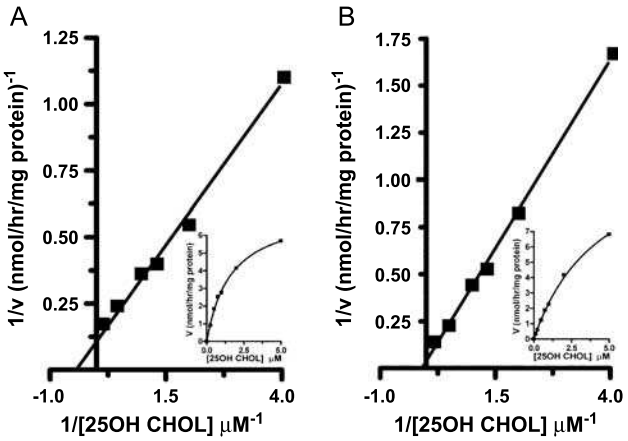

Figure 2. Kinetics of 25-hydroxycholesterol metabolism by (A) *CYP11A1a* and (B) *CYP11A1b* expressed in COS1 cells. (A) *CYP11A1a* Apparent K_m = 1.62 μM; *V* value = 7.5 nmol · h^{-1}· mg protein and (B) *CYP11A1b* Apparent K_m = 4.53 μM; *V* value = 13.1 nmol · h^{-1}· mg protein. Results are representative of three independent experiments.

on the StAR protein to deliver the cholesterol substrate into the mitochondrial membrane (12). The action of StAR was circumvented by providing the cells with 25-hydroxycholesterol as substrate, which readily diffuses from the extracellular environment to the mitochondria. The side-chain cleavage of 25-hydroxycholesterol requires the same three oxidative steps as cholesterol. 22R-hydroxycholesterol used by previous groups bypasses the 22-hydroxylation step (13). In initial experiments both constructs converted approximately 88% of the 25-hydroxycholesterol (1 μM) to pregnenolone after 6 h. Pregnenolone was not detected in untransfected cells after 6 h. Typical HPLC analyses of the metabolism of 25-hydroxycholesterol to pregnenolone by the constructs are shown in Fig. 1.

Conversion assays using concentrations of 25-hydroxycholesterol ranging from 0.125 to 5 μM were preformed in triplicate. Lineweaver-Burk analysis of data yielded apparent K_m (K_{mapp}) values of 1.62 and 4.53 μM and V values of 7.5 and 13.1 nmol · h^{-1}· mg protein for *CYP11A1a* and *CYP11A1b*, respectively (Fig. 2). In addition to Lineweaver-Burk analysis, K_{mapp} and V values were determined by direct linear plots. The K_{mapp} values of 1.82 and 5.25 μM and V values of 7.76 and 13.94 nmol · h^{-1}· mg protein for *CYP11A1a* and *CYP11A1b*, respectively, did not differ significantly from the values obtained by Lineweaver-Burk analysis.

Modeling

The *CYP11A1a* and *CYP11A1b* constructs were homology modeled using *CYP102* and *CYP2C5* as templates (4). In *CYP11A1a* the S141N substitution lies in the D helix

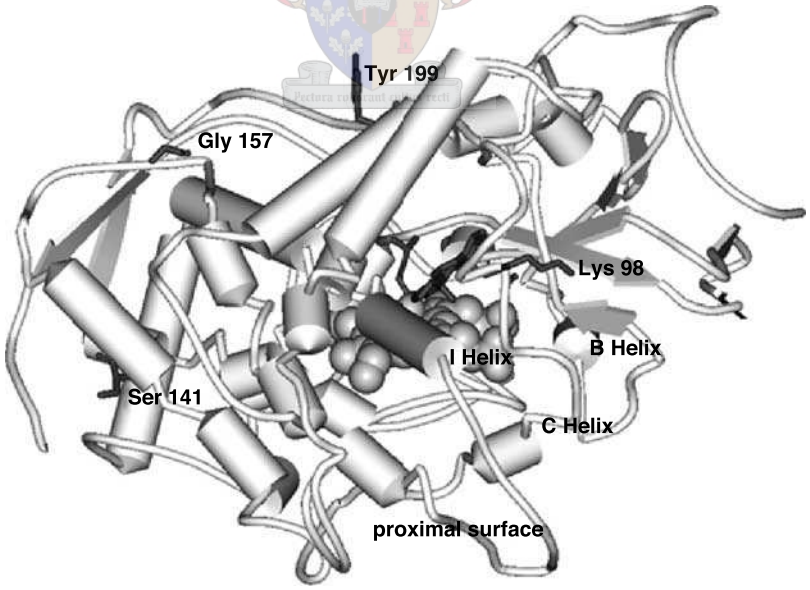

Figure 3. A three-dimensional model of construct *CYP11A1b*, with cholesterol as substrate, showing the I98K substitution, which lies between the B and C helices. Serine 141, which lies in the D helix, glycine 157, which lies at the start of the E helix, and tyrosine 199, which lies in the F helix, are also indicated. (For color photos please see http://www.sun.ac.za/biochem/swart/CYP11A1.)

within a helix turn, the G157W substitution lies at the start of the E helix and the Y199H substitution lies in the F-helix. Structural analysis indicated that these substitutions do not appear to influence the three-dimensional structure of *CYP11A1* significantly. The Ile residue at position 98 in the *CYP11A1a* construct lies between the B and C helices in close proximity to the heme group in the active site. The model revealed that the side chain of this residue is turned towards the substrate in the active pocket and associates with other hydrophobic residues *viz.* Pro85, Pro86, Trp87, Val88, and Ala89. In construct *CYP11A1b* however, a positively charged Lys residue replaces the hydrophobic Ile residue. The side chain of this residue is turned outwards away from the hydrophobic residues in this pocket, as shown in Fig. 3.

DISCUSSION

The K_{mapp} value of a complex enzyme like *CYP11A1* is influenced by a number of factors such as the membrane environment, redox partner type and availability, and the substrate used (cholesterol versus hydroxy derivatives). The K_{mapp} values obtained in different heterologous expression systems can therefore not be compared directly with one another. The K_{mapp} values of 1.62 and 4.53 μM, obtained for *CYP11A1a* and *CYP11A1b*, respectively, in this study were, however, determined under the same conditions and is a useful parameter to compare the activities of the two recombinant enzymes. The difference in K_{mapp} values could be correlated to the structural differences seen in the constructed models.

Baboon *CYP11A1b* has a lower substrate affinity than *CYP11A1a* for 25-hydroxycholesterol, which can be attributed to the I98K substitution lying in a highly conserved domain between the B and C helices. These helices play an essential role in substrate selectivity and redox partner interaction in the structurally determined cytochromes P450 (5,6). The three-dimensional structure of *CYP11A1* indicates that this domain between these helices lies in the hydrophobic pocket in close proximity to the heme group in the active site. In *CYP11A1a*, the Ile residue at position 98 points inwards and associates with other hydrophobic residues in this pocket to form a stable structure. The I98K substitution in *CYP11A1b* results in this residue turning outwards, possibly destabilizing this structural domain. A structural change of this domain would impact on substrate interaction in the active site and could account for the increased K_{mapp} (2.7 fold). This indicates that residues in the B and C helices in the N-terminal have an important functional role in *CYP11A1* activity. This finding is substantiated by previous studies, which demonstrated the functional relevance of N-terminal amino acids of human *CYP11B2* in substrate recognition (7). In addition, destabilization of the B and C helices would impact on the position and shape of the I helix, which plays a critical role in catalysis, (14) possibly contributing to the difference in the catalytic activities.

In conclusion, the results presented here show that the amino acid substitution I98K decreases the substrate affinity of baboon *CYP11A1* by possibly destabilizing the B and C helices in the N-terminal. Taken together, our data provides further evidence of the importance of the N-terminal in the catalytic activity of mitochondrial cytochromes P450. The 98% homology shared between the mature forms of human and baboon *CYP11A1* indicates that future structure/function relationship studies

preformed with the baboon enzyme could contribute toward a greater understanding of *CYP11A1* enzymology.

ACKNOWLEDGMENTS

The authors wish to thank the NRF, the University of Stellenbosch, and the Wilhelm Frank Bursary Fund for financial support. Human pCI-neo Adx was a generous gift from Robert C. Tuckey.

REFERENCES

1. Chung B-C, Matteson KJ, Voutilainen R, Mohandas TK, Miller WL. Proc Natl Acad Sci U S A 1986; 83:8962–8966.
2. Woods ST, Sadleir J, Downs T, Triantopoulos T, Headlam M, Tuckey RC. Arch Biochem Biophys 1998; 353:109–115.
3. Vilchis F, Chávez B, Larrea F, Timossi C, Montiel F. Gen Comp Endocrinol 2002; 126:279–286.
4. Usanov SA, Graham S, Lepesheva GI, Azeva TN, Strushkevich NV, Gilep AA, Estabrook RW, Peterson JA. Biochemistry 2002; 41:8310–8320.
5. Peterson JA, Graham SE. Structure 1998; 6:1079–1085.
6. Graham-Lorence S, Peterson JA. FASEB J 1996; 10:206–214.
7. Bechtel S, Belkina N, Bernhardt R. Eur J Biochem 2002; 296:1118–1127.
8. Swart AC, Brown N, Kolar N, Swart P. Endocr Res 2000; 26:1011–1018.
9. Swart AC, Kolar NW, Lombard N, Mason JI, Swart P. Eur J Biochem 2002; 269:5608–5616.
10. Hurt EC, van Loon APGM. Trends Biochem Sci 1986; 11:204–207.
11. von Heijne G. EMBO J 1986; 5:1335–1342.
12. Stocco DM, Clark BJ. Endocr Rev 1996; 17:221–244.
13. Lambeth JD, Kitchen SE, Farooqui AA, Tuckey R, Kamin H. J Biol Chem 1982; 257:1876–1884.
14. Ravichandran KG, Boddupalli SS, Hasemann CA, Peterson JA, Deisenhofer J. Science 1993; 261:731–736.

CHAPTER 6

EVIDENCE FOR THE FUNCTIONAL ROLE OF RESIDUES IN THE B´-C LOOP OF BABOON CYTOCHROME P450 SIDE-CHAIN CLEAVAGE (CYP11A1) OBTAINED BY SITE-DIRECTED MUTAGENESIS, KINETIC ANALYSIS AND HOMOLOGY MODELLING.

Evidence for the functional role of residues in the B´-C loop of baboon cytochrome P450 side-chain cleavage (CYP11A1) obtained by site-directed mutagenesis, kinetic analysis and homology modelling.

Karl-Heinz Storbeck[a], Pieter Swart[a], Sandra Graham[b] and Amanda C. Swart[a*]

[a]Department of Biochemistry, University of Stellenbosch, Stellenbosch 7602, South Africa

[b]Department of Biochemistry, University of Texas Southwestern Medical Centre, Dallas, Texas, USA

*Address correspondence to: Amanda C. Swart, Department of Biochemistry, University of Stellenbosch, Private Bag X1, Matieland, 7602, South Africa; Tel: +27-21-8085862; Fax +27-21-8085863; Email: acswart@sun.ac.za

Abstract

In an effort to gain further insight into the structure/function relationship of cytochrome P450 side-chain cleavage (CYP11A1), this enzyme was investigated in the Cape baboon (Papio ursinus). Four constructs were cloned and characterised in nonsteroidogenic mammalian COS1 cells. Recombinant baboon CYP11A1 cDNA yielded an apparent K_m value of 1.64 μM for 25-hydroxycholesterol. The single amino acid substitutions, I98K and I98Q resulted in a 2.8 and 1.7 fold increases in apparent K_m values, respectively. Conversely, the introduction of the mutation, K103A, resulted in a 1.8 fold decrease in apparent K_m. A homology model of CYP11A1, based on the crystal structures of CYP102 and CYP2C5, revealed that residues 98 and 103 lie within the B´-C loop and contribute to the spatial orientation and structural integrity of this domain. Based on these results we propose a topological model of the baboon CYP11A1 active pocket, which is supported by substrate docking analysis and kinetic studies.

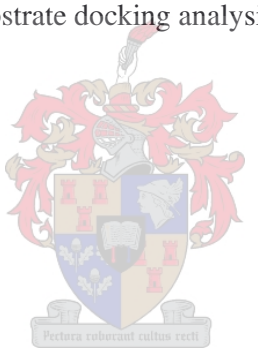

Keywords: cytochrome P450 side-chain cleavage, CYP11A1, P450scc, cholesterol, homology model, structure/function, B´-C loop, baboon

1. Introduction

In humans cytochrome P450 side-chain cleavage (CYP11A1) catalyses the conversion of cholesterol to pregnenolone and isocaproic aldehyde, the first step in adrenal steroidogenesis. This reaction consists of three consecutive monooxygenations: a 22-hydroxylation, 20-hydroxylation and the cleavage of the C_{20}-C_{22} bond to produce pregnenolone and isocaproic aldehyde. Each monooxygenation reaction requires electrons to activate molecular oxygen and these are provided by NADPH via adrenodoxin reductase (AR) and adrenodoxin (Adx), with Adx acting as an electron shuttle between AR and CYP11A1.

CYP11A1 is an insoluble hydrophobic hemoprotein, intimately associated with the inner mitochondrial membrane and has, to date, not been crystallised. In humans a single gene encoding CYP11A1 was located on chromosome 15 [1]. The N-terminal, comprising a presequence of 39 amino acid residues, targets the enzyme to the inner mitochondrial membrane and is cleaved upon mitochondrial uptake [2]. Sequence alignments of deduced amino acid residues of CYP11A1 from various species have allowed the prediction of steroid- and heme-binding domains with some success [3-6]. Catalytic and binding studies have indicated that amino acid residues in the active pocket of CYP11A1 interact via hydrogen bonds with the 3β-hydroxyl group of cholesterol as well as the 20α-hydroxyl and 22(R)-hydroxyl groups of the reaction intermediates [7-10]. Cholesterol and the intermediates have also been shown to occupy slightly different positions in the active pocket of CYP11A1 [2,11]. In bovine CYP11A1, Y93 and Y94 have been identified by site-directed mutagenesis to interact with the side chain of cholesterol [11], while a further study by Woods et al. suggested that I461 lies in close proximity to the side chain of cholesterol [2]. In the absence of a solved crystal structure, neither the three-dimensional structure of the enzyme nor the residues that constitute its active pocket have, to date, been accurately identified from sequence alignments, site-directed mutagenesis or kinetic studies. When combined with homology modelling, however, these techniques provide a powerful tool for the investigation of the structure/function of an enzyme such as CYP11A1.

The crystal structures of P450cam isolated from *Pseudomonas putida*, P450BM-P (the heme domain of the fusion protein BM-3) from *Bacillus megaterium* and P450terp from *Pseudomonas saccharophiai* have been solved [12-15] and comparisons revealed that these soluble bacterial cytochromes P450 share a common structural core even though these proteins differ in terms of solubility, sequence identity, redox partners and

substrate specificity [16]. These findings were confirmed when the first mammalian cytochrome P450, rabbit CYP2C5, was crystallised by modifying the N-terminal sequence thus removing the transmembrane domain to yield a protein which could readily be displaced from membranes. In addition, amino acid residue changes were made in the G helix to minimise protein aggregation [17,18]. Similar techniques have subsequently been used to solve the crystal structures of a number of other mammalian cytochromes P450, which to date include: human CYP2C9 [19,20], human CYP2C8 [21], rabbit CYP2B4 [22-24] and human CYP3A4 [25,26].

Until recently, homology models of mammalian cytochromes P450 have been based solely on the structurally determined bacterial cytochromes P450, which share less than 20% identity with the mammalian enzymes [27]. The availability of the crystal structures of more closely related mammalian cytochromes P450 has contributed towards the reliability of homology models for cytochromes P450 [27,28].

Five homology models of CYP11A1 have been reported to date — three based on the bacterial cytochromes CYP101 [29] and CYP102 [30,31], and two based on the mammalian cytochromes P450 CYP2C5 [32] and CYP2B4 [33]. These models were instrumental in identifying amino acid residues essential for the interaction with Adx [31], membrane binding domains [32] and residues that affect the electrochemical gradient of CYP11A1 [33]. Even though CYP11A1 has been studied and modelled extensively, little is known about the residues that form the active pocket and interact with the substrate and hydroxyl reaction intermediates.

Although the highly conserved structures play a role in protein folding and heme binding, it is the regions of greatest structural difference that influence substrate recognition and binding [16]. One such region, the B´-C loop, meanders in and out of the heme pocket and has been identified as the first of six putative substrate recognition sites (SRS 1) [16,34]. Specific residues within the B´-C loop have been shown to contribute towards substrate specificity and hydroxylation regioselectivity in both bacterial [12,13,16,35] and mammalian cytochromes P450 [34,36-43]. Furthermore, flexibility of B´-C loop, together with the F-G loop, has been shown to be important in allowing substrates access to the buried active pocket of the cytochromes P450. Crystal structures of CYP2C5 [17,18], CYP2C8 [21], CYP2C9 [19,20], and of CYP2B4 bound with a phenylimidazole inhibitor [23], show closed conformations with no observable substrate access channel. However, the structure of inhibitor-free CYP2B4 demonstrates a large open substrate access channel, formed by the repositioning of helices B´ to C

and F through G [24]. In CYP2C5 the B´-C loop adopts different orientations when bound with the substrates dicofenac or 4-methyl-*N*-methyl-*N*-benzenesulfonamide, further illustrating the importance of this domain [18].

In the Cape Baboon, a primate species more closely related to humans than any other species investigated thus far, CYP11A1 cDNA (GenBank accession no. AY 702067) encodes the predicted 521 amino acid protein containing a putative 39 amino acid N-terminal presequence and shares 98% amino acid identity with human CYP11A1 [44]. This study aims to characterize baboon CYP11A1 cDNA and to determine the influence of amino acid residue substitutions in the B′-C loop on structure/function relationship of baboon CYP11A1 using homology modelling. Employing site-directed mutagenesis and molecular modelling our group has previously shown that the amino acid substitution, I98K, in the B´-C loop results in a substantial increase in the K_m of baboon CYP11A1 [44]. The reported importance of the B´-C loop in the catalytic activity of cytochromes P450 prompted a further investigation of the role of residue 98 in this domain. Therefore, the influence of this side chain on substrate affinity was investigated by site-directed mutagenesis, introducing the amino acid substitution I98Q. As the introduction of a charged lysine residue at position 98 of the B´-C loop resulted in a decrease in substrate affinity, the potential importance of the highly conserved charged residue K103 was highlighted. The functional role of this residue was subsequently investigated by introducing the amino acid substitution K103A. A three-dimensional model of CYP11A1 was constructed based on the crystal structures of CYP102 and CYP2C5, the first homology model of CYP11A1 to be based on both a bacterial and mammalian cytochrome P450. Both residues, I98 and K103, were found to be important in maintaining the structural integrity of helices B´ through C, playing an important role in substrate binding. The kinetic data obtained from the amino substitutions I98K, I98Q and K103A, coupled to substrate docking studies has also permitted us to predict the orientation of cholesterol in the active pocket of baboon CYP11A1 and the residues forming the active pocket. We therefore present the first topological model for the active pocket of CYP11A1 determined by both site-directed and homology modelling.

2. Materials and methods

2.1. Animals

Adrenal glands were obtained from normal adult Cape Baboons, bred in Kwazulu Natal and in the Western Cape, South Africa, and housed in the animal units of the University of Cape Town Medical School and the University of Stellenbosch Medical School. All anaesthetic and surgical procedures complied with the 'Principles of Laboratory Care' and the 'NIH Guide for the Care and Use of Laboratory Animals' and were approved by the Animal Research and Ethics committee of both Universities. Adrenals were collected over a period of eight years from 20 groups consisting of between two and four baboons. The surgically removed adrenal glands were flash frozen and stored in liquid N_2.

2.2. Reagents

25-[26,27-^{3}H]-hydroxycholesterol was purchased from PerkinElmer Life Sciences (Boston, MA, USA). 25-Hydroxycholesterol, Dulbecco's modified Eagle's medium, Hepes, diethylaminoethyl-dextran, Chloroquine and antibiotics were all from Sigma Chemical Co. (St Louis, MO, USA). COS-1 cells were obtained from the American Type tissue Culture Collection (Manassas, VA, USA). Penicillin-streptomycin, trypsin-EDTA and Dulbecco's PBS were purchased from Gibco-BRL (Gaithersburg, MD, USA). Fetal calf serum and bacterial culture media were purchased from Highveld Biological (Lyndhurst, RSA) and Difco Laboratories (Detroit, MI, USA), respectively. Plasmid vectors, restriction enzymes and T4 Ligase were purchased from Promega Biotech (Madison, WI, USA). PWO DNA polymerase and ribonucleotide triphosphates were purchased from Roche Diagnostics (Mannheim, Germany). Primers were purchased from Integrated DNA technologies (Coralville, IA, USA). Nucleobond® AX plasmid preparation kits were purchased from Macherey-Nagel (Duren, Germany) and Qiquick® gel extraction kits from Southern Cross Biotechnology (Cape Town, RSA). A Pierce BCA™ protein assay kit was purchased from Pierce (Rockford, IL, USA). All other chemicals were of the highest analytical grade and purchased from scientific supply houses.

2.3. RNA isolation and reverse transcriptase-polymerase chain reaction (RT-PCR)

Total RNA was extracted from baboon adrenal cortex tissue using the High Pure™ RNA tissue Kit (Roche) according to the manufacturers instructions. Polyadenylated (poly A^+) RNA was prepared using a mRNA Capture kit (Roche) and RT-PCR was carried out using the Titan™ One Tube RT-PCR system (Roche) according to the manufacturers instructions. The reverse transcription reaction was performed at 50°C for 30 min after which themocycling was carried out directly.

The RT-PCR products were gel purified and subjected to a second round of amplification using either Taq DNA polymerase (Thermoprime, Advanced Biotechnologies) prior to ligation into the pTargeT™ mammalian expression vector system (Promega) according to the manufacturers instructions or high fidelity DNA polymerase (Roche) for direct cDNA sequence analysis. All amplification reactions were preformed with primers complementary to the 5' and 3' ends of human CYP11A1, (GenBank accession no. M 14565) and are shown in Table 1. Plasmid constructs were screened by restriction digestion analysis and positive clones were subsequently subjected to sequence analysis. All DNA sequencing was preformed on an ABI Prism 3100 Genectic Analyzer (Applied Biosystems, Johannesurg, RSA).

Table 1
Primer sequences used in baboon CYP11A1 amplifications. Primers complementary to the 5' and 3' ends of human CYP11A1, (GenBank accession no. M 14565) Left primer (LP) and right primer (RP) respectively and the site-directed mutagenesis primers, K98QLP, K98QRP, K103ALP, K103ARP, T291ALP and T291ARP. A *Xho*1 restriction site (underlined) was incorporated in the sense primer. The codons for the changed amino acid are represented in bold characters in I98QLP, K103ALP and T291ALP.

Primer	Oligonucleotide sequence
LP (Sense)	5'-<u>CTCGAG</u>CTGTGGGGACAGC-3'
RP (Antisense)	5'-AGTGACGACCCAACGAAG-3'
I98QLP (Sense)	5'-CCAATATTACCAGAGACCC**ATA**GGAGTCCTG-3'
I98QRP(Antisense)	5'-TGGGTCTCTGGTAATATTGGTGATAGGCG –3'
K103ALP (Sence)	5'-ACCCATAGGAGTCCTGTT**GGC**GAAGTCAGC-3'
K103ARP (Antisence)	5'-AACAGGACTCCTATGGGTCTCTGGTAATATTG-3'
T291ALP (Sence)	5'-GGCAGGAGGGGTGGAC**GCG**ACGTCCAT-3'
T291ARP (Antisence)	5'-GTCCACCCCTCCTGCCAGCATCTCTGTG-3'

2.4. Site-directed mutagenesis

Site-directed mutagenesis of baboon CYP11A1 was carried out using the Gene Tailor^{TM} site-directed mutagenesis system (Invitrogen) according to the manufactures instructions using the mutagenic primers listed in Table 1. Mammalian expression construct CYP11A1 was used as the template. This construct contains the cDNA encoding baboon CYP11A1. The desired mutations, I98Q, K103A and T291A were confirmed by direct DNA sequence analysis.

2.5. Enzymatic assays in transiently cotransfected COS-1 cells

COS-1 cells were grown at 37°C and 5% CO_2 in Dulbecco's modified Eagle's medium (DMEM) supplemented with 10% fetal calf serum, 1% penicillin-streptomycin, 4 mM L-glutamine and 25 mM glucose. Baboon CYP11A1 plasmid constructs were cotransfected with a pCI-neo/human Adx construct into COS-1 cells, using the DEAE-Dextran method [45]. COS-1 cells were grown to confluence in 6 cm diameter dishes and each dish plated to five 6 cm diameter and grown overnight. The cells were washed with 4ml fetal calf serum-free medium containing Hepes (20 mM) medium and cotransfected with 5 μg of a baboon CYP11A1 plasmid construct and 5 μg of pCI-neo/human Adx/ml Hepes medium supplemented with 250 μg DEAE-dextran. The medium was removed after 1h and 10 ml DMEM containing chloroquine to a final concentration of 5.2 μg/ml was added and the cells incubated for an additional 5h. The medium was subsequently removed and replaced with DMEM. The same protocol was followed to determine the catalytic activity of recombinant human CYP11A1, using pECE/human CYP11A1. Control transfection reactions were preformed using the mammalian expression vector pCI-neo (Promega). After 72h enzyme activity was assayed by adding 25-hydroxycholesterol and [^{3}H]25-hydroxycholesterol as substrate. Aliquots of 0.5 mL, were removed at specific time intervals. The steroid metabolites were extracted with dichloromethane (10 volumes) and the dichloromethane phase was evaporated under N_2. The dried steroid residue was redisolved in 120 μL methanol prior to HPLC analysis. On the completion of each experiment, the cells were washed with and collected in 0.1M phosphate buffer, pH 7.4. The cells were homogenised with a

small glass homogeniser and the protein content of the homogenate determined by the Pierce BCA method according to the manufactures instructions.

2.6. Separation and quantification of steroids

Chromatography was preformed on a Waters (Milford, MA, USA) high performance liquid chromatograph attached to a WISP^{TM} automatic injector (Waters) and a Flo-One liquid scintillation spectrophotometer (Radiomatic, Tampa, FL). The ratio of scintillant to column element was 3:1. Metabolites of 25-hydroxycholesterol were isocratically separated on a Novapak® C18 column with acetonitrile/isopropanol (50/50) at a flow rate of 1ml·min^{-1} for 10 min. Kinetic constants were determined by non-linear regression using GraphPad Prism (version 4) software (GraphPad Software, San Diego, CA) and by direct linear plots [46].

2.7. Modelling

A homology model of baboon CYP11A1 was constructed using the program Modeler from the Insight II suite of programs from Accelrys (San Diego, CA) on an Octane Silicon Graphics workstation. A sequence alignment of CYP11A1 with CYP102 and CYP2C5 was generated and then refined manually to take advantage of certain known conserved sequences among the cytochromes P450, as shown in figure 1. The Modeler program was then employed to generate an initial model of CYP11A1 using the coordinates of CYP102 [14] and CYP2C5 [18] as the templates. Molecular dynamic simulations were subsequently preformed using Discover from Accelyrs using the cvff force field. The model was soaked in a layer of water and the pH set to 7.4 in order to charge the residues. Energy minimizations were preformed using either steepest descent or conjugate gradient in the Discover package and were carried out from 8000 to 12000 steps per run until the derivative was less than 0.1. The heme and its thiolate ligand were held fixed during all minimizations.

The substrate cholesterol was initially hand docked into the active pocket of CYP11A1 such that the carbon to be oxidized was oriented towards and within 2Å of the heme ferrous oxygen. The complex was them minimized as described above. Several orientations above the heme in the active pocket were considered, and the one

presented is that which reached a minimum and without inappropriate conflicts between the protein and the substrate.

```
CYP11A1:  FNEIPSPGDNGWLNLYHFWRETGTHKVHLHHVQNFQKYGPIYREKLGNVESVYVID  64
P450BMP:  TIKEMPQPKTFGELKNL--PLLNTDKPVQALMKIADELGEIFKFEAPGRVTRYLSS  54
CYP2C5 :  GKLPPGPTPFPIIGNILQI--DAKDISKSLTKFSECYGPVFTVYLGMKPTVVLHG  79
             A' Helix                A Helix     β1-1    β1-2

CYP11A1:  PEDVALLFKSEGPNPERFLIP-PWVAYHQYYQRPIGVLL---KK            104
P450BMP:    QRLIKEACDES---RFDKNLSQALKFV-RDFAGDGLFTSWTH             92
CYP2C5 :    YEAVKEALVDL-GEEFAGRGSV-PILE-KVSKGLGIAFS--N            116
           B helix       β1-5    B' Helix

CYP11A1:  SAAWKKDRVAL-NQEVMAPETTKNFLPLLDAVSRDFVSVLHRRIKKAGSGNFSGD 158
P450BMP:  EKNWKKAHNILL-PSFSQQ-----AMKGYHAMMVDIAVQLVQKWERLNADEHIEV 141
CYP2C5 :  AKTWKEMRRFSLMTLRNFG----MGKRSIEDRIQEEARCLVEELRKTNASPCD   165
           C Helix    C' Helix            D Helix          β3-1

CYP11A1:  ISDDLFRFAFESITNVIFGERQGM-LEEVVNPEAQRFIDAIYQMFHTSVPMLNL   211
P450BMP:    PEDMTRLTLDTIGLCGFNYRFNSFYRDQPHPFITSMVRALDEAM-NKLQRAN    192
CYP2C5 :  PTFILGCAPCNVICSVIFHNRFDYKDEEF-LKLMESLHENVELLGTPWLQVYNNFP 220
             E Helix                        F Helix

CYP11A1:     PPDLFRLFRTKTWKDHVAAWDVIFSKADMYTENFYWELRQK             252
P450BMP:     PDDPAYDENKRQFQEDIKVMND--LVDKIIADRKASGEQ-SD            231
CYP2C5 :  ALLDYFPGIHKTLLKNADYIKNFIMEKVKEHQKLLDVNN-PR               261
                        G Helix

CYP11A1:  GNVHHDYRGILYRLLGDSKMSFEDIKANVTEMLAGGVDTTSMTLQWHLYEMAR   305
P450BMP:  DLLTHMLNGKDPET-GEPL-DDENIRYQIITFLIAGHETTSGLLSFALYFLVK   282
CYP2C5 :  DFIDCFLIKMEQEN-NLEF-TLESLVIAVSDLFGAGTETTSTTLRYSLLLLK   312
           H Helix                      I Helix

CYP11A1:  NLKVQDMLRAEVLAARRQAQGDMATMLQLVPLLKASIKETLRLHPISV         353
P450BMP:  NPHVLQKAAEEAARVLVDPVPSYKQVKQL-KYVGMVLNEALRLWPTA         328
CYP2C5 :  HPEVAARVQEEIERVIGRHRSPCMQDRSRMPYTDAVIHEIQRFIDLLP         360
               J Helix       J' Helix   K Helix

CYP11A1:  TLQRYLV-NDLVL-RGYMIPAKTLVQVA-IYALGREPTFFF-DPENFDPTRW    401
P450BMP:  PAFSLYAKEDTVLGGEYPLEKGDELMVL-IPQLHRDKTIWGDDVEEFRPERF    379
CYP2C5 :  TNLPHAVTRDVRF-RNYFIPKGTDIITS-LTSVLHDEKAFP-NPKVFDPGHF    409
          β1-4   β2-1     β2-2  β1-3    K' Helix

CYP11A1:  L--SKD-KNITYFRNLGFGWGVRQCLGRRIAELEMTIFLINMLE            442
P450BMP:  ENPSA---IPQH-AFKPFGNGQRACIGQQFALHEATLVLGMMLK            419
CYP2C5 :  LDESGNFKKSDY--FMPFSAGKRMCVGEGLARMELFLFLTSILQ            451
                                    L Helix

CYP11A1:  NFRVEIQHLS-DVGTTFNLILMPEKPISFTFWPFNQEATQQ               482
P450BMP:  HFDFEDHTN---YELDIKE-TLTLKPEGFVVKAKSKKIPLGGI             458
CYP2C5 :  NFKLQSLVEPKDLDITAVVNGFVSVPPSYQLCFIPIH                   487
          B3-3         β4-1     β4-2    β3-2
```

Fig. 1. Alignment of the deduced amino acid sequence of baboon CYP11A1 with CYP102 and CYP2C5 used to construct the three-dimensional model. Helical and sheet elements are underlined and labelled.

3. Results

3.1Characterization of CYP11A1

The RT-PCR amplification of baboon mRNA yielded a single 1566bp product, which was subjected to either a second round of amplification using high fidelity polymerase for direct sequence analysis or Taq DNA polymerase prior to ligation into the pTargeT^{TM} mammalian expression vector system. Sequence analysis of baboon CYP11A1 cDNA (GenBank accession no. AY 702067) revealed 8 amino acids differences when compared to human CYP11A1 viz. T124A, F155Y, M240I, E243Q, N254S, I262M, R322H and G367D. Seven amino acid differences were evident when constructs CYP11A1a, CYP11A1b and CYP11A1c were compared to baboon CYP11A1 cDNA (table 2).

Three single mutants of CYP11A1, I98Q, K103A and T291A, were created using the primers listed in table 1. The successful insertion of the intended mutations was confirmed by direct sequence analysis.

Table 2
Corresponding amino acid residues of baboon CYP11A1 cDNA and the constructs, CYP11A1a, CYP11A1b, CYP11A1c, I98Q, K103A and T291A. Amino acid substitutions are shown in bold.

Position	Baboon CYP11A1 cDNA	CYP11A1a	CYP11A1b	CYP11A1c	I98Q	K103A	T291A
98	I	I	**K**	I	**Q**	I	I
103	K	K	K	K	K	**A**	K
141	S	**N**	S	S	S	S	S
157	G	**W**	G	G	G	G	G
199	Y	**H**	Y	Y	Y	Y	Y
240	M	M	M	**V**	M	M	M
291	T	T	T	**S**	T	T	**A**
443	N	N	N	**S**	N	N	N

3.2. Enzymatic activity of baboon CYP11A1 mutants in COS-1 cells

The plasmids were cotransfected with a pCI-neo/human Adx construct into COS-1 cells to analyze the enzymatic activity of the CYP11A1 constructs. Endogenous renodoxin reductase and renodoxin support low levels of CYP11A1 activity in COS-1

cells, with the addition of Adx increasing the activity of CYP11A1 [45]. The cells were incubated with 25-hydroxycholesterol and assayed for the conversion to pregnenolone to assess enzyme activity. The use of 25-hydroxycholesterol as substrate, which readily diffuses from the extracellular environment to the mitochondria, circumvented the action of the StaR protein which limits the rate at which cholesterol enters the mitochondria [47]. In addition, the side-chain cleavage of 25-hydroxycholesterol requires the same three oxidative steps as cholesterol, unlike the commonly used 22R-hydroxycholesterol, which bypasses the 22-hydroxylation [8]. Although 25-hydroxycholesterol binds slightly stronger to CYP11A1 than cholesterol, it is still relatively weakly bound compared to 22R-hydroxyl or 20α-hydroxyl derivatives [9]. Conversion assays using concentrations of 25-hydroxycholesterol ranging from 0.125 to 5 μM were preformed in triplicate. K_m and V values determined by direct linear plots (data not shown) did not differ significantly from the values obtained by non-linear regression (table 3). As the K_m value of a complex enzyme like CYP11A1 is influenced by a number of factors which include the membrane environment, redox partner type, the substrate and its and availability, the K_m values obtained using different heterologous expression systems cannot be directly compared to one another. Human CYP11A1 was therefore also assayed in order to allow comparison of human and baboon CYP11A1 constructs in the same cellular environment.

Table 3
Summary of kinetics of 25-hydroxycholesterol metabolism by baboon CYP11A1 constructs expressed in COS1 cells. The initial reaction rates of 25-hydroxycholesterol metabolism were determined by linear regression for each substrate concentration. At least four time points were used for each rate determination. The R-squared value for all initial rate regression was always higher than 0.95. K_m values are expressed as the mean ± SEM of three experiments. All K_m values were compared to baboon CYP11A1 cDNA with an unpaired *t* test. *p<0.01, †p<0.0005.

Construct	**K_m (μM)**	**V (nmol·h^{-1}·mg^{-1} total protein)**
CYP11A1 cDNA	1.64 ± 0.13	11.47 ± 0.41
CYP11A1a	1.62 ± 0.12	7.51 ± 0.25
CYP11A1b	4.53 ± 0.38†	13.05 ± 0.66
CYP11A1c	1.86 ± 0.28	9.06 ± 0.28
I98Q	2.81 ± 0.25*	18.92 ± 0.88
K103A	0.94 ± 0.23*	6.21 ± 0.55
Human CYP11A1	1.95 ± 0.16	11.64 ± 0.47

No significant differences in K_m values were observed between baboon and human CYP11A1, indicating that none of the eight amino acid differences influence substrate binding. The same observation was made for CYP11A1a and CYP11A1c, which each differ from the cDNA by three amino acid residues (table 2). In contrast, CYP11A1b (I98K) and the mutant I98Q have K_m values that are 2.8 and 1.7 fold greater than CYP11A1 cDNA, respectively, illustrating the catalytic importance of the residue at this position (Fig. 2). Conversely, the mutant K103A has a K_m value that is 1.8 fold less than CYP11A1 cDNA. No detectable pregnenolone was produced by the mutant T291A after six hours (data not shown).

Unlike the K_m values, which are not dependent on enzyme concentration and can be directly compared to one another if obtained under identical experimental conditions, the V values are influenced by enzyme concentration. The observed variations in V values may therefore result from differing transfection efficiencies. It is, however, interesting to note that the V values obtained for the human and bovine CYP11A1, expressed under identical conditions, did not differ significantly.

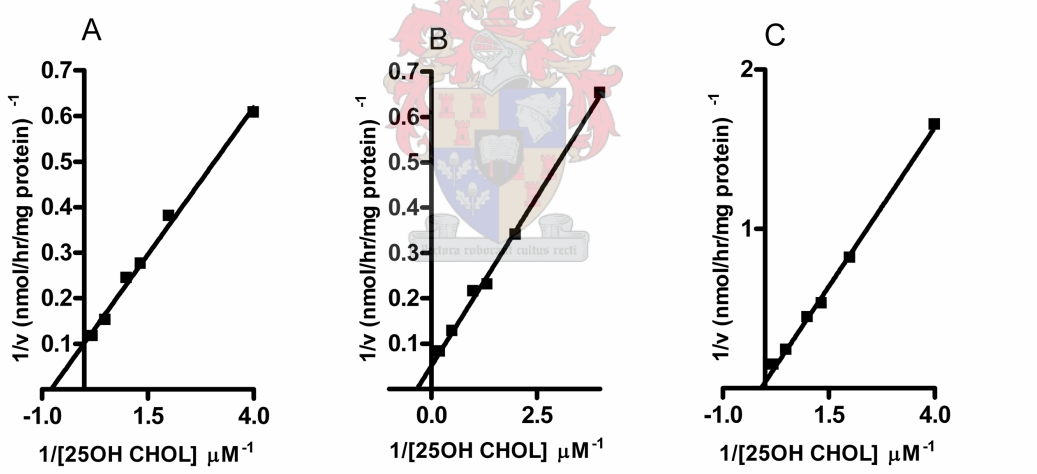

Fig. 2. Kinetics of 25-hydroxycholesterol metabolism by baboon CYP11A1: (A) CYP11A1 cDNA, (B) CYP11A1/Q and (C) CYP11A1b expressed in COS1 cells**.** (A) CYP11A1 cDNA Apparent K_m = 1.640 μM; V value = 11.47 nmol·h^{-1}·mg protein, (B) CYP11A1/Q Apparent K_m = 2.809 μM; V value = 18.92 nmol·h^{-1}·mg protein and (C) CYP11A1b Apparent K_m = 4.530 μM; V value = 13.05 nmol·h^{-1}·mg protein. Results are representative of three independent experiments.

3.3. Modelling

A homology model of CYP11A1 was constructed using the coordinates of CYP102 and CYP2C5 (Fig. 1). We are the first group to incorporate both bacterial and

mammalian cytochrome P450 structural templates. Although the B´ helix is absent in the crystal structure of CYP2C5, a B´ helix was incorporated in the three-dimensional model, as baboon CYP11A1 appears to have a B´ helix similar to CYP102, as determined by the length and amphipathic nature of the residues in this region. Similarly, a B´ helix was also incorporated in the bovine CYP11A1 model of Headman et al., which was based on CYP2C5 [32]. The four tryptophan residues, W20, W27, W231 and W224, which were identified by this group as residues possibly involved in membrane binding, are conserved in our model and located on the distal face of the enzyme. The proximal face has a net positive charge and includes three of the four residues identified in bovine CYP11A1 by Usanov et al. believed to play a role in Adx interaction (K404, K405 and R427). The fourth residue, K268, is replaced by a Gly residue in baboon and human CYP11A1. However, an Arg residue present at position 265 in these species, but absent in the bovine enzyme, may therefore be important for Adx interaction in these species.

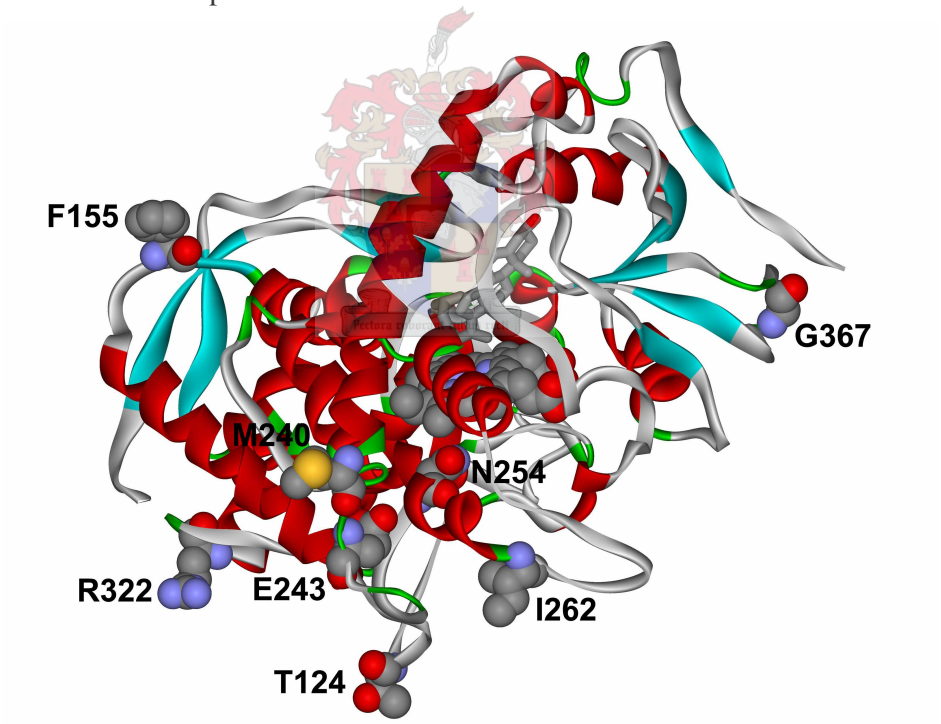

Fig. 3. Computer model of the three-dimensional structure of baboon CYP11A1. The heme and docked cholesterol are visible in the active pocket. The side chains of the amino acid residues, Thr124, Phe155, Met240, Glu243, Asp254, Ile262, Arg322 and Gly367 are indicated. In human CYP11A1 these residues are replaced by Ala, Tyr, Ile, Gln, Ser, Met, His and Asp, respectively.

In our model, the eight amino acid differences observed between baboon cDNA and human CYP11A1 as well as those in CYP11A1a, lie on the surface of the predicted protein structure. The position of the eight amino acid differences between baboon and

human CYP11A1 are indicated in Fig. 3. Five of the amino acid differences, M240I, E243Q, N254S, I262M and R322H, lie within helixes and one, F155Y, lies in a beta sheet. The substitutions T124A and G367D are located in loop regions and are therefore not expected to influence the three dimensional structure of the enzyme as was confirmed by the similar K_m values (table 3).

In CYP11A1a the S141N substitution lies within a turn in the D helix, the G157W substitution lies at the N-terminal of the E helix and the Y199H substitution lies within a turn in the F-helix. In CYP11A1c, two substitutions lie on the surface of the predicted protein structure. M240V lies within a turn in the G helix and N443S lies in the beta sheet β3-3. Structural analysis indicated that these substitutions do not influence the three-dimensional structure of CYP11A1 significantly.

In CYP11A1c, the third substitution, T291S, lies in the middle of the I helix within the active pocket and faces towards the heme (Fig. 6). This conservative substitution does not appear to influence the structure of the I helix and does not affect the activity of the enzyme (table 3). However, the mutation T291A abolished enzymatic activity as was observed for a similar mutation T252A in CYP101 [48].

In both baboon and human CYP11A1, an isoleucine residue at position 98 lies in the B´-C loop. Since this region differs in length, amino acid composition and orientation between different cytochromes P450 [12-15,18], homology modelling of this loop remains difficult with the orientation and positioning of the side-chains remaining uncertain. We previously hypothesised that the side chain of I98 is associated with other hydrophobic residues *viz.* P85, P86, W87, V88 and A89. Our current model based on the crystal structures of CYP102 and CYP2C5 shows that this residue faces directly towards the I helix, and may influence the orientation and stabilisation of the B´-C loop. The construct CYP11A1b has a positively charged lysine replacing this hydrophobic residue, resulting in a 2.8 fold increase in K_m. Subsequent modelling of CYP11A1b, showed that the side chain of K98 points outwards away from the I helix, resulting in a dramatic change in the shape and orientation of the B´ through C helices (Fig. 4). Using both models, we examined the orientation of cholesterol docked in the active pocket. Docking studies revealed a substantial change in the orientation of cholesterol in the active pocket of CYP11A1b, as a result of the structural change of the B´ through C helices (Fig. 4).

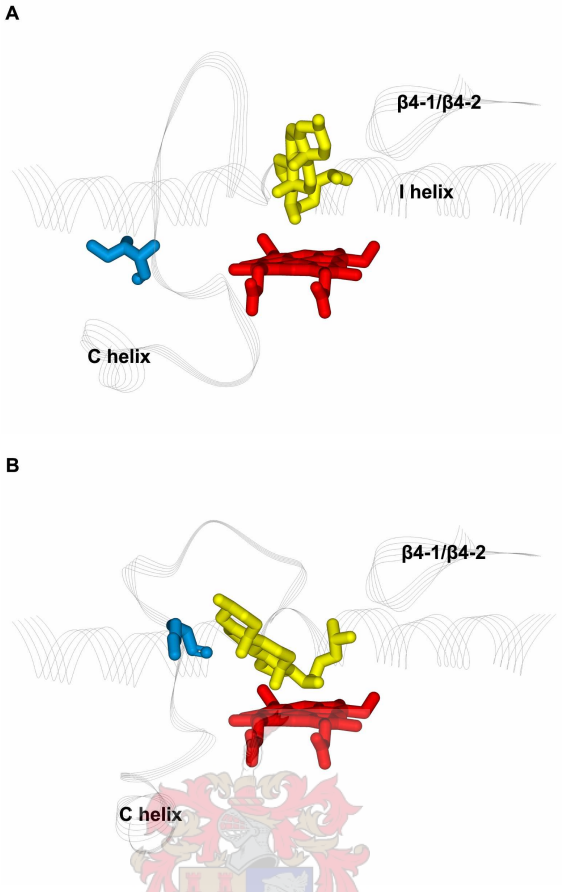

Fig. 4. Putative positions of residue 98 in the B´-C loop of baboon CYP11A1: A) Ile in CYP11A1 cDNA, B) Lys in CYP11A1b.

Two positively charged residues, K103 and K104, lie in the B´-C loop, just N-terminal of the C helix, and the mutation K103A resulted in a 1.8 fold decrease in K_m. It is evident from our model that K103 does not interact directly with the docked substrate, but may nevertheless contribute towards the stabilisation of the B´-C loop. Furthermore, K103 interacts with R421, which in turn is associated with the heme propionate in the active pocket. Since the B´-C loop enters the active pocket on the same level as the heme plane, K103 may be important in orientating the heme in the active pocket by stabilising the B´-C loop via its association with R421 (Fig. 5).

The constructed three-dimensional model was subsequently used to examine the likely binding orientation of cholesterol and its interactions with CYP11A1. Cholesterol was docked manually into the active pocket of the homology model of CYP11A1. Several orientations of cholesterol docked in the active pocket were considered, but only one reached a minimum without inappropriate conflicts between the protein and the substrate when minimised. Residues found within 5Å of the docked cholesterol were

identified and are listed in table 4. The results indicate that each of the predicted residues lies within one of the six SRS's as predicted by Goto [34].

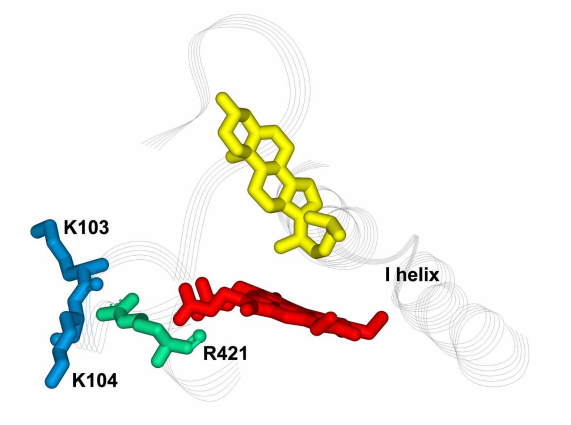

Fig. 5. Putative positions of K103, K104 and R421 in the homology model of baboon CYP11A1 cDNA.

4. Discussion

The absence of the crystal structure of CYP11A1 has complicated deductions pertaining to the structure/function relationships and the three-dimensional orientation of residues in the active pocket. Site-directed mutagenesis can identify amino acid residues important for catalytic activity, but cannot predict their three dimensional orientations in space and thus the mechanism by which they exert a kinetic effect albeit in the active pocket, on substrate binding, or via an indirect mechanism. Site-directed mutagenesis can, however, be used together with molecular modelling as a powerful tool for structure/function investigations [31].

Kinetic analysis revealed that the amino acid residue differences between baboon CYP11A1 cDNA and human CYP11A1 (Fig. 3) do not influence the enzymatic activity significantly as is seen by the similar K_m values (table 3). These amino acid residues located on the surface of the molecule do not affect the structural integrity of the enzyme since, conforming to the paradigm that positions most tolerable to a variety of substitutions are those on the exterior of an enzyme [49-55].

Table 4
Substrate docking results with model of baboon CYP11A1 cDNA. Residues that interact with the docked cholesterol are listed, together with their location and the distance between the nearest atoms of each residue and the docked substrate. Only residues within 5Å of docked cholesterol were considered. The seventeen CYP11A1 sequences available on Genbank were aligned and the conservation of each residue determined. The seventeen species aligned are: human (**NM_000781**), baboon (**AY702067**), cow (**NM_176644**), goat (**D50058**), sheep (**D50057**), horse (**AF031664**), pig (**NM_214427**), mouse (**NM_019779**), hamster (**AF323965**), rat (**NM_017286**), rabbit (**S59219**), chicken (**NM_001001756**), dog (**XM_535539**), zebra finch (**AY633556**), rainbow trout (**S57305**), zebrafish (**NM_152953**) and channel catfish (**AF063836**).

Residue	Shortest distance (Å)	Located	Conserved
Trp87	1.84	B´ helix (SRS1)	17/17
Tyr93	3.90	B´ helix (SRS1)	14/17[a]
Leu101	3.54	B´-C Loop (SRS1)	17/17
Phe194	1.78	F helix (SRS2)	17/17
Ile198	2.45	F helix (SRS2)	5/17[b]
Met201	1.73	F helix (SRS2)	17/17
Thr204	3.81	F-G Loop (SRS3)	17/17
Ser205	4.19	F-G Loop (SRS3)	12/17[c]
Val206	4.14	F-G Loop (SRS3)	12/17[d]
Gly287	1.25	I Helix (SRS4)	17/17
Thr291	1.04	I helix (SRS4)	16/17[e]
Met294	1.92	I helix (SRS4)	14/17[f]
Ile351	1.03	K helix/ β1-4 (SRS5)	12/17[g]
Ser352	3.52	K helix/ β1-4 (SRS5)	12/17[h]
Gln356	3.64	K helix/ β1-4 (SRS5)	16/17[i]
Arg357	2.68	K helix/ β1-4 (SRS5)	17/17
Leu462	0.88	B4-1/ β4-2 (SRS6)	17/17
Met463	2.77	B4-1/ β4-2 (SRS6)	8/17[j]
Pro464	1.53	B4-1/ β4-2 (SRS6)	17/17

[a] Phe in zebra finch and channel catfish; His in pig
[b] Val in all other species
[c] Thr in chicken, zebra finch, rainbow trout and channel catfish
[d] Ser in chicken, zebrafish and rainbow trout; Ala in zebra finch; Cys in channel catfish
[e] Ser in zebra fish
[f] Ile in rainbow trout and channel catfish; Phe in zebrafish
[g] Val in chichen, zebra finch, zebrafish, rainbow trout and channel catfish
[h] Ala in horse, chichen, zebra finch, zebrafish, rainbow trout and channel catfish
[i] Pro in zebrafish
[j] Thr in bovine, goat and sheep; Ile in horse and zebra finch; Val in chicken and channel catfish; Leu in rainbow trout

The catalytic importance of T291 in the active pocket of baboon CYP11A1 was illustrated with the T291S and T291A substitutions. Most cytochromes P450 have a highly conserved threonine residue at this position in the I Helix, believed to play a critical role in dioxygen activation [48,56]. This residue is believed to accept a hydrogen bond from the hydroperoxy (Fe(III)-OOH) intermediate which promotes the second protonation on the distal oxygen atom, leading to O-O bond cleavage [57]. A T252S mutation at this alignment position in CYP101 resulted in the mutant exhibiting essentially the same monooxygenase activity as that of the wild-type enzyme. The T252A mutant, however, exhibited less than 10% of the monooxygenase activity and

approximately 85% of the oxygen consumed was converted to H_2O_2 [48]. In baboon CYP11A1, T291 lies in the middle of the I helix, facing towards the heme. The T291S mutation did not influence enzymatic activity significantly, while the expressed T291A mutant was inactive, demonstrating the importance of a residue with a hydroxyl group at this key position in the active pocket.

One of the most variable domains amongst the cytochromes P450 is the B´-C loop, which forms part of SRS 1 [16,34]. The differences in length, amino acid composition and orientation of this domain permit the cytochromes P450 to catalyse the hydroxylation of an array of diverse substrates [16]. The adaptive positioning of the B´ helix in CYP2C5, reflects the relatively weak interactions of this domain with the rest of the protein structure when different substrates are bound. The B´ helix is flanked by two GXG motifs which contribute to the flexibility of this region in the CYP2 family and the regions preceding and following the GXG motifs, which includes the B´-C loop, are stabilized by interactions with adjacent domains [58,59]. In baboon CYP11A1, I98 appears to stabilise the B´ through C helices through interactions with the I helix. In all of the crystallised mammalian cytochromes P450, a large hydrophobic residue, corresponding to I98 in the B´-C loop is orientated towards the I helix in a similar manner – I112 in CYP2C5, V113 in CYP2B4, L110 in CYP2C8, F110 in CYP2C9 and S116 in CYP3A4. In each case, these residues appear to stabilise the B´ through C helices by interactions with the I helix.

The introduction of a polar or charged amino acid residue into a critical position within the B´-C loop can destabilise this domain and subsequently influence substrate binding. The charged lysine residue at this position in CYP11A1b results in a dramatic change in the shape and orientation of the B´ through C helices as this residue points outwards and no longer stabilises this domain through interactions with the I helix. The structural change of this domain in turn results in a substantial change in the orientation of cholesterol in the active pocket, with the 3β-hydroxyl group being shifted by more than 8Å, resulting in a marked decrease in substrate affinity (table 3). A polar glutamine residue at this position partially restores catalytic activity as it allows for a more favourable conformation of the B´ through C helices and orientation of cholesterol in the active pocket.

While a hydrophobic residue at the N-terminal of the B´-C loop is essential for the orientation of this domain, a charged lysine residue at the C-terminal of the B´-C loop plays a role in orientating the heme in the active pocket. Usanov et al. have previously

shown that mutation of this residue to glutamine results in reduced enzymatic activity possibly due to the destabilisation of the heme in the active pocket [31]. Mutating K103 to alanine yielded a similar decrease in enzymatic activity, but unexpectedly resulted in a greater affinity for the cholesterol substrate (table 3). In our model, K103 and K104 interact with R421, which is in turn associated with the heme propionate (Fig. 5). K103 is therefore essential in maintaining the correct orientation of the heme in the active pocket by stabilising the B´-C loop and via its association with R421. Taken together, our results as well as those of Usanov et al. [31], suggest that mutations of K103 may change the orientation of the heme in the active pocket that results in cholesterol binding more tightly, but in an orientation that is not optimal for side-chain cleavage.

Docking studies were further used to predict the orientation of cholesterol in the active pocket, and to identify residues that may interact with the docked cholesterol. In the most favourable orientation cholesterol binds with its side chain orientated towards the beta plates, β4-1 and β4-2, within SRS6 and the 3β-hydroxyl orientated towards the B´ helix within SRS1 (Fig. 4) [34]. In this orientation the 22(R)-hydrogen of cholesterol is located in line with the heme iron approximately perpendicular to the heme plane (3.51Å from iron) as was predicted by Heyl et al. [9] and similar to the orientation of testosterone docked in the active pocket of a CYP2B1 model [58]. Furthermore, Negishi et al. have provided evidence that the C3 position of steroids interact with residue A117 in CYP2A4 and V117 in CYP2A5, which are situated within SRS1 [60].

This orientation of cholesterol offers a feasible explanation for the ability of human CYP11A1 to catalyse the side chain-cleavage of cholesterol sulphate and cholesterol esters with acyl chain lengths of up to four carbons [10]. The crystal structures of CYP2C5, CYP2C9 and CYP2B4 have revealed that the B´ through C helices exhibit significant flexibility [18,20,23]. An induced fit model of substrate binding was proposed for CYP2C5 since the B´ helix adopts different orientations depending on the bound substrate [18]. The additional carbon atoms in the fatty acid esters could therefore be accommodated by the flexibility of this domain, allowing the fatty acid esters to bind in the active pocket with K_m values similar to that of cholesterol, but in an orientation not optimal for side chain cleavage, as was observed by the decreased turnover rate [Robert Tuckey, personal communication, 10].

Residues important for orientating cholesterol in the active pocket are W87, Y93, F194, I198, T291, M294, S352, R357, L462 and P464. W87 and Y93 both lie within the B´ helix, while F194 and I198 lie in the F helix. These residues all interact with

cholesterol via hydrophobic interactions. Pikuleva et al. have previously mutated Y93 and Y94 and found that mutating Y94 decreased binding of cholesterol, 22(R)-hydroxycholesterol and 25-hydroxycholesterol, while mutating Y93 affected only the binding of cholesterol [11]. In our model, Y93 is 3.90Å from the nearest atom in cholesterol (Fig. 6). The hydroxycholesterols may therefore be bound in an orientation that is further removed and unaffected by Y93. Y94, however, is pointed away from the active pocket and the influence of this residue on the binding of cholesterol and its hydroxyl derivatives is probably via an indirect mechanism resulting from a change in the spatial orientation of the B´ through C helices. T291 and M294 are located in the I helix and interact with the side-chain of cholesterol, pushing it towards the beta sheets, β4-1 and β4-2, where it interacts with L462 and P464 (Fig. 6). Woods et al. have previously mutated I461 to Leu and found that this mutation caused a decrease in the catalytic rate constant with cholesterol as substrate, increased K_m for 22(R)-hydroxycholesterol, but did not affect the kinetic constants for 20α-hydroxycholesterol. This suggested that the side chains of cholesterol, 22(R)-hydroxycholesterol and 20α-hydroxycholesterol occupy slightly different positions in the active pocket, with I461 in close proximity to the side chain binding site [2]. Although I461 does not interact directly with the side chain of cholesterol in our model, it is situated within β4-1 and β4-2, adjacent to residues, L462 and P464, which do.

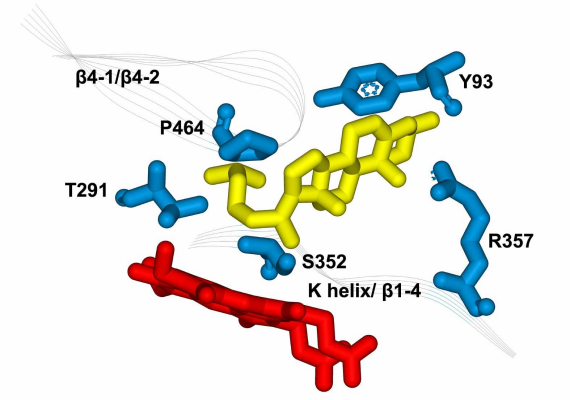

Fig. 6. Putative positions of the active site residues T93, T291, S352, R357 and P464, in the homology model of baboon CYP11A1 cDNA.

The binding of different 3β-hydroxysteroids has lead to the proposal that hydrogen bonding between the 3β-oxygen of cholesterol and a residue in the active pocket is important for substrate binding [9]. No such hydrogen bond was detected in

our model with docked cholesterol. However, R357, located in the loop between the K helix and β1-4 in SRS5, is pointed towards the docked cholesterol and is within 4Å of the 3β-hydroxyl group (Fig. 6). It is possible that a hydrogen bond may form between R357 and the 3β-oxygen of the reaction intermediates 22(R)-hydroxycholesterol and 22,20-dihydroxycholesterol, facilitating the 20α-hydroxylation and the cleavage of the 20-22 bond [2,9,11]. This hypothesis is supported by the observation that the derivatives of cholesterol, 22(R)-hydroxyl- and/or a 20α-hydroxycholesterol, bind significantly tighter to CYP11A1 than do cholesterol or 25-hydroxycholesterol. S352, located in the loop between the K helix and β1-4, is pointed towards the heme in the active pocket, in an orientation favourable for hydrogen bonding with the 22(R)-hydroxyl group, a bond believed to be responsible for mediating the orientation of the intermediate in the subsequent 20α-hydroxylation as shown in figure 6 [9]. Such a shift in the orientation of 22(R)-hydroxycholesterol towards S352 would result in the intermediate being orientated further from Y93, offering a feasible explanation for the effect of this residue on the binding of cholesterol, but not that of 22(R)-hydroxycholesterol [11].

The data obtained in this study demonstrates that valuable insight into the structure/function of CYP11A1 may be gleaned from using homology modelling since the enzyme is not amenable to the standard crystallization techniques. We have shown that amino acid changes on the surface of CYP11A1 do not impact greatly on the catalytic activity of the enzyme even though the changes may not all be conservative. The importance and the flexibility of the B´ through C helices as a substrate binding domain have been confirmed in a mitochondrial cytochrome P450. Furthermore, this study added to previous evidence in the literature strongly indicating that cholesterol is bound in the active pocket of CYP11A1 with the 3β-hydroxyl group interacting with the B´ helix, while the side chain interacts with beta plates, β4-1 and β4-2. These results have provided evidence for a topological model of the active pocket of CYP11A1.

Acknowledgments

The authors wish to thank the NRF, the University of Stellenbosch and the Wilhelm Frank Bursary Fund for financial Support. Human pCI-neo Adx and human pECE-CYP11A1 were generous gifts from Robert C. Tuckey and Walter L. Miller, respectively.

References

[1] B.C. Chung, K.J. Matteson, R. Voutilainen, T.K. Mohandas, W.L. Miller, Human cholesterol side-chain cleavage enzyme, P450scc: cDNA cloning, assignment of the gene to chromosome 15, and expression in the placenta, Proc. Natl. Acad. Sci. USA. 83 (1986) 8962-8966.

[2] S.T. Woods, J. Sadleir, T. Downs, T. Triantopoulos, M. Headlam, R.C. Tuckey, Expression of catalytically active human cytochrome P450scc in Escherichia coli and mutagenesis of isoleucine-462, Arch. Biochem. Biophys. 353 (1998) 109-115.

[3] K. Morohashi, Y. Fujii-Kuriyama, Y. Okada, K. Sogawa, T. Hirose, S. Inayama, T. Omura, Molecular cloning and nucleotide sequence of cDNA for mRNA of mitochondrial cytochrome P450(SCC) of bovine adrenal cortex, Proc. Natl. Acad. Sci. USA. 81 (1984) 4647-4651.

[4] E. Okuyama, T. Okazaki, A. Furukawa, R. Wu, Y. Ichikawa, Molecular cloning and nucleotide sequences of cDNA clones of sheep and goat adrenocortical cytochrome P450scc (CYP11A1), J. Steroid Biochem. Mol. Biol. 57 (1996) 179-185.

[5] O. Nomura, O. Nakabayashi, K. Nishimori, S. Mizuno, The cDNA cloning and transient expression of a chicken gene encoding cytochrome P450scc, Gene. 185 (1997) 217-222.

[6] F. Vilchis, B. Chávez, F. Larrea, C. Timossi, F. Montiel, The cDNA cloning and tissue expression of the cytochrome P450scc from Syrian Hamster (Mesocricetus auratus), Gen. Comp. Endocrinol. 126 (2002) 279-286.

[7] R.C. Tuckey, K.J. Cameron, Side-chain specificities of human and bovine cytochromes P450scc, Eur. J. Biochem. 217 (1993) 209-215.

[8] J.D. Lambeth, S.E. Kitchen, A.A. Farooqui, R.C. Tuckey, H. Kamin, Cytochrome P450scc substrate interactions, J. Biol. Chem. 257 (1982) 1876-1884.

[9] B.L. Heyl, D.J. Tyrrell, J.D. Lambeth, Cytochrome P-450scc-substrate interactions. Role of the 3β- and side chain hydroxyls in binding to oxidized and reduced forms of the enzyme, J. Biol. Chem. 261 (1986) 2743-2749.

[10] R.C. Tuckey, J. Lawrence, K.J. Cameron, Side-chain cleavage of cholesterol esters by human P450scc, J. Steroid Biochem. Mol. Biol. 58 (1996) 605-610.

[11] I.A. Pikuleva, R.L. Mackman, N. Kagawa, M.R. Waterman, P.R. Ortiz de Montellano, Active-site topology of bovine cholesterol side-chain cleavage cytochrome P450 (P450scc) and evidence for interaction of tyrosine 94 with the side chain of cholesterol, Arch. Biochem. Biophys. 322 (1995) 189–197.

[12] T.L. Poulos, B.C. Finzel, I.C. Gunsalus, G.C. Wagner, J. Kraut, The 2.6-Å crystal structure of Pseudomonas putida cytochrome P-450, J.Biol. Chem. 260 (1985) 16122-16130.

[13] T.L Poulos, B.C. Finzel, A.J. Howard, High-resolution crystal structure of cytochrome P450cam, J. Mol. Biol. 195 (1987) 687-700.

[14] K.G. Ravichandran, S.S. Boddupalli, C.A. Hasemann, J.A. Peterson, J. Deisenhofer, Crystal structure of hemoprotein domain of P450BM-3, a prototype for microsomal P450's, Science 261 (1993) 731-736.

[15] C.A. Hasemann, K.G. Ravichandran, J.A. Peterson, J. Deisenhofer, Crystal structure and refinement of cytochrome P450terp at 2.3 Å resolution, J. Mol. Biol. 236 (1994) 1169-1185.

[16] S. Graham-Lorence, J.A. Peterson, P450s: Structural similarities and functional differences, FASEB J. 10 (1996) 206-214.

[17] J. Cosme, E.F. Johnson, Engineering microsomal cytochrome P450 2C5 to be a soluble, monomeric enzyme: Mutations that alter aggregation, phospholipid dependence of catalysis, and membrane binding, J. Biol. Chem. 275 (2000) 2545-2553.

[18] M.R. Wester, E.F. Johnson, C. Marques-Soares, S. Dijols, P.M. Dansette, D. Mansuy, C.D. Stout, Structure of a substrate complex of mammalian cytochrome P450 2C5 at 2.3Å resolution: Evidence for multiple substrate binding modes, Biochemistry. 42 (2003) 9335-9345.

[19] P.A. Williams, J. Cosme, A. Ward, H.C. Angove, V.D. Matak, H. Jhoti, Crystal structure of human cytochrome P450 2C9 with bound warfarin, Nature 424 (2003) 464–468.

[20] M.R. Wester, J.K. Yano, G.A. Schoch, C. Yang, K.J. Griffin, C.D. Stout, E.F. Johnson, The structure of human cytochrome P450 2C9 complexed with flurbiprofen at 2.0-Å Resolution, J. Biol. Chem. 279 (2004) 35630–35637.

[21] G.A. Schoch, J.K. Yano, M.R. Wester, K.J. Griffin, C.D. Stout, E.F. Johnson, Structure of Human Microsomal Cytochrome P450 2C8: Evidence for a peripheral fatty acid binding site, J. Biol. Chem. 279 (2004) 9497–9503.

[22] E.E. Scott, Y.A. He, M.R. Wester, M.A, White, C.C. Chin, J.R. Halpert, E.F. Johnson, C.D. Stout, An open conformation of mammalian cytochrome P450 2B4 at 1.6 A° resolution, Proc. Natl. Acad. Sci. USA. 100 (2003) 13196–13201.

[23] E.E. Scott, M.A. White, Y.A. He, E.F. Johnson, C.D. Scout, J.R. Halbert, Structure of Mammalian Cytochrome P450 2B4 Complexed with 4-(4-Chlorophenyl)imidazole at 1.9-Å Resolution: Insight into the range of P450 conformations and the coordination of redox partner binding, J. Biol. Chem. 279 (2004) 27294-27301.

[24] E.E. Scott, H. Liu, Y.A. He, W. Li, J.R. Halpert, Mutagenesis and molecular dynamics suggest structural and functional roles for residues in the N-terminal portion of the cytochrome P450 2B1 I helix, Arch. Biochem. Biophys. 423 (2004) 266-276.

[25] P.A. Williams, J. Cosme, D.M. Vinkovic´, A. Ward, H.C. Angove, P.J. Day, C. Vonrhein, I.J. Tickle, H. Jhoti, Crystal structures of human cytochromeP450 3A4 bound to metyrapone and progesterone, Science 305 (2004) 683–686.

[26] J.K. Yano, M.R. Wester, G.A. Schoch, K.J. Griffin, C.D. Stout, E.F. Johnson, The structure of human microsomal cytochrome P450 3A4 determined by X-ray crystallography to 2.05 Å resolution, J. Biol. Chem. 279 (2004) 38091–38094.

[27] C.A. Kemp, J.D. Marechala, M.J. Sutcliffe, Progress in cytochrome P450 active site modelling, Arch. Biochem. Biophys. 433 (2005) 361–368.

[28] S.B. Kirton, C.A. Kemp, N.P. Tomkinson, S. St.-Gallay, M.J. Sutcliffe, Impact of incorporating the 2C5 crystal structure into comparative models of cytochrome P450 2D6, Proteins 49 (2002) 216-231.

[29] S. Vijayakumar, J.C. Salerno, Molecular modeling of the 3-D structure of Cytochrome P-450scc, Biochim. Biophys. Acta. 1160 (1992) 281–286.

[30] D.F.V. Lewis, P. Lee-Robichaud, Molecular modelling of steroidogenic cytochromes P450 from families CYP11, CYP17, CYP19 and CYP21 based on the CYP102 crystal structureJ. Steroid Biochem. Mol. Biol. 66 (1998) 217-233.

[31] S.A. Usanov, S. Graham, G.I Lepesheva, T.N. Azeva, N.V. Strushkevich, A.A. Gilep, R.W. Estabrook, J.A. Peterson, Probing the Interaction of Bovine Cytochrome P450scc (CYP11A1) with Adrenodoxin: Evaluating Site-Directed Mutations by Molecular Modeling, Biochemistry. 41 (2002) 8310-8320.

[32] M.J. Headlam, M.C. Wilce, R.C. Tuckey, The F–G loop region of Cytochrome P450scc (CYP11A1) interacts with the phospholipid membrane, Biochim. Biophys. Acta. 1617 (2003) 96–108.

[33] V. Sivozhelezova, C. Nicolinia, Homology modeling of cytochrome P450scc and the mutations for optimal amperometric sensor, J. Theor. Biol. 234 (2005) 479–485.

[34] O. Gotoh, Substrate recognition sites in cytochrome P450 family 2 (CYP2). Proteins inferred from comparative analysis of amino acid and coding nucleotide sequences, J. Biol. Chem. 267 (1992) 83-90.

[35] J.A. Peterson, S.E. Graham, A close family resemblance: the importance of structure in understanding cytochromes P450, Structure. 6 (1998) 1079-1085.

[36] T. Aoyama, K. Korzekwa, K. Nagata, M. Adesnik, A. Reiss, D.P. Lapenson, J. Gillette, H.V. Gelboin, D.J. Waxman, F.J. Gonzalez, Sequence requirements for cytochrome P4502B1 catalytic activity: Alterations of the stereospecificity and regionselectivity of steroid hydroxylation by a simultaneous change of two hydrophobic amino acid residues to phenylalanine, J. Biol. Chem. 264 (1989) 21327-21333.

[37] T. Kronbach, T.M. Larabee, E.F. Johnson, Hybrid cytochromes P450 identify a substrate binding domain in P4502C5 and P4502C4, Proc. Natl. Acad. Sci. USA. 86 (1989) 8262-8265.

[38] T. Kronbach, E.F. Johnson, An inhibitory monoclonal antibody binds in close proximity to a determinant for substrate binding in cytochrome P4502C5, J. Biol. Chem. 266 (1991) 6215-6220.

[39] T. Kronbach, B. Keper, E.F. Johnson, A hypervariable region of P4502C5 confers progesterone 21-hydroxylase activity to P4502C1, Biochemistry. 30 (1991) 6097-6102.

[40] R.P.L. Lindberg, M. Negishi, Alterations of mouse cytochrome P450coh substrate specificity by mutation of a single amino acid residue, Nature. 339 (1989) 632-634.

[41] M. Christou, M.J. Mitchell, T. Aoyama, H.V. Gelboin, F.J. Gonzalez, C.R. Jefcoate, Selective suppression of the catalytic activity of cDNA-expressed cytochrome P4502B1 towards polycyclic hydrocarbons in the microsomal membrane: Modifications of this effect by specific amino acid substitutions, Biochemistry. 31 (1992) 2835-2841.

[42] E.F. Johnson, T. Kronbach, M. Hsu, Analysis of the catalytic specificity of cytochrome P450 enzymes through site-directed mutagenesis, FASEB J. 6 (1992) 700-705.

[43] J.R. Halbert, Y. He, Engineering of cytochrome P450 2B1 specificity. Conversion of an androgen 16 beta-hydroxylase to a 15 alpha-hydroxylase, J. Biol. Chem. 268 (1993) 4453-4457.

[44] K. Storbeck, P. Swart, S. Graham, A.C. Swart, The Influence of the Amino Acid Substitution I98K on the Catalytic Activity of Baboon Cytochrome P450 Side-Chain Cleavage (CYP11A1), Endocr. Res. 30 (2004) 761-767.

[45] M.X. Zuber, J.I. Mason, E.R. Simpson, M.R. Waterman, Simultaneous transfection of COS-1 cells with mitochondrial and microsomal steroid hydroxylases: Incorporation of a steroidogenic pathway into nonsteroidogenic cells, Proc. Natl. Acad. Sci. USA. 85 (1988) 699-703.

[46] R. Eisenthal, A. Cornish-Bowden, The direct linear plot. A new graphical procedure for estimating enzyme kinetic parameters, Biochern. J. 139 (1984) 715-720.

[47] D.M. Stocco, B.J. Clark, Regulation of the acute production of steroids in steroidogenic cells, Endocr. Rev. 17 (1996) 221-244.

[48] M. Imai, H. Shimada, Y. Watanabe, Y. Matsushima-Hibiya, R. Makino, H. Koga, T. Horiuchi, Y. Ishimura, Uncoupling of the cytochrome P450cam monooxygenase reaction by a single mutation, threonine 252 to alanine or valine: A possible role of the hydroxy amino acid in oxygen activation, Proc. Natl. Acad. Sci. USA. 86 (1989) 7823-7827.

[49] J.F. Reidhaar-Olson, R.T. Sauer, Combinatorial cassette mutagenesis as a probe of the informational content of protein sequences, Science. 241 (1988) 53-57.

[50] J.U. Bowie, J.F. Reidhaar-Olson, W.A. Lim, R.T. Sauer, Deciphering the message in protein sequences: tolerance to amino acid substitutions, Science. 247 (1990) 1306-1310.

[51] D. Rennell, S.E. Bouvier, L.W. Hardy, A.R. Poteete, Systematic mutation of bacteriophage-T4 lysozyme, J. Mol. Biol. 222 (1991) 67-87.

[52] T.C. Terwilliger, H.B. Zabin, M.P. Horvath, W.S. Sandberg, P.M. Schlunk, In vivo characterization of mutants of the bacteriophage f1 gene V protein isolated by saturation mutagenesis, J. Mol. Biol. 236 (1994) 556-571.

[53] J. Suckow, P. Markiewicz, L.G. Kleina, J. Miller, B. Kisters-Woike, B. Muller-Hill, Genetic studies of the Lac repressor XV: 4000 single amino acid substitutions and analysis of the resulting phenotypes on the basis of the protein structure, J. Mol. Biol. 261 (1996) 509-523.

[54] W. Huang, J. Petrosino, M. Hirsch, P.S. Shenkin, T. Palzkill, Amino acid sequence determinants of b-lactamase structure and activity, J. Mol. Biol. 258 (1996) 688-703.

[55] D.D. Axe, N.W. Foster, A.R. Fersht, A search for single substitutions that eliminate enzymatic function in a bacterial ribonuclease, Biochemistry. 37(1998) 7157-7166.

[56] S.A. Martinis, W.M. Atkins, P.S. Stayton, S.G. Sligar, A conserved residue of cytochrome P450 is involved in heme-oxygen stability and activation, J. Am. Chem. Soc. 111 (1989) 9252-9253.

[57] S. Nagano, T.L. Poulos, Crystallographic study on the dioxygen complex of wild-type and mutant cytochrome P450cam: Implications for the dioxygen activation mechanism, J. Biol. Chem. 280 (2005) 31659 – 31663.

[58] W. Honma, W. Li, H. Liu, E.E. Scott, J.R. Halbert, Functional role of residues in the helix B´ region of cytochrome P450 2B1, Arch. Biochem. Biophys. 435 (2005) 157-165.

[59] E.F. Johnson, Deciphering substrate recognition by drug-metabolizing cytochromes P450, Drug Metab. Dispos. 31 (2003) 1532–1540.

[60] M. Negishi, T. Uno, T.A. Darden, T. Sueyoshi, L.G. Pedersen, Structural flexibility and functional versatility of mammalian P450 enzymes, FASEB J. 10 (1996) 683-689.

CHAPTER 7
GENERAL DISCUSSION

The aim of this study was to investigate CYP11A1, an essential enzyme in adrenal steroidogenesis, by structure/function analysis. The absence of the crystal structure of CYP11A1 has complicated deductions pertaining to structure/function relationships. Sequence alignments of deduced amino acid residues of CYP11A1 from various species have allowed the prediction of steroid- and heme-binding domains with some success [193,207,208,210], while site-directed mutagenesis and kinetic studies have identified residues of catalytic importance in the active pocket [194,270]. In the absence of a solved crystal structure, neither the three-dimensional structure of the enzyme nor the residues that constitute its active pocket have, to date, been accurately identified from sequence alignments, site-directed mutagenesis or kinetic studies. This study therefore aimed to couple data acquired from site-directed mutagenesis and kinetic analysis to structural data obtained from homology modelling, thereby allowing for deductions pertaining to structure/function to be made.

The majority of the homology models of mammalian cytochromes P450 currently available have been generated based on the crystal structures of bacterial enzymes, which share less than 20% homology with the mammalian enzymes [212]. However, comparisons of the soluble bacterial cytochromes P450 revealed that these enzymes do share a common structural core even though these proteins differ in terms of solubility, sequence homology, redox partners and substrate specificity. Since the regions of greatest structural difference play a role in substrate recognition and binding [7], the precise orientation of residues involved in substrate recognition and binding have been difficult to predict using such models. The recent solving of several mammalian cytochromes P450 crystal structures has, however, greatly improved the accuracy of homology modelling. Homology modelling of the cytochromes P450 becomes a powerful tool for investigating an enzyme such as CYP11A1 when combined with techniques such as site-directed mutagenesis and kinetic studies.

In an effort to gain further insight into the structure/function relationship of this essential enzyme, CYP11A1 was characterised in the Cape baboon (Papio ursinus), a species closely related to humans. Baboon CYP11A1 cDNA was previously synthesised by isolating total RNA and mRNA from the adrenals of randomly selected Cape

baboons. The RT-PCR amplification of baboon mRNA yielded a single 1566bp product. During this study the cDNA fragment was amplified by high fidelity DNA polymerase and subjected to direct sequence analysis (GenBank accession no. AY 702067). Baboon CYP11A1 cDNA encodes a predicted 521 amino acid protein, 97% homologous to human CYP11A1 [203]. The putative 39 amino acid presequence is 85% homologous to the human mitochondrial targeting sequence, containing several basic and hydroxylated residues, as well as hydrophobic regions, conforming to the general rule for this domain [271,272]. The mature enzyme shares 98% amino acid homology with mature human CYP11A1, exhibiting eight amino acid differences.

Subsequent to a second round PCR and ligation into a mammalian expression vector system, sequence analysis identified three constructs, CYP11A1a, CYP11A1b and CYP11A1c. Three amino substitutions, S141N, G157W and Y199H, were identified in CYP11A1a, CYP11A1b was found to contain a single amino acid substitution, I98K and three amino acid substitutions, M240V, T291S and N443S, were identified in CYP11A1c when compared to baboon cDNA. These substitutions possibly result from the second round PCR amplification with Taq DNA polymerase prior to ligation into the mammalian expression vector system as this polymerase is not subject to a high degree of stringency. The possibility that different CYP11A1 isoforms are present in the baboon can, however, not be excluded and an effort is currently underway to sequence the baboon genomic DNA.

The three constructs were coexpressed in nonsteroidogenic COS-1 cells with a human adrenodoxin construct and the enzyme activity assayed using 25-hydroxycholesterol as substrate. CYP11A1a, CYP11A1b and CYP11A1c yielded K_m values of 1.62, 4.53 and 1.86 μM, respectively. These kinetic studies therefore suggested that the single amino acid substitution I98K in CYP11A1b has a substantial effect on the enzymatic activity of CYP11A1. The role of this residue was further investigated by constructing a homology model of CYP11A1b based on the crystal structure of the bacterial enzyme CYP102 and rabbit CYP2C5. Structural analysis revealed that in CYP11A1a the S141N substitution lies in the D helix within a helix turn, the G157W substitution at the N-terminal of the E helix and the Y199H substitution in the F-helix. None of these three amino acid substitutions were expected to influence the three-dimensional structure of CYP11A1 significantly. However, the single amino acid substitution, I98K, in CYP11A1b is located in the B´-C loop, a domain associated with substrate binding [8]. The three-dimensional model of

CYP11A1b revealed that the side chain of K98 was turned outwards away from the hydrophobic residues in this pocket. It was hypothesised from this model that the side chain of I98 in CYP11A1a would be turned towards the substrate in the active pocket, associated with other hydrophobic residues viz. P85, P86, W87, V88, and A89 in the active pocket. These preliminary results indicated that I98 might play an important role in the orientation of the B´-C loop, influencing substrate binding. The introduction of a charged lysine residue at position 98 was believed to destabilise this structural domain and cause the observed 2.8 fold increase in K_m in CYP11A1b.

The potential influence of the abovementioned amino acid substitutions were further investigated by cloning and expressing wild type baboon CYP11A1 cDNA. The cDNA was obtained using site-directed mutagenesis, mutating K98 in construct CYP11A1b to isoleucine. Wild type baboon and human CYP11A1 were subsequently coexpressed in nonsteroidogenic COS-1 cells together with a human adrenodoxin construct and the enzyme activity was assayed using 25-hydroxycholesterol as substrate. These constructs yielded K_m values of 1.64 and 1.95 μM for baboon and human CYP11A1, respectively. These values, together with that obtained for CYP11A1a and CYP11A1c, do not differ statistically from each other and confirmed our previous hypothesis that the three amino acid substitutions present in CYP11A1a, which has a K_m value of 1.62 μM, do not affect the enzymatic activity of CYP11A1.

A homology model of the baboon CYP11A1 cDNA was constructed based on the crystal structures of CYP102 and CYP2C5. Structural analysis revealed that the eight amino acid residue differences between baboon and human CYP11A1 are located on the surface of the model and are therefore not expected to alter the three-dimensional structure of CYP11A1 significantly. This conforms to the paradigm that positions most tolerable to a variety of substitutions are those on the exterior of an enzyme [273-279]. Six of the eight changes lie within helixes or beta sheet, while the two least conservative substitutions, T124A and G367D, are located in loop regions. These changes did not influence the affinity of the enzyme for its substrate as was confirmed by the similar K_m values of the expressed enzymes. Similarly, two of the three substitutions observed in CYP11A1c are located on the exterior of the enzyme – the M240V substitution lies within a turn in the G helix and N443S lies in the beta sheet, β3-3.

One of the three substitutions in CYP11A1c, T291S, lies in the middle of the I helix within the active pocket and faces towards the heme. A highly conserved threonine residue at this alignment position is present in the majority of the cytochromes

P450, and is believed to play a critical role in dioxygen activation [280,281]. It has been postulated that this threonine residue accepts a hydrogen bond from the hydroperoxy (Fe(III)-OOH) intermediate that promotes the second protonation on the distal oxygen atom, leading to O-O bond cleavage [282]. The mutation of the T252 residue to serine in CYP101 resulted in the mutant exhibiting essentially the same monooxygenase activity as that of the wild-type enzyme. The mutant T252A, however, exhibited less than 10% of the monooxygenase activity observed in the wild type. Approximately 85% of the oxygen consumed by the T252A mutant was converted to H_2O_2 [280]. In the baboon construct, CYP11A1c, the substitution T291S did not result in a significant change in enzymatic activity, as is reflected by the K_m value of 1.86 μM. obtained from kinetic studies. However, when this residue was mutated to alanine, the conversion of 25-hydroxycholesterol was negligible, further demonstrating the importance of a residue with a hydroxyl group at this key position.

The homology model together with the kinetic analysis clearly demonstrated that of the amino acid substitutions seen in the constructs (CYP11A1a, CYP11A1b and CYP11A1c), only one, I98K, influenced the three-dimensional structure and enzymatic activity of CYP11A1. Both baboon and human CYP11A1 have an isoleucine residue at position 98 in the B´-C loop. A preliminary model of CYP11A1b, indicated that the side chain of I98 could turn towards the substrate in the active pocket, associating with other hydrophobic residues *viz.* P85, P86, W87, V88 and A89. However, subsequent modelling of the CYP11A1 cDNA subsequently revealed that this residue faces directly towards the I helix and appears to stabilise the B´ through C helices. Similarly, in all the crystal structures of the mammalian cytochromes P450 obtained to date, a large hydrophobic residue at a similar alignment position in the B´-C loop is orientated towards the I helix – I112 in CYP2C5, V113 in CYP2B4, L110 in CYP2C8, F110 in CYP2C9 and S116 in CYP3A4.

The adaptive positioning of the B´ helix in CYP2C5, reflects the relatively weak interactions of this domain with the rest of the protein structure with different substrates bound to the enzyme. The B´ helix is flanked by two GXG motifs that contribute to the flexibility of this region in the CYP2 family [283]. The loop regions preceding and following the GXG motifs, which include the B´-C loop, are stabilized by interactions with adjacent structures [283,284]. In CYP2C5 and CYP2B4 bound with a phenylimidazole inhibitor, I112 and V113 lie directly after the second GXG motif in

each enzyme, respectively, while in CYP2C8 and CYP2C9, L110 and F110 lie in the second GXG motif of each enzyme, respectively. In each case, the abovementioned residues appear to stabilise the B´ through C helices by interactions with the I helix.

Residues within the B´ through C helices have previously been shown to be important determinants of substrate selectivity, sterio- and regiospecificity. Aoyama et al. showed that the mutation I114F in rat CYP2B1 was essential when expressing a double mutant (L58F, I114F) that exhibited the altered regiospecificity for steroid hydroxylation seen in an allelic form of CYP2B2 [285]. Halbert and He observed that the mutations I114V and I114A resulted in a decrease in 16β-OH:16αOH and an increases in 15α-OH:16-OH androgen ratios in rat CYP2B1 for both mutations [286]. In rabbit CYP2C4 and CYP2C5, residue 113 is responsible for the >10-fold difference in K_m for progesterone 21-hydroxylation [287]. In addition, the introduction of the point mutation V113A confers progesterone 21-hydroxylase activity to rabbit CYP2C1 which has no detectable progesterone 21-hydroxylase activity [288]. Lindberg and Negishi have shown that the mutation V117A is one of three mutations that confer coumarin 7-hydroxylase activity to mouse CYP2A4, a steroid 15α-hydroxylase [289]. The lower coumarin hydroxylase activity of an allelic form of CYP2C5 found in some inbred strains of mice has also been attributed to a mutation at this position [290]. The abovementioned studies further strengthen the hypothesis that the orientation of the B´ through C helices is essential in binding the substrate in the correct orientation for hydroxylation.

In CYP11A1, I98 may therefore play an important role in orientating the B´ through C helices and stabilising the substrate binding domain as was clearly demonstrated by the single substitution, I98K, in construct CYP11A1b. The model of CYP11A1b shows that the side chain of K98 points outwards away from the I helix resulting in a dramatic change in the shape and orientation of the B´ through C helices. Furthermore, docking studies revealed that destabilisation of this substrate binding domain resulted in a substantial change in the orientation of cholesterol in the active pocket with the 3β-hydroxyl group being shifted by more than 8Å. This finding explains the marked decrease in substrate affinity detected during the kinetic studies. The introduction of a polar residue, glutamine, at this position partially restores substrate affinity as it is expected to allow a more favourable conformation of the B´ through C helices and of the orientation of cholesterol in the active pocket.

Further inspection of the B´-C loop revealed a lysine residue at position 103, which is conserved in all species for which the sequences of CYP11A1 were available. Given the detrimental effect on substrate affinity by the insertion of a lysine residue into position 98, it was decided to investigate the role played by the conserved lysine at position 103. Usanov et al. have previously shown that the mutation of this residue to glutamine resulted in reduced enzymatic activity possibly due to the destabilisation of the heme in the active pocket [178]. Mutating K103 to alanine yielded a similar decrease in enzymatic activity, but unexpectedly resulted in a greater affinity for the cholesterol substrate. The homology model revealed that K103 and K104 interact with R421, which is in turn associated with the heme propionate. K103 is therefore essential in maintaining the correct orientation of the heme in the active pocket by stabilising the B´-C loop and by its association with R421. Taken together, our findings and those of Usanov et al. [178] suggest that mutations of K103 may change the orientation of the heme in the active pocket that results in cholesterol binding more tightly, but not in an orientation optimal for side-chain cleavage.

The abovementioned results demonstrate the use of homology modelling in understanding experimental results. Results obtained by site-directed mutagenesis and kinetic studies may well be useful in identifying catalytically important amino acids, but the precise role of these residues cannot be determined in the absence of a three-dimensional structure. Conversely, it is important to incorporate experimental results into any modelling exercise, as this is an effective way to verify the validity of a model. Only once the accuracy of a model has been verified experimentally can it be used as a predictive tool. The site-directed mutagenesis and kinetic analysis used during this study were preformed independently of the homology modelling. The strong agreement of the experimental results with those obtained from the model suggested that our model was in fact valid. Furthermore our model was in agreement with results obtained by other groups [31,32], allowing its use as a predictive tool in this study.

Docking studies were carried out in an effort to predict the orientation of cholesterol in the active pocket and to identify residues that may interact with the docked substrate. In the most favourable orientation obtained, cholesterol was bound with its side chain orientated towards beta plates, β4-1 and β4-2, within SRS6 and with the 3β-hydroxyl of C3 orientated towards the B´ helix within SRS1 [8]. In this orientation the 22(R)-hydrogen of cholesterol is located in line with the heme iron, approximately perpendicular to the heme plane (3.51Å from iron) as was also predicted

by Heyl et al. [268] and similar to the orientation of testosterone docked in the active pocket of a CYP2B1 model [283]. Furthermore, the proposed orientation of cholesterol offered a feasible explanation for the ability of human CYP11A1 to catalyse the side-chain cleavage of cholesterol sulphate and cholesterol esters with acyl chain lengths of up to four carbons [269]. As the B´ through C helices have been shown to exhibit significant flexibility [219,220,222,225], with an induced fit model of substrate binding proposed for CYP2C5 [220], the additional carbon atoms in the fatty acid esters could therefore be accommodated by the flexibility of this domain. This would permit the fatty acid esters to bind in the active pocket with K_m values similar to that of cholesterol, but in an orientation not optimal for side chain cleavage as was observed by the decreased turnover rate [Robert Tuckey, personal communication, 269].

In addition to using docking studies to determine the orientation of the cholesterol substrate in the active pocket of CYP11A1, residues important for mediating this orientation were identified and are listed in chapter 6. The involvement of five of these residues could be supported by results obtained in previous studies.

The first of these residues is T291, which as previously mentioned lies in the I helix directed towards the substrate bound above the heme and plays a critical role in dioxygen activation [48,56]. With cholesterol docked with the side chain orientated towards beta plates, β4-1 and β4-2, we identified a direct hydrophobic interaction between the side chain and this domain, specifically with P464. This is well supported by a previous group, who used site-directed mutagenesis in combination with substrate binding studies to show that an adjacent residue, I461, lies in close proximity to the side chain binding site. The results of Woods et al. further suggest that the side chains of cholesterol, 22(R)-hydroxycholesterol and 20α-hydroxycholesterol occupy slightly different positions in the active pocket [194].

Subsequent to the first hydroxylation at C22, a hydrogen bond responsible for mediating the orientation of the intermediate for the subsequent 20α-hydroxylation is believed to form between the 22(R)-hydroxyl group and a residue within the active pocket [268]. Our model reveals that S352, located in the loop between the K helix and β1-4, is pointed towards the heme in the active pocket, in an orientation favourable for hydrogen bonding with the 22(R)-hydroxyl group. Site-directed mutagenesis may be employed in the future to test this prediction.

Furthermore, previous binding studies using a variety of 3β-hydroxysteroids has lead to the proposal that hydrogen bonding between the 3β-oxygen of cholesterol and a

residue in the active pocket is important for substrate binding [268]. No hydrogen bond was detected in our model with the docked cholesterol. However, R357, located in the loop between the K helix and β1-4 in SRS5, is pointed towards the docked cholesterol and is within 4Å of the 3β-hydroxyl group. We therefore suggest that a hydrogen bond may form between R357 and the 3β-oxygen of the reaction intermediates 22(R)-hydroxycholesterol and 22,20-dihydroxycholesterol, further facilitating the 20α-hydroxylation and the cleavage of the 20-22 bond [194,268,270]. This hypothesis is supported by the observation that the derivatives of cholesterol, 22(R)-hydroxyl- and/or a 20α-hydroxycholesterol, bind significantly tighter to CYP11A1 than do cholesterol or 25-hydroxycholesterol. The catalytic importance of R357 may also be verified in future by site-directed mutagenesis and homology modelling.

Previous studies, however, support our hypothesis for the interaction of S352 and R357 with the reaction intermediates. In our model Y93 is 3.90Å from the nearest cholesterol atom and has a hydrophobic interaction with the substrate. After the first hydroxylation, the interaction of the intermediates with S352 and R357 would result in them being bound in an orientation that is further removed and unaffected by Y93. This is well supported by the data obtained by Pikuleva et al., who showed that Y93 is important for the binding of cholesterol, but not for the reaction intermediate 22(R)-hydroxycholesterol [270].

The data obtained in this study demonstrates that valuable insight into the structure/function of CYP11A1 may be gleaned from using site directed mutagenesis, kinetic analyses in combination with homology modelling since the enzyme is not amenable to the standard crystallization techniques. We have shown that amino acid changes on the surface of CYP11A1 do not impact on the catalytic activity of the enzyme, even though the changes are not all conservative. The importance and the flexibility of the B´ through C helices as a substrate binding domain have been confirmed in a mitochondrial cytochrome P450. Furthermore, this study added to evidence in previously published literature strongly indicating that cholesterol is bound in the active pocket of CYP11A1 with the 3β-hydroxyl group interacting with the B´ helix, while the side chain interacts with beta plates, β4-1 and β4-2. These results have provided evidence for a topological model of the active pocket of CYP11A1. Our model is the first to use both bacterial and mammalian cytochrome P450 crystal structures as templates, and has allowed us to identify catalytically important residues in the putative active pocket. This study has therefore laid a strong foundation from which future

studies may build in order to determine the role of these residues in the catalytic activity of CYP11A1 and bring us one step closer to understanding the catalytic cycle of this essential enzyme.

REFERENCES

1. **Vander A, Sherman J and Luciano D** 2001 In: Human physiology, the mechanisms of body function 8th ed. McGraw-Hill Companies, Inc., 1221 Avenue of the Americas, New York, NY 10020.:265-287, 505-519, 593-625

2. **Mason JI** 2002 In: Genetics of steroid biosynthesis and function. Taylor and Francis, 11 New Fetter Lane, London, EC4P 4EE.:1-35,115-144

3. **Payne AH and Hales DB** 2004 Overview of Steroidogenic Enzymes in the Pathway from Cholesterol to Active Steroid Hormones. Endocr. Rev. 5:947–970

4. **Boyd GS and Simpson ER** 1968 Studies on the conversion of cholesterol to pregnenolone in bovine adrenal mitochondria. In: McKern, KW, ed. Functions of adrenal cortex. New York: Appleton-Century Crofts. 1:49–76

5. **Burstein S and Gut M** 1976 Intermediates in the conversion of cholesterol to pregnenolone: kinetics and mechanism. Steroids 28:115-311

6. **Chothia C and Lesk AM** 1986 The relation between the divergence of sequence and structure in proteins. EMBO J. 5:823–826

7. **Graham-Lorence S and Peterson JA** 1996 P450s: Structural similarities and functional differences. FASEB J. 10:206-214

8. **Gotoh O** 1992 Substrate recognition sites in cytochrome P450 family 2 (CYP2). Proteins inferred from comparative analysis of amino acid and coding nucleotide sequences. J. Biol. Chem. 267:83-90

9. **Poulos TL, Finzel BC, Gunsalus IC, Wagner GC and Kraut J** 1985 The 2.6-Å crystal structure of Pseudomonas putida cytochrome P-450. J. Biol. Chem. 260:16122-16130

10. **Poulos TL, Finzel, BC and Howard AJ** 1987 High-resolution crystal structure of cytochrome P450cam. J. Mol. Biol. 195:687-700

11. **Peterson JA and Graham SE** 1998 A close family resemblance: the importance of structure in understanding cytochromes P450. Structure 6:1079-1085

12. **Young B and Heath JW** 2000 In: Wheather's Functional Histology a text and colour atlas 4th ed. Harcourt Publishers Limited, Harcourt Place, 32 Jamesfown Road, London NW1 7B7.:319-322

13. **Ehrhart-Bronstein M, Hinson JP, Bornstein SR, Scherbaum WA and Vinson GP** 1998 Intraadrenal interactions in the regulation of adrenocortical steroidogenesis. Endocr. Rev. 19:101–143

14. **Morrison SF and Cao WH** 2000 Different adrenal sympathetic preganglionic neurons regulate epinephrine and norepinephrine secretion. Am. J. Physiol. Reg. Integ. Comp. Physiol. 279: R1763–R1775

15. **Brown N, Swart P, Fenhalls G, Stevens L, Kolar NW and Swart AC** 2002 Baboon CYP11B1: The localization and catalytic activity in baboon adrenal tissue. Endocr. Res. 28:477-484

16. **Ganong WF** 1995 In: Review of medical physiology 17th ed. Prentice-Hall International Inc.:306-351

17. **Teebken OE and Scheumann GF** 2000 Differenciated corticosteroid production and regulation after selective transplantation of cultured and noncultured adrenocortical cells in the adrenalectomixed rat. Transplantation 70:836-843

18. **Fortak W and Kmiec B** 1968 About occurrence of the chromophilic cells in the adrenal cortex of white rats. Endokrynol. Pol. 19:117–128

19. **Kmiec B** 1968 Histologic and histochemical observations on regeneration of the adrenal medulla after enucleation in white rats. Folia. Morphol. (Warsz) 27:238–245

20. **Palacios G and Lafraga M** 1975 Chromaffin cells in the glomerular zone of adult rat adrenal cortex. Cell Tissue Res. 164:275–278

21. **Gallo-Payet N, Pothier P and Isler H** 1987 On the presence of chromaffin cells in the adrenal cortex: their possible role in adrenocortical function. Biochem. Cell Biol. 65:588–592

22. **Bornstein SR, Ehrhart-Bornstein M, Usadel H, Böckmann M and Scherbaum WA** 1991 Morphological evidence for a close interaction of chromaffin cells with cortical cells within the adrenal gland. Cell Tissue Res. 265:1–9

23. **Funder JW** 2005 The nongenomic actions of aldosterone. Endocr. Rev. 26:313-321

24. **Olefsky JM** 2001 Nuclear receptor minireview series. J. Biol. Chem. 276:36836-36864

25. **Farman N and Rafestin-Oblin ME** 2001 Multiple aspects of mineralocorticoid selectivity. Am. J. Physiol. Renal Physiol. 280:F181–F192

26. **Strickland I, Kisich K, Hauk PJ, Vottero A, Chrousos GP, Klemm DJ and Leung DYM** 2001 High constitutive glucocorticoid receptor β in human neutrophils enables them to reduce their spontaneous rate of cell death in response to corticosteroids. J. Exp. Med. 193:585–593

27. **Rosenfeld MG and Glass CK** 2001 Coregulation codes of transcriptional regulation by nuclear receptors. J. Biol. Chem. 276:36865-36868

28. **Palmer LG** 2001 Intracellular pH as a regulator of Na+ transport. J. Membr. Biol. 184:305-311

29. **Meneton P, Loffing J and Warnock DG** 2004 Sodium and potassium handling by the aldosterone-sensitive distal nephron: the pivotal role of the distal and connecting tubule. Am. J. Physiol. Renal. Physiol. 287:F593–F601

30. **Yoo D, Kim BY, Campo C, Nance L, King A, Maouyo D, and Welling PA** 2003 Cell surface expression of the ROMK (Kir 1.1) channel is regulated by the aldosterone-induced kinase, SGK-1, and protein kinase A. J. Biol. Chem. 278:23066–23075

31. **Yun CC, Palmada M, Embark HM, Fedorenko O, Feng Y, Henke G, Setiawan I, Boehmer C, Weinman EJ, Sandrasagra S, Korbmacher C, Cohen P, Pearce D, and Lang F** 2002 The serum and glucocorticoid-inducible kinase SGK1 and the Na/H exchange regulating factor NHERF2 synergize to stimulate the renal outer medullary K channel ROMK1. J. Am. Soc. Nephrol. 13:2823–2830

32. **Kwon TH, Nielsen J, Masilamani S, Hager H, Knepper MA, Frokler J, and Nielsen S** 2002 Regulation of collecting duct AQP3 expression: response to mineralocorticoid Am. J. Physiol. Renal. Physiol. 283:F1403–F1421

33. **Nakada T, Furuta H, Katayama T, Sumiya H and Shimazaki J** 1989 The effect of adrenal surgery on plasma atrial natriuretic factor and sodium escape phenomenon in patients with primary aldosteronism. J. Urol. 142:13-18

34. **Ngarmukos C and Grekin RJ** 2001 Nontraditional aspects of aldosterone physiology. Am. J. Physiol. Endocrinol. Metab. 281:E1122–E1127

35. **Dallman MF, la Fleur SE, Pecoraro NC, Gomez F, Houshyay H and Akana SF** 2004 Minireview: Glucocorticoids—food intake, abdominal obesity, and wealthy nations in 2004. Endocrinology 145:2633–2638

36. **Gold R, Buttgereit F and Toyka KV** 2001 Mechanism of action of glucocorticosteroid hormones: possible implications for therapy of neuroimmunological disorders. J. Neuroimmunol.117:1–8

37. **Gagliardo R, Vignola AM and Bonsignore G** 2001 Role of glucocorticosteroid receptors in bronchial asthma. Recenti. Prog. Med. 92:542-545

38. **Breen KM, Billings HJ, Wagenmaker ER, Wessinger EW and Karsch FJ** 2005 Endocrine basis for disruptive effects of cortisol on preovulatory events. Endocrinology 146:2107-2115

39. **Kita H, Jorgensen RK, Reed CE, Dunnette SL, Swanson MC, Bartemes KR, Squillace D, Blomgren J, Bachman K and Gleich GL** 2000 Mechanism of topical glucocorticoid treatment of hay fever: IL-5 and eosinophil activation during natural allergen exposure are suppressed, but IL-4, IL-6, and IgE antibody production are unaffected. J. Allergy Clin. Immunol. 106:521-529

40. **Kaliner M** 1985 Mechanisms of glucocorticosteroid action in bronchial asthma. J. Allergy. Clin. Immunol. 76:321-329

41. **Sanner BM, Meder U, Zidek W and Tepel M** 2002 Effects of glucocorticoids on generation of reactive oxygen species in platelets. Steroids 67:715-719

42. **Reid SD and Perry SF** 1991 the effects and physiological consequences of raised levels of cortisol on rainbow trout (Oncorhynchus mykiss) erythrocyte beta-adrenoreceptors. J. Exp. Biol. 158:217-240

43. **Beck SG and Handa RJ** 2004 Dehydroepiandrosterone (DHEA): A misunderstood adrenal hormone and spine-tingling neurosteroid? Endocrinology 145:1039-1041

44. **Ibanez L, Dimartino-Nardi J, Potau N and Saenger P** 2000 Premature adrenarche: Normal variant or forerunner of adult disease? Endocr. Rev. 21:671–696

45. **Siiteri PK** 2005 Editorial: The continuing saga of dehydroepiandrosterone (DHEA) J. Clin. Endocrinol. Metab. 90:3795-3769

46. **Hiort O** 2002 Androgens and puberty. Best Pract. Res. Clin. Endocrinol. Metab. 16:31-41

47. **Arnold JT, Le H, McFann KK, and Blackman MR** 2004 Comparative effects of DHEA vs. testosterone, dihydrotestosterone, and estradiol on proliferation and gene expression in human LNCaP prostate cancer cells. Am J Physiol. Endocrinol. Metab. 288:E573–E584

48. **Vermeulen A, Kaufman JM, Goemaere S and van Pottelberg I** 2002 Estradiol in elderly men. Aging Male 5:98-102

49. **Buvat J** 2003 Androgen therapy with dehydroepiandrosterone. World J. Urol. 21:346–355

50. **Suárez C, Vela J, García-Tornadú I and Becu-Villalobos D** 2005 Dehydroepiandrosterone (DHEA) modulates GHRH, somatostatin and angiotensin II action at the pituitary level. J. Endocrinol. 185:165–172

51. **Hajszan T, MacLusky NJ and Leranth C** 2004 Dehydroepiandrosterone increases hippocampal spine synapse density in ovariectomized female rats. Endocrinology 145:1042–1045

52. **Nelson DR, Koymans L, Kamataki T, Stegeman JJ, Feyereisen R, Waxman D, Waterman MR, Gotoh O, Coon MJ, Estabrook RW, Gunsulus IC and Nebert DW** 1996 P450 superfamily: update on new sequences, gene mapping, accession numbers and nomenclature. Pharmacogenetics 6:1–42

53. **Lewis DFV** 2001 In: Guide to cytochromes P450: Structure and function. Taylor and Francis, 11 New Fetter Lane, London EC4P 4EE.:1-17

54. **Garfinkel D** 1958 Studies on pig liver microsomes. I. Enzymic and pigment composition of different microsomal fractions. Arch. Biochem. Biophys. 77:493-509

55. **Klingenberg M** 1968 Pigment of rat liver microsomes. Arch. Biochem. Biophys. 75:376-386

56. **Omura T and Sato R** 1962 A new cytochrome in liver microsomes. J. Biol. Chem. 237:1375-1376

57. **Omura T and Sato R** 1964 The carbon monoxide-binding pigment of liver microsomes. J. Biol. Chem. 239:2379-2385

58. **White RE and Coon MJ** 1980 Oxygen activation by cytochrome P450. Ann. Rev. Biochem. 49:315-356

59. **Schlichting I, Berendzen J, Chu K, Stock AM, Maves SA, Benson DE, Sweet RM, Ringe D, Petsko GA and Sligar SG** 2000 The catalytic pathway of cytochrome P450cam at atomic resolution. Science 287:1615-1622

60. **Slabbert JT** 2003 Identification of two CYP17 alleles in the South African Angora goat. MSc thesis, Univ. Stellenbosch

61. **Porter TD and Coon MJ** 1991 Multiplicity of isoforms, substrates, and catalytic and regulatory mechanisms. J. Biol. Chem. 266:13469-13472

62. **Penning TM** 1997 Molecular endocrinology of hydroxysteroid dehydrogenases. Endocr. Rev. 18:281–305

63. **Thomas JL, Myers RP and Strickler RC** 1989 Human placental 3-hydroxy-5-ene-steroid dehydrogenase and steroid 5-4-ene-isomerase: purification from mitochondria and kinetic profiles, biophysical characterization of the purified mitochondrial and microsomal enzymes. J. Steroid Biochem. 33:209–217

64. **Thomas JL, Frieden C, Nash WE and Strickler RC** 1995 An NADH induced conformational change that mediates the sequential 3-hydroxysteroid dehydrogenase/isomerase activities is supported by affinity labelling and the time-dependent activation of isomerase. J. Biol. Chem. 270:21003–21008

65. **Thomas JL, Duax WL, Addlagatta A, Brandt S, Fuller RR and Norris W** 2003 Structure/function relationships responsible for coenzyme specificity and the isomerase activity of human type 1 3-hydroxysteroid dehydrogenase/isomerase. J. Biol. Chem. 278:35483–35490

66. **Rheaume E, Lachance Y, Zhao HF, Breton N, Dumont M, deLaunoit Y, Trudel C, Luu-The V, Simard J and Labrie F** 1991 Structure and expression of a new complementary DNA encoding the almost exclusive 3 -hydroxysteroid dehydrogenase/5- 4-isomerase in human adrenals and gonads. Mol. Endocrinol. 5:1147–1157

67. **Pelletier G, Li S, Luu-The V, Tremblay Y, Belanger A and Labrie F** 2001 Immunoelectron microscopic localization of three key steroidogenic enzymes (cytochrome P450(scc), 3 -hydroxysteroid dehydrogenase and cytochrome P450(c17)) in rat adrenal cortex and gonads. J. Endocrinol. 171:373–383

68. **Suzuki T, Sasano H, Takeyama J, Kaneko C, Freije WA, Carr BR and Rainey WE** 2000 Developmental changes in steroidogenic enzymes in human postnatal adrenal cortex: immunohistochemical studies. Clin. Endocrinol. (Oxf) 53:739–747

69. **You L** 2004 Steroid hormone biotransformation and xenobiotic induction of hepatic steroid metabolising enzymes. Chem. Biol. Interact. 147:233-246

70. **Martin G, Pilon A, Albert C, Valle M, Hum DW, Fruchart JC, Najib J, Clavey V and Staels B** 1999 Comparison of expression and regulation of the high-density lipoprotein receptor SR-BI and the low-density lipoprotein receptor in human adrenocortical carcinoma NCI-H295. Eur. J. Biochem. 261:481-491

71. **Liu J, Heikkila P, Meng QH, Kahri AI, Tikkanen MJ and Voutilainen R** 2000 Expression of low and high density lipoprotein receptor genes in human adrenals. Eur. J. Endocrinol. 142:677–682

72. **Swarnakar S, Reyland ME, Deng J, Azhar S, and Williams DL** 1998 Selective uptake of low density lipoprotein-cholesteryl ester is enhanced by inducible apolipoprotein E expression in cultured mouse adrenocortical cells. J. Biol. Chem. 273:12140–12147

73. **von Eckardstein A, Nofer JR and Assmann G** 2001 High density lipoproteins and arteriosclerosis role of cholesterol efflux and reverse cholesterol transport. Arterioscler. Thromb. Vasc. Biol. 21:13-27

74. **Connelly MA and Williams DL** 2004 SR-BI and HDL cholesterol ester metabolism. Endocr. Res. 30:697–703

75. **Kraemer FB, Shen WJ, Harada K, Patel S, Osuga JI, Ishibashi S and Azhar S** 2004 Hormone-sensitive lipase is required for high-density lipoprotein cholesterol ester-supported adrenal steroidogenesis. Mol. Endocrinol. 18:549–557

76. **Sun Y, Wang N and Tall AR** 1999 Regulation of adrenal scavenger receptor-BI expression by ACTH and cellular cholesterol pools. J. Lip. Res. 40:1799-1805

77. **Guo IC, Hu MC and Chung BC** 2003 Transcriptional regulation of CYP11A1 J. Biomed. Sci. 10:593-598

78. **Carrasco GA and Van de Kar LD** 2003 Neuroendocrine pharmacology of stress. Eur. J. Pharmacol. 463:235-272

79. **Beuschlein F, Fassnacht M, Klink A, Allolio B and Reincke M** 2001 ACTH-receptor expression, regulation and role in adrenocortical tumor formation. Eur. J. Endocrinol. 144:199-206

80. **Lodish H, Berk A, Zipursky SL, Matsudaira P, Baltimore D and Darnell J** 2000 In: Molecular cell biology 4th ed. WH Freeman and Company, 41 Madison Avenue, New York, NY 10010.:862-871

81. **Evans MJ, Kitson NE, Livesey JH and Donald RA** 1993 The effect of cortisol on the secretion of ACTH by the anterior pituitary cells of the horse in culture. J. Endocrinol. 137:403-412

82. **Bradbury MJ, Akana SF and Dallman MF** 1994 Roles of type I and II corticosteroid receptors in regulation of basal activity in the hypothalamo-pituitary-adrenal axis during the diurnal trough and the peak: Evidence for a nonadditive effect of combined receptor occupation. Endocrinology 134:1286-1296

83. **Dijkstra I, Binnekade R and Tilders FJH** 1996 Diurnal variation in resting levels of corticosterone is not mediated by variation in adrenal responsiveness to adrenocorticotropin but involves splanchnic nerve integrity. Endocrinology 137:540–547

84. **Bornstein SR, Ehrhart-Bornstein M, Scherbaum WA, Pfeiffer EF and Holst JJ** 1990 Effects of splanchnic nerve stimulation on the adrenal cortex may be mediated by chromaffin cells in a paracrine manner. Endocrinology 127:900–906

85. **Edwards AV and Jones CT** 1987 The effect of splanchnic nerve stimulation on adrenocortical activity in conscious calves. J. Physiol. 382:385–396

86. **Edwards AV, Jones CT and Bloom SR** 1986 Reduced adrenal cortical sensitivity to ACTH in lambs with cut splanchnic nerves. J. Endocrinol. 110:81–85

87. **Ehrhart-Bornstein M, Bornstein SR, Trzeciak WH, Usadel H, Gu¨ se-Behling H, Waterman MR and Scherbaum WA** 1991 Adrenaline stimulates cholesterol side chain cleavage cytochrome P450 mRNA accumulation in bovine adrenocortical cells. J. Endocrinol. 131:R5–R8

88. **Tschernitz C, Laslop A, Eiter C, Kroesen S and Winkler H** 1995 Biosynthesis of large dense-core vesicles in PC12 cells: effects of depolarization and second messengers on the mRNA levels of their constituents. Brain. Res. Mol. Brain. Res. 31:131–140

89. **Eskay RL and Eiden LE** 1992 Interleukin-1a and tumor necrosis factor-α differentially regulate enkephalin, vasoactive intestinal polypeptide, neurotensin, and substance P biosynthesis in chromaffin cells. Endocrinology 130:2252–2258

90. **Usadel H, Bornstein SR, Ehrhart-Bornstein M, Kreysch HG and Scherbaum WA** 1993 Gap junctions in the adrenal cortex. Horm. Metab. Res. 25:653–654

91. **Bronstein SR and Chrousos GP** 1999 Adrenocorticotropin (ACTH)- and non-ACTH-mediated regulation of the adrenal Cortex: neural and immune inputs. J. Clin. Endocrinol. Met. 84:1729-1736

92. **Holzwarth MA, Cunningham LA and Kleitman N** 1987 The role of adrenal nerves in the regulation of adrenocortical functions. Ann. NY Acad. Sci. 512:449–464

93. **Holzwarth MA** 1984 The distribution of vasoactive intestinal peptide in the rat adrenal cortex and medulla. J. Auton. Nerv. Syst. 11:269–283

94. **Kuramoto H, Kondo H and Fujita T** 1987 Calcitonin gene-relatedpeptide (CGRP)-like immunoreactivity in scattered chromaffincells and nerve fibers in the adrenal gland of rats. Cell Tissue Res. 247:309–315

95. **Kuramoto H, Kondo H and Fujita T** 1986 Neuropeptide tyrosine (NPY)-like immunoreactivity in adrenal chromaffin cells and intraadrenal nerve fibers of rats. Anat. Rec. 214:321–328

96. **Hinson JP and Kapas S** 1996 Effect of splanchnic nerve section and compensatory adrenal hypertrophy on rat adrenal neuropeptide content. Regul. Pept. 61:105–109

97. **Engeland WC and Gann DS** 1989 Splanchnic nerve stimulation modulates steroid secretion in hypophysectomized dogs. Neuroendocrinology 50:124–131

98. **Hinson JP and Vinson GP** 1990 Calcitonin gene-related peptide stimulates adrenocortical function in the isolated perfused rat adrenal gland in situ. Neuropeptides 16:129–133

99. **Hinson JP, Cameron LA, Purbrick A and Kapas S** 1994 The role of neuropeptides in the regulation of adrenal vascular tone: effects of vasoactive intestinal polypeptide, substance P, neuropeptide Y, neurotensin, Met-enkephalin, and Leu-enkephalin on perfusion medium flow rate in the intact perfused rat adrenal. Regul. Pept. 51:55–61

100. **Hinson JP, Vinson GP and Whitehouse BJ** 1986 The relationship between perfusion medium flow rate and steroid secretion in the isolated perfused rat adrenal gland in situ. J. Endocrinol. 111:391–396

101. **Hinson JP, Vinson GP, Pudney J and Whitehouse BJ** 1989 Adrenal mast cells modulate vascular and secretory responses in the intact adrenal gland of the rat. J. Endocrinol. 121:253–260

102. **Hinson JP, Vinson GP, Kapas S and Teja R** 1991 The relationship between adrenal vascular events and steroid secretion: the role of mast cells and endothelin. J. Steroid Biochem. Mol. Biol. 40:381–389

103. **Jones CT, Edwards AV and Bloom SR** 1990 The effect of changes in adrenal blood flow on adrenal cortical responses to adrenocorticotrophin in conscious calves. J. Physiol. (Lond) 429:377–386

104. **Hinson JP, Vinson GP, Kapas S and TejaR** 1991 The role of endothelin in the control of adrenocortical function: stimulation of endothelin release by ACTH and the effects of endothelin-1 and endothelin-3 on steroidogenesis in rat and human adrenocortical cells. J. Endocrinol. 128:275–280

105. **Cameron LA and Hinson JP** 1993 The role of nitric oxide derived from L-arginine in the control of steroidogenesis, and perfusion medium flow rate in the isolated perfused rat adrenal gland. J. Endocrinol. 139:415–423

106. **Bornstein SR, Ehrhart M, Scherbaum WA and Pfeiffer EF** 1990 Adrenocortical atrophy of hypophysectomized rats can be reduced by corticotropin releasing hormone (CRH). Cell Tissue Res. 260:161–166

107. **van Oers JWAM, Hinson JP, Binnekade R and Tilders FJH** 1992 Physiological role of corticotropin-releasing factor in the control of adrenocorticotropin-mediated corticosterone release from the rat adrenal gland. Endocrinology 130:282–288

108. **Azar ST, Turner A and Melby JC** 1992 Corticotropin-independent effect of ovine corticotropin-releasing hormone on cortisol release in man. Am. J. Med. Sci. 303:217–221

109. **Andreis PG, Neri G and Nussdorfer GG** 1991 Corticotropin-releasing hormone (CRH) directly stimulates corticosterone secretion by the rat adrenal gland. Endocrinology 128:1198–1200

110. **Andreis PG, Neri G, Mazzocchi G, Musajo FG and Nussdorfer GG** 1992 Direct secretagogue effect of corticotropin-releasing factor on the rat adrenal cortex: the involvement of the zona medullaris. Endocrinology 131:69–72

111. **Clark BJ and Stocco DM** 1996 StAR-A Tissue Specific Acute Mediator of Steroidogenesis. TEM 7:227-233

112. **Clark BJ and Stocco DM** 1997 Steroidogenic acute regulatory protein: The StAR still shines brightly. Mol. Cell Endocrinol. 134:1-8

113. **Stocco DM and Clark BJ** 1996 Role of the Steroidogenic Acute Regulatory Protein (StAR) in Steroidogenesis. Biochem. Pharmacol. 51:197-205

114. **Jefcoate C** 2002 High-flux mitochondrial cholesterol trafficking, a specialized function of the adrenal cortex. J. Clin. Invest. 110:881-890

115. **Rocchi S, Gaillard I, Obberghen EV, Chambaz EM and Vilgrain I** 2000 Adrenocorticotrophic hormones stimulates phosphotyrosine phosphatase SHP2 in bovine adrenocortical cells: phosphorylation and activation by camp-dependent protein kinase. Biochem. J. 352:483-490

116. **Soto EA, Kliman HJ, Strauss JF and Paavola LG** 1986 Gonadotropins and cyclic adenosine 3',5'-monophosphate (cAMP) alter the morphology of cultured human granulosa cells. Biol. Reprod. 34:559-569

117. **Garren LD, Gill GN, Masui H and Walton GM** 1971 On the mechanism of action of ACTH. Recent Prog. Horm. Res. 27:443-478

118. **Privalle CT, McNamara BC, Dhariwal MC and Jefcoate CR** 1987 ACTH control of cholesterol side-chain cleavage at adrenal mitochondrial cytochrome P450scc. Regulation of intramitochondrial cholesterol transfer. Mol. Cell. Endocrinol. 53:87-101

119. **Lambeth JD, Xu XX and Glover M** 1987 Cholesterol sulphate inhibits adrenal mitochondrial cholesterol side-chain cleavage at a site distinct from cytochrome P450scc. Evidence for an intramitochondrial cholesterol translocator. J. Biol. Chem. 262:9181-9188

120. **Elliot ME, Goodfriend TL and Jefcoate CR** 1993 Bovine adrenal glomerulosa and fasiculata cells exibit 28.5-kilodalton proteins sensitive to angiotensin, other agonists, and atrial natriuretic peptide. Endocrinology 133:1669-1677

121. **Bose HS, Lingappa VR and Miller WL** 2002 Rapid regulation of steroidogenesis by mitochondrial protein import. Nature 417:87-91

122. **Koehler CM** 2000 Protein translocation pathways of the mitochondrion. FEBS Lett. 476:27-31

123. **Tuckey RC, Headman MJ, Bose HS and Miller WL** 2002 Transfer of cholesterol between phospholipid vesicles mediated by the steroidogenic acute regulatory protein (StAR). J. Biol. Chem. 277:47123-47128

124. **Artemenko IP, Zhao D, Hales DB, Hales KH and Jefcoate CR** 2001 Mitochondrial processing of newly synthesized StAR, but not total StAR, mediates cholesterol transfer to cytochrome P450 side-chain cleavage enzyme in adrenal cells. J. Biol. Chem. 276:46583-46596

125. **Christensen K, Bose HS, Harris FM, Miller WL and Bell JD** 2001 Binding of StAR to synthetic membranes suggests an active molten globule. J. Biol. Chem. 276:17044-17051

126. **Papadopoulos V** 1998 Structure and function of the peripheral benzodiazepine receptor in steroidogenic cells. Proc. Soc. Exp. Biol. Med. 217:130-142

127. **Li H, Degenhardt B, Tobin D, Yao Z, Tasken K and Papadopoulos** V 2001 Identification, localization, and function of PAP7: a peripheral-type benzodiazepine receptor and PKA (RIα)-associated protein. Mol. Endocrinol. 15:2211-2228

128. **Maloberti P, Mele PG, Neuman I, Cornejo Maciel F, Cano F, Bey P, Paz C and Podesta EJ** 2000 Regulation or arachidonic acid release in steroidogenesis: role of a new acyl-CoA thioesterase (ARTISt). Endocr. Res. 26:653-662.

129. **Guo IC, Huang C and Chung BC** 1992 Differential regulation of the CYP11A1 (P450scc) and ferrodoxin genes in the adrenal and placental cells. DNA Cell Biol. 12:849-860

130. **Lala DS, Rice DA and Parker KL** 1992 Steroidogenic factor I, a key regulator of steroidogenic enzyme expression, is the mouse homolog of fushi tarazu-factor I. Mol. Endocrinol 6:1249–1258

131. **Morohashi K, Honda S, Inomata Y, Handa H and Omura T** 1992 A common trans-acting factor, Ad4-binding protein, to the promoters of steroidogenic P-450s. J. Biol. Chem. 267:17913–17919

132. **Parker KL and Schimmer BP** 1995 Transcriptional regulation of the genes encoding the cytochrome P-450 steroid hydroxylases. Vitam. Horm. 51:339–370

133. **Guo IC and Chung BC** 1999 Protein binding activity and cyclic AMP responsiveness of a weak Sp1 site in proximal promoter of human CYP11A1 gene. J. Genet. Mol. Biol. 10:9-18

134. **Guo IC, Tsai HM and Chung BC** 1994 Actions of two different cAMP-responsive sequences and an enhancer of the human CYP11A1 (P450scc) gene in adrenal Y1 cells. J. Biol. Chem. 269:6362-6369

135. **Takayama K, Morohashi K, Honda S, Hara N and Omura T** 1994 Contribution of Ad4BP, a steroidogenic cell-specific transcription factor, to regulation of the human CYP11A and bovine CYP11B genes through there distal promoters. J. Biochem. (Tokyo) 116:193-203

136. **Watanabe N, Inoue H and Fujii-Kuriyama Y** 1994 Regulatory mechanisms of cAMP-dependent and cell-specific expression of the human steroidogenic cytochrome P450scc (CYP11A1) gene. Eur. J. Biochem. 222:825-834

137. **Chou SJ, Lai KN and Chung B** 1996 Charactorization of the upstream sequence of the human CYP11A1 gene for cell type-specific expression. J. Biol. Chem. 271:22125-22129

138. **Guo IC and Chung BC** 1999 Cell-type specificity of human CYP11A1 TATA box. J. Steroid Biochem. Mol. Biol. 69:329-334

139. **Chen C and Guo IC** 2000 Effect of cAMP on protein binding activities of three elements in upstream promoter of human CYP11A1 gene. Life Sci. 67;2045-2049

140. **Chung BC, Guo IC and Chou SJ** 1997 Transcriptional regulation of the CYP11A1 and ferredoxin genes. Steroids 62:37-42

141. **Hu MC, Hsu HJ, Guo IC and Chung BC** 2004 Function of CYP11A1 in animal models. Mol. Cell Endocrinol. 215:95-100

142. **Hu MC, Hsu NC, Pai CI, Wang CKL and Chung BC** 2001 Functions of the upstream and proximal steroidogenic factor 1 (SF-1)-binding sites in the CYP11A1 promoter in basal transcription and hormone response. Mol. Endocrinol. 15:812-818

143. **Jacob AL and Lund J** 1998 Mutations in the activation function-2 core domain of steroidogenic factor-1 dominantly suppresses PKA-dependent transactivation of the bovine CYP17 gene. J. Biol. Chem. 273:13391-13394

144. **Ishimura K and Fujita H** 1997 Light and electron microscopic immunohistochemistry of the localization of adrenal steroidogenic enzymes. Microsc. Res. Tech. 36:445–453

145. **Pelletier G, Li S, Luu-The V, Tremblay Y, Belanger A and Labrie F** 2001 Immunoelectron microscopic localization of three key steroidogenic enzymes (cytochrome P450(scc), 3 -hydroxysteroid dehydrogenase and cytochrome P450(c17)) in rat adrenal cortex andgonads. J. Endocrinol. 171:373–38377:98–102

146. **Oonk RB, Parker KL, Gibson JL and Richards JS** 1990 Rat cholesterol side-chain cleavage cytochrome P-450 (P-450scc) gene. Structure and regulation by cAMP in vitro. J. Biol. Chem. 265:22392–22401

147. **Payne AH and Youngblood GL** 1995 Regulation of expression of steroidogenic enzymes in Leydig cells. Biol. Reprod. 52:217–225

148. **Strauss JF, Martinez F and Kiriakidou M** 1996 Placental steroid hormone synthesis: unique features and unanswered questions. Biol. Reprod. 54:303–311

149. **Compagnone NA, Bulfone A, Rubenstein JL and Mellon SH** 1995 Expression of the steroidogenic enzyme P450scc in the central andperipheral nervous systems during rodent embryogenesis. Endocrinology 136:2689–2696

150. **Slominski A, Zjawiony J, Wortsman J, Semak I, Stewart J, Pisarchik A, Sweatman T, Marcos J, Dunbar C and Tuckey RC** 2004 A novel pathway for sequential transformation of 7-dehydrocholesterol and expression of the P450scc system in mammalian skin. Eur. J. Biochem. 271:4178–4188

151. **Young MJ, Clyne CD, Cole TJ and Funder JW** 2001 Cardiac steroidogenesis in the normal and failing heart. J. Clin. Endocrinol. Metab. 86:5121–5126

152. **White PC** 2003 Aldosterone: direct effects on and production by the heart. J. Clin. Endocrinol. Metab. 88:2376–2383

153. **Voutilainen R and Miller WL** 1986 Developmental expression of genes for the steroidogenic enzymes P450scc (20,22-desmolase), P450c17 (17α-hydroxylase/17,20-lyase), and P450c21 (21-hydroxylase) in the human fetus. J. Clin. Endocrinol. Metab. 63:1145–1150

154. **Narasaka T, Suzuki T, Moriya T and Sasano H** 2001 Temporal and spatial distribution of corticosteroidogenic enzymes immunoreactivity in developing human adrenal. Mol. Cell Endocrinol. 174:111–120

155. **Mesiano S, Coulter CL and Jaffe RB** 1993 Localization of cytochrome P450 cholesterol side-chain cleavage, cytochrome P450 17α -hydroxylase/17, 20-lyase, and 3-hydroxysteroid dehydrogenase isomerase steroidogenic enzymes in human and rhesus monkey fetal adrenal glands: reappraisal of functional zonation. J. Clin. Endocrinol. Metab. 77:1184–1189

156. **Chemes H** 1996 Leydig cell development in humans. In: Payne AH, Hardy MP and Russell LD, eds. The Leydig cell. Vienna, IL: CacheRiver Press.:175–202

157. **Camacho AM, Kowarski A, Migeon CJ and Brough A** 1968 Congenital adrenal hyperplasia due to a deficiency of one of the enzymes involved in the biosynthesis of pregnenolone. J. Clin. Endocrinol. Metab. 28:153-161

158. **Miller WL** 1997 Congenital lipoid adrenal hyperplasia; the human gene knockout of the steroidogenic acute regulatory protein. J. Mol. Endocrinol. 19:227-240

159. **Degenhart HJ, Visser KHA, Boon H and O'Doherty NJD** 1972 Evidence for deficiency of 20α cholesterol hydroxylase activity in adrenal tissue of patient with lipoid adrenal hyperplasia. Acta. Endocrinol. (Copenh) 71:512-518

160. **Hauffa BP, Miller WL, Grumbach MM, Conte FA and Kaplan SL** 1985 Congenital adrenal hyperplasia due to deficient cholesterol side-chain cleavage activity (20,22 desmolase) in a patient treated for 18 years. Clin. Endocrinol. (Oxf) 23;481-493

161. **Yang X, Iwamoto, K, Wang M, Artwohl J, Mason JI and Pand S** 1993 Inherited Congenital Adrenal Hyperplasia in the Rabbit Is Caused by a Deletion in the Gene Encoding Cytochrome P450 Cholesterol Side-Chain Cleavage Enzyme. Endocrinology 132:1977-1982

162. **Okuyama E, Nishi N, Onishi S, Itoh S, Ishii Y, Miyanaka H, Fujita K and Ichikawa Y** 1997 A novel splicing junction mutation in the gene for the steroidogenic acute regulatory protein causes congenital lipoid adrenal hyperplasia. J. Clin. Endocrinol. Metab. 82:2337-2342

163. **Bose HS, Sugawara T, Strauss JF and Miller WL** 1996 the pathophysiology and genetics of congenital lipoid hyperplasia. New Engl. J. Med. 335:1870-1878

164. **Miller WL** 1988 Molecular biology of steroid hormone synthesis. Endocr. Rev. 9:295-318

165. **Miller WL** 1998 Why nobody has P450scc (20,22 Desmoslase) deficiency. J. Clin. Endocrinol. Metab. 83:1399-1400

166. **Csapo AI, Pulkkinen MO and Wiest WB** 1973 Effects of luteectomy and progesterone replacement theropy in early pregnant patients. Am. J. Obstet. Gynecol. 115:759-765

167. **Csapo AI and Pulkkinen MO** 1978 Indispensibility of the human corpus luteum in the maintenance of early pregnancy: luteectomy evidence. Obstet. Gynecol. Surv. 83:69-81

168. **Tajima T, Fujieda K, Kouda N, Nakae J and Miller WL** 2001 Heterozygous mutation in the cholesterol side-chain cleavage enzyme (P450scc) gene in a patient with 46,XY Sex reversal and adrenal insufficiency. J. Clin. Endocrinol. Metab. 86:3820-3825

169. **Katsumata N, Ohtake M, Hojo T, Ogawa E, Hara T, Sato N and Tanaka T** 2002 Compound heterozygous mutations in the cholesterol side-chain cleavage enzyme gene (CYP11A1) causes congenital adrenal insufficiency in humans. J. Clin. Endocrinol. Metab. 87:3808-3813

170. **Hiort O, Holterhus PM, Werner R, Marschke C, Hoppe U, Partsch CJ, Riepe FG, Achermann JC and Struve D** 2005 Homozygous Disruption of P450 Side-Chain Cleavage (CYP11A1) Is Associated with Prematurity, Complete 46,XY Sex Reversal, and Severe Adrenal Failure. J. Clin. Endocrinol. Metabol. 90:538-541

171. **Franks S, Gharani N and Gilling-Smith C** 1999 Polycystic ovary syndrome: evidence for a primary disorder of ovarian steroidogenesis. J. Steroid. Biochem. Mol. Biol. 69:269-272

172. **Stone D and Hechter O** 1954 Studies on ACTH action in perfused bovine adrenals: the site of action of ACTH in corticosteroidogenesis. Arch. Biochem. 51:457-469

173. **Simpson ER and Boyd GS** 1966 The cholesterol side-chain cleavage system of the adrenal cortex: a mixed-function oxidase. Biocherm. Biophys. Res. Commun. 24:10-17

174. **Hume R and Boyd GS** 1978 Cholesterol metabolism and steroid-hormone production. Biochem. SOC. Trans. 6:893-898

175. **Schulster D, Burstein SH and Cooke BA** 1976 Biosynthesis of steroid hormones. In: Schulster D, Burstein S, Cooke BA, eds. Molecular endocrinology of the steroid hormones. London, New York, Sydney, Toronto, Wiley and Sons.:44–77

176. **Lambeth JD, Kitchen SE, Farooqui AA, Tuckey R and Kamin H** 1982 Cytochrome P-450scc Substrate Interactions: Studies of binding and catylytic activity using hydroxycholesterols. J. Biol. Chem. 257:1876-1884

177. **Hlavica P, Schulze J and Lewis DFV** 2003 Functional interaction of cytochrome P450 with its redox partners: a critical assessment and update of the topology of predicted contact regions. J. Inorg. Biochem. 96:279-297

178. **Usanov SA, Graham SE, Lepesheva GI, Azeva TN, Strushkevich NV, Gilep AA, Estabrook RW and Peterson JA** 2002 Probing the Interaction of Bovine Cytochrome P450scc (CYP11A1) with Adrenodoxin: Evaluating Site-Directed Mutations by Molecular Modelling. Biochemistry 41:8310-8320

179. **Tuls J, Geren L, Lambeth JD and Millet F** 1987 The use of a specific fluorescence probe to study the interaction of adrenodoxin with adrenodoxin reductase and cytochrome P-450scc. J. Biol. Chem. 262:10020-10025

180. **Tuls J, Geren L, Lambeth JD and Millet F** 1989 Fluorescein isothiocyanate specifically modifies lysine 338 of cytochrome P-450scc and inhibits adrenodoxin binding. J. Biol. Chem. 264:16421-16425

181. **Adamovich TB, Pikuleva IA, Usanov ST and Chashchin VL** 1989 Study of the role of lysine residues of the cholesterol hydroxylating cytochrome P-450 by a method of chemical modification. Biochemistry (Moscow) 54:1206-1216

182. **Adamovich TB, Pikuleva IA, Chashchin VL and Usanov SA** 1989 Selective chemical modification of cytochrome P-450SCC lysine residues. Identification of lysines involved in the interaction with adrenodoxin. Biochim. Biophys. Acta 996:247-253

183. **Tsubaki M, Iwamoto Y, Hiwatashi A and Ichikawa Y** 1989 Inhibition of electron transfer from adrenodoxin to cytochrome P-450scc by chemical modification with pyridoxal 5'-phosphate: identification of adrenodoxin-binding site of cytochrome P-450scc. Biochemistry 28:6899-6907

184. **Wada A and Waterman MR** 1992 Identification by site-directed mutagenesis of two lysine residues in cholesterol side chain cleavage cytochrome P450 that are essential for adrenodoxin binding J. Biol. Chem. 267:2877-22882

185. **Geren LM, O'Brien P, Stonehouerner J and Millett F** 1984 Identification of specific carboxylate groups on adrenodoxin that are involved in the interaction with adrenodoxin reductase. J. Biol. Chem. 259:2155-2160

186. **Coghlam VM and Vickery LE** 1991 Site-specific Mutations in Human Ferredoxin That Affect Binding to Ferredoxin Reductase and Cytochrome P45Oscc. J. Biol. Chem. 266:18606-18612

187. **Coghlan VM and Vickery LE** 1992 Electrostatic interactions stabilizing ferredoxin electron transfer complexes. Disruption by "conservative" mutations. J. Biol. Chem. 267:8932-8935

188. **Zollner A, Hannemann F, Lisurek M and Bernhardt R** 2002 Deletions in the loop surrounding the iron-sulphur cluster of adrenodoxin severely affect the interactions with its native redox partners adrenodoxin reductase and cytochrome P450scc (CYP11A1) J. Inorg. Biochem. 91:644-654

189. **Lambeth JD, Seybert DW and Kamin H** 1979 Ionic effects on adrenal steroidogenic electron transport. The role of adrenodoxin as an electron shuttle. J. Biol. Chem. 254:7255-7264

190. **Schiffler B, Kiefer M, Wilken A, Hannemann F, Adolph HW and Bernhardt R** 2001 The Interaction of Bovine Adrenodoxin with CYP11A1 (Cytochrome P450scc) and CYP11B1 (Cytochrome P45011β). J. Biol. Chem. 276:36225–36232

191. **Tuckey RC, McKinley AJ and Headman MJ** 2001 Oxidised adrenodoxin acts as a competitive inhibitor of cytochrome P450scc in mitochondria from human placenta. Eur. J. Biochem. 268:2338-2343

192. **Cao P and Bernhardt R** 1999 Interaction of CYP11B1 (cytochrome P45011β) with CYP11A1 (cytochrome P450scc) in COS-1 cells. Eur. J. Biochem. 262:720-726

193. **Morohashi K, Fujii-Kuriyama Y, Okada Y, Sogawa K, Hirose T, Inayama S and Omura T** 1984 Molecular cloning and nucleotide sequence of cDNA for mRNA of mitochondrial cytochrome P450(SCC) of bovine adrenal cortex. Proc. Natl. Acad. Sci. USA. 81:4647-4651

194. **Woods ST, Sadleir J, Downs T, Triantopoulos T, Headlam M and Tuckey RC** 1998 Expression of catalytically active human cytochrome P450scc in Escherichia coli and mutagenesis of isoleucine-462. Arch. Biochem. Biophys. 353:109-115

195. **Matocha MF and Waterman MR** 1984 Discriminatory Processing of the Precursor Forms of Cytochrome P-450scc, and Adrenodoxin by Adrenocortical and Heart Mitochondria. J. Biol. Chem. 259:8672-8678

196. **Matocha MF and Waterman MR** 1985 Synthesis and Processing of Mitochondrial Steroid Hydroxylases in vivo maturation of the precursor forms of cytochrome P450scc, cytochrome P45011β and adrenodoxin. J. Biol. Chem. 260:12259-12265

197. **Zuber MX, Mason JI, Simpson ER and Waterman MR** 1988 Simultaneous transfection of COS-1 cells with mitochondrial and microsomal steroid hydroxylases: Incorporation of a steroidogenic pathway into nonsteroidogenic cells. Proc. Natl. Acad. Sci. USA 85:699-703

198. **Harikrishna JA, Black SM, Szklarz GD and Miller WL** 1993 Construction of Fusion Enzymes of the Human Cytochrome P450scc System. DNA Cell Biol. 12:371-379

199. **Black SM, Harikrishna JA, Szklarz GD and Miller WL** 1994 The mitochondrial environment is required for activity of the cholesterol side-chain cleavage enzyme, cytochrome P450scc. Proc. Natl. Acad. Sci. USA 91:7247-7251

200. **Lambeth JD, Kamin H and Seybert DW** 1980 Phosphatidylcholine vesicle reconstituted cytochrome P-450scc. Role of the membrane in control of activity and spin state of the cytochrome. J. Biol. Chem. 255:8282-8288

201. **Lambeth JD** 1981 Cytochrome P-450scc. Cardiolipin as an effector of activity of a mitochondrial cytochrome P-450. J. Biol. Chem. 256:4757-4762

202. **Schwarz D, Kisselev P, Wessel R, Pisch S, Bornscheuer U and Schmid RD** 1997 Possible involvement of nonbilayer lipids in the stimulation of the activity of cytochrome P450SCC (CYP11A1) and its propensity to induce vesicle aggregation. Chem. Phys. Lipids 85:91-99

203. **Chung BC, Matteson KJ, Voutilainen R, Mohandas TK and Miller WL** 1986 Human cholesterol side-chain cleavage enzyme, P450scc: cDNA cloning, assignment of the gene to chromosome 15, and expression in the placenta. Proc. Natl. Acad. Sci. USA. 83:8962-8966

204. **Morohashi K, Sogawa K, Omura T and Fujii-Kuriyama Y** 1987 Gene structure of human cytochrome P-450(SCC), cholesterol desmolase. J. Biochem. (Tokyo) 101:879–887

205. **Oonk RB, Krasnow JS, Beattie WG, Richards JS** 1989 Cyclic AMP dependent and -independent regulation of cholesterol side chain cleavage cytochrome P-450 (P-450scc) in rat ovarian granulosa cells and corpora lutea. cDNA and deduced amino acid sequence of ratP-450scc. J. Biol. Chem. 264:21934–21942

206. **Rice DA, Kirkman MS, Aitkene LD, Mouw AR, Schimmer BP and Parker KL** 1990 Analysis of the Promoter Region of the Gene Encoding Mouse Cholesterol Side-chain Cleavage Enzyme. J. Biol. Chem. 265:11713-11720

207. **Vilchis F, Chávez B, Larrea F, Timossi C and Montiel F** 2002 The cDNA cloning and tissue expression of the cytochrome P450scc from Syrian Hamster (Mesocricetus auratus). Gen. Comp. Endocrinol. 126:279-286

208. **Nomura O, Nakabayashi O, Nishimori K and Mizuno S** 1997 The cDNA cloning and transient expression of a chicken gene encoding cytochrome P450scc. Gene 185:217-222

209. **Mulheron GW, Stone RT, Miller WL and Wise T** 1989 Nucleotide sequence of cytochrome P450 cholesterol side-chain cleavage cDNA isolated from porcine testis. Nucleic Acids Res. 17:1773

210. **Okuyama E, Okazaki T, Furukawa A, Wu R and Ichikawa Y** 1996 Molecular cloning and nucleotide sequences of cDNA clones of sheep and goat adrenocortical cytochrome P450scc (CYP11A1). J. Steroid Biochem. Mol. Biol. 57:179-185.

211. **Hsu HJ, Hsiaoa P, Kuo MW and Chung BC** 2002 Expression of zebrafish cyp11a1 as a maternal transcript and in yolk syncytial layer. Gene Expr. Pat. 2:219–222

212. **Kemp CA, Marechala JD and Sutcliffe MJ** 2005 Progress in cytochrome P450 active site modeling. Arch. Biochem. Biophys. 433:361–368

213. **Lewis DFV and Lee-Robichaud P** 1998 Molecular modelling of steroidogenic cytochromes P450 from families CYP11, CYP17, CYP19 and CYP21 based on the CYP102 crystal structure. J. Steroid Biochem. Mol. Biol. 66:217-233

214. **Schwede T, Kopp J, Guex N and Peitsch MC** 2003 SWISS-MODEL: an automated protein homology-modeling server. Nucleic Acids Res. 31:3381–3385

215. **Ravichandran KG, Boddupalli SS, Hasemann CA, Peterson JA and Deisenhofer J** 1993 Crystal structure of hemoprotein domain of P450BM-3, a prototype for microsomal P450's. Science 261:731-736

216. **Hasemann CA, Ravichandran KG, Peterson JA and Deisenhofer J** 1994 Crystal structure and refinement of cytochrome P450terp at 2.3 Å resolution. J. Mol. Biol. 236:1169-1185

217. **Cupp-Vickery JR, Li H and Poulos TL** 1994 Preliminary crystallographic analysis of an enzyme involved in erythromycin biosynthesis: cytochrome P450eryF. Proteins 20:197–201

218. **Cosme J and Johnson EF** 2000 Engineering microsomal cytochrome P450 2C5 to be a soluble, monomeric enzyme: Mutations that alter aggregation, phospholipid dependence of catalysis, and membrane binding. J. Biol. Chem. 275:2545-2553

219. **Wester MR, Johnson EF, Marques-Soares C, Dansette PM, Mansuy D, and Stout CD** 2003 Structure of a substrate complex of mammalian cytochrome P450 2C5 at 2.3Å resolution: Evidence for multiple substrate binding modes. Biochemistry 42:6370-6379

220. **Wester MR, Johnson EF, Marques-Soares C, Dijols S, Dansette PM, Mansuy D and Stout CD** 2003 Structure of mammalian cytochrome P450 2C5 complexed with diclofenac at 2.1 Å resolution: Evidence for an induced fit model of substrate binding. Biochemistry 42:9335-9345

221. **Williams PA, Cosme, J, Ward A, Angove HC, Matak VD and Jhoti H** 2003 Crystal structure of human cytochrome P450 2C9 with bound warfarin. Nature 424:464–468

222. **Wester MR, Yano JK, Schoch GA, Yang C, Griffin KJ, Stout CD and Johnson EF** 2004 The structure of human cytochrome P450 2C9 complexed with flurbiprofen at 2.0-Å Resolution. J. Biol. Chem. 279:35630–35637

223. **Schoch GA, Yano JK, Wester MR, Griffin KJ, Stout CD and Johnson EF** 2004 Structure of Human Microsomal Cytochrome P450 2C8: Evidence for a peripheral fatty acid binding site. J. Biol. Chem. 279:9497–9503

224. **Scott EE, He YA, Wester MR, White MA, Chin CC, Halpert JR, Johnson EF and Stout CD** 2003 An open conformation of mammalian cytochrome P450 2B4 at 1.6 A° resolution. Proc. Natl. Acad. Sci. USA 100:13196–13201

225. **Scott EE, White MA, He YA, Johnson EF, Scout CD and Halbert JR** 2004 Structure of Mammalian Cytochrome P450 2B4 Complexed with 4-(4-Chlorophenyl)imidazole at 1.9-Å Resolution: Insight into the range of P450 conformations and the coordination of redox partner binding. J. Biol. Chem. 279:27294-27301

226. **Williams PA, Cosme J, Vinkovic´ DM, Ward A, Angove HC, Day PJ, Vonrhein C, Tickle IJ and Jhoti H** 2004 Crystal structures of human cytochromeP450 3A4 bound to metyrapone and progesterone. Science 305:683–686

227. **Yano JK, Wester MR, Schoch GA, Griffin KJ, Stout CD and Johnson EF** 2004 The structure of human microsomal cytochrome P450 3A4 determined by X-ray crystallography to 2.05 Å resolution. J. Biol. Chem. 279:38091–38094

228. **Berman HM, Westbrook J, Feng Z, Gilliland G, Bhat TN, Weissig H, Shindyalov IN and Bourne PE** 2000 The Protein Data Bank. Nucleic Acids Res. 28:235–242

229. **Altschul SF, Madden TL, Schaffer AA, Zhang J, Zhang Z, Miller W and Lipman DJ** 1997 Gapped BLAST and PSI-BLAST: a new generation of protein database search programs. Nucleic Acids Res. 25:3389–3402

230. **Kirton SB, Kemp CA, Tomkinson NP, St.-Gallay S and Sutcliffe MJ** 2002 Impact of incorporating the 2C5 crystal structure into comparative models of cytochrome P450 2D6. Proteins 49:216-231

231. **John B and Sali A** 2003 Comparative protein structure modeling by iterative alignment, model building and model assessment. Nucleic Acids Res. 31:3982-3992

232. **Pieper U, Eswar N, Stuart AC, Ilyin VA and Sali A** 2002 MODBASE, a database of annotated comparative protein structure models. Nucleic Acids Res. 30:255-259

233. **Rost B** 1998 Marrying structure and genomics. Structure 6:259-263

234. **Sanchez R and Sali A** 1998 Large-scale protein structure modeling of the Saccharomyces cerevisiae genome. Proc. Natl. Acad. Sci. USA 95:13597-13602

235. **Venclovas C, Zemla A, Fidelis K and Moult J** 2001 Comparison of performance in successive CASP experiments. Proteins 5:163-170

236. **Guex N and Peitsch MC** 1997 SWISS-MODEL and the Swiss-PdbViewer: an environment for comparative protein modeling. Electrophoresis 18:2714–2723

237. **Sutcliffe MJ, Haneef I, Carney D and Blundell TL** 1987 Knowledge based modelling of homologous proteins, Part I: Three- dimensional frameworks derived from the simultaneous superposition of multiple structures. Protein Eng. 1:377–384

238. **Sutcliffe MJ, Hayes FR and Blundell TL** 1987 Knowledge based modelling of homologous proteins, Part II: Rules for the conformations of substituted side chains. Protein Eng. 1:385–392

239. **Sali A and Blundell TL** 1993 Comparative protein modelling by satisfaction of spatial restraints. J. Mol. Biol. 234:779–815

240. **Szklar GD** 2005 Homology modelling of protein structures. 14th International Conference on Cytochromes P450: Biochemistry, Biophysics and Bioinformatics. Dallas, Texas, USA, May 31-June 5, 2005

241. **Leach AR** 2001 In: Molecular modelling: Principles and applications 2nd ed. Pearson Education Limited, Edinburgh Gate, Harlow, Essex, CM20 2JE.:165-302

242. **Eswar N, John B, Mirkovic N, Fiser A, Ilyin VA, Pieper U, Stuart AC, Marti-Renom MA, Madhusudhan MS, Yerkovich B and Sali A** 2003 Tools for comparative protein structure modeling and analysis. Nucleic Acids Res. 31:3375–3380

243. **Pontius J, Richelle J and Wodak SJ** 1996 Deviations from standard atomic volumes as a quality measure for protein crystal structures. J. Mol. Biol. 264:121–136

244. **Rodriguez R, Chinea G, Lopez N, Pons T and Vriend G** 1998 Homology modeling, model and software evaluation: three related resources. Bioinformatics 14:523–528

245. **Luthy R, Bowie JU and Eisenberg D** 1992 Assessment of protein models with three-dimensional profiles. Nature 356:83–85

246. **Laskowski RA, Moss DS and Thornton JM** 1993 Main-chain bond lengths and bond angles in protein structures. J. Mol. Biol. 231:1049–1067

247. **Rupasinghe S, Baudry J and Schuler MA** 2003 Common active site architecture and binding strategy of four phenylpropanoid P450s from Arabidopsis thaliana as revealed by molecular modeling. Protein Eng. 16:721-731

248. **Hasemann CA, Kurmbail RG, Boddupalli SS, Peterson JA and Deisenhofer J** 1995 Structure and function of cytochromes P450: a comparative analysis of three crystal structures. Structure 3:41-62

249. **Graham-Lorence S, Amarneh B, White RE, Peterson JA and Simpson ER** 1995 A three-dimensional model of aromatase cytochrome P450. Protein Sci. 4:1065-1080

250. **Raag R and Poulos TL** 1989 Crystal structure of the carbon monoxide-substrate-cytochrome P450cam ternary complex. Biochemistry 28:7586-7592

251. **Raag R, Martinis SA, Sligar SG and Poulos TL** 1991 Crystal structure of the cytochrome P450cam active site mutant Thr252Ala. Biochemistry 30:11420-11429

252. **Wade RC, Winn PJ, Schlichting I and Sudarko** 2004 A survey of active site access channels in cytochromes P450. J. Inorganic Biochemistry 98:1175-1182

253. **Li HY and Poulos TL** 1997 The structure of the cytochrome p450BM-3 haem domain complexed with the fatty acid substrate, palmitoleic acid. Nat. Struct. Biol. 4:140-146

254. **Haines DC, Tomchick DR, Machius M and Peterson JA** 2001 Pivotal role of water in the mechanism of P450BM-3. Biochemistry 40:13456-13465

255. **Dunn AR, Dmochowski IJ, Bilwes AM, Gray HB and Crane BR** 2001 Probing the open state of cytochrome P450cam with ruthenium-linker substrates. Proc. Natl. Acad. Sci. USA 98:12420–12425

256. **Zerbe K, Pylypenko O, Vitali F, Zhang W, Rouset S, Heck M, Vrijbloed JW, Bischoff D, Bister B, Sussmuth RD, Pelzer S, Wohlleben W, Robinson JA and Schlichting I** 2002 Crystal Structure of OxyB, a Cytochrome P450 Implicated in an Oxidative Phenol Coupling Reaction during Vancomycin Biosynthesis. J. Biol. Chem. 277:47476-47485

257. **Podust L.M, Kim Y, Arase M, Neely BA, Beck BJ, Bach H, Sherman DH, Lamb DC, Kelly SL and Waterman MR** 2003 The 1.92-Å Structure of Streptomyces coelicolor A3(2) CYP154C1. A new monooxygenase that functionolizes macrolide ring systems. J. Biol. Chem. 278:12214-12221

258. **Negishi M, Uno T, Darden TA, Sueyoshi T and Pedersen LG** 1996 Structural flexibility and functional versatility of mammalian P450 enzymes. FASEB J. 10:683-689

259. **Negishi M, Iwasaki M, Juvonen RO, Sueyoshi T, Darden TA and Pedersen LG** 1996 Structural flexibility and functional versatility of cytochrome P450 and rapid evolution. Mut. Res. 350:43-50

260. **Vijayakumar S and Salerno JC** 1992 Molecular modeling of the 3-D structure of Cytochrome P-450scc. Biochim. Biophys. Acta. 1160:281–286

261. **Tsujita M and lchikawa Y** 1993 Substrate-binding region of cytochrome P-450scc (P-450X1A1). Identifcation and primary structure of the cholesterol binding region in cytochrome P-450scc. Biochim. Biophys. Acta 1161:124-130

262. **Headlam MJ, Wilce and MC Tuckey RC** 2003. The F–G loop region of Cytochrome P450scc (CYP11A1) interacts with the phospholipid membrane. Biochim. Biophys. Acta. 1617:96–108

263. **Shank-Retzlaff ML, Raner GM, Coon MJ and Sligar SG** 1998 Membrane topology of cytochrome P450 2B4 in Langmuir-Blodgett monolayers, Arch. Biochem. Biophys. 359:82– 88

264. **Blum H, Leigh JS, Salerno JC and Ohnishi T** 1978 The orientation of bovine adrenal cortex cytochrome P-450 in submitochondrial particle multilayers, Arch. Biochem. Biophys. 187:153– 157

265. **Kamin H, Batie C, Lambeth JD, Lancaster J, Graham Land Salerno JC** 1985 Paramagnetic probes of multicomponent electron-transfer systems, Biochem. Soc. Trans. 13:615– 618

266. **Sivozhelezova V and Nicolinia C** 2005 Homology modeling of cytochrome P450scc and the mutations for optimal amperometric sensor. J. Theor. Biol. 234:479–485

267. **Tuckey RC and Cameron KJ** 1993 Side-chain specificities of human and bovine cytochromes P450scc. Eur. J. Biochem. 217:209-215

268. **Heyl BL, Tyrrell DJ and Lambeth JD** 1986 Cytochrome P-450scc-substrate interactions. Role of the 3β- and side chain hydroxyls in binding to oxidized and reduced forms of the enzyme. J. Biol. Chem. 261:2743-2749

269. **Tuckey RC, Lawrence J and Cameron KJ** 1996 Side-chain cleavage of cholesterol esters by human P450scc. J. Steroid Biochem. Mol. Biol. 58:605-610

270. **Pikuleva IA, Mackman RL, Kagawa N, Waterman MR and Ortiz de Montellano PR** 1995 Active-site topology of bovine cholesterol side-chain cleavage cytochrome P450 (P450scc) and evidence for the interaction of tyrosine 94 with the side chain of cholesterol. Arch. Biochem. Biophys. 322:189–197

271. **Hurt EC and van Loon APGM** 1986 How proteins find mitochondria and intramitochondrial compartments. Trends Biochem. Sci. 11:204–207

272. **von Heijne G** 1986 Mitochondrial targeting sequences may form amphiphilic helices. EMBO J. 5:1335–1342

273. **Reidhaar-Olson JF and Sauer RT** 1988 Combinatorial cassette mutagenesis as a probe of the informational content of protein sequences. Science. 241:53-57

274. **Bowie JU, Reidhaar-Olson JF, Lim WA and Sauer RT** 1990 Deciphering the message in protein sequences: tolerance to amino acid substitutions. Science. 247:1306-1310

275. **Rennell D, Bouvier SE, Hardy LW and Poteete AR** 1991 Systematic mutation of bacteriophage-T4 lysozyme. J. Mol. Biol. 222:67-87

276. **Terwilliger TC, Zabin HB, Horvath MP, Sandberg WS and Schlunk PM** 1994. In vivo characterization of mutants of the bacteriophage f1 gene V protein isolated by saturation mutagenesis. J. Mol. Biol. 236:556-571

277. **Suckow J, Markiewicz P, Kleina LG, Miller J, Kisters-Woike B and Muller-Hill B** 1996 Genetic studies of the Lac repressor XV: 4000 single amino acid substitutions and analysis of the resulting phenotypes on the basis of the protein structure. J. Mol. Biol. 261:509-523

278. **Huang W, Petrosino J, Hirsch M, Shenkin PS and Palzkill T** 1996 Amino acid sequence determinants of b-lactamase structure and activity. J. Mol. Biol. 258:688-703

279. **Axe DD, Foster NW and Fersht AR** 1998 A search for single substitutions that eliminate enzymatic function in a bacterial ribonuclease. Biochemistry 37:7157-7166

280. **Imai M, Shimada H, Watanabe Y, Matsushima-Hibiya Y, Makino R, Koga H, Horiuchi T and Ishimura Y** 1989 Uncoupling of the cytochrome P450cam monooxygenase reaction by a single mutation, threonine 252 to alanine or valine: A possible role of the hydroxy amino acid in oxygen activation. Proc. Natl. Acad. Sci. USA 86:7823-7827

281. **Martinis SA, Atkins WM, Stayton PS and Sligar SG** 1989 A conserved residue of cytochrome P450 is involved in heme-oxygen stability and activation. J. Am. Chem. Soc. 111:9252-9253

282. **Nagano S and Poulos TL** 2005 Crystallographic study on the dioxygen complex of wild-type and mutant cytochrome P450cam: Implications for the dioxygen activation mechanism. J. of Biol. Chem. 280:31659 – 31663

283. **Honma W, Li W, Liu H, Scott EE and Halbert JR** 2005 Functional role of residues in the helix B´ region of cytochrome P450 2B1. Arch. Biochem. Biophys. 435:157-165

284. **Johnson EF** 2003 Deciphering substrate recognition by drug-metabolizing cytochromes P450. Drug Metab. Dispos. 31:1532–1540

285. **Aoyama T, Korzekwa K, Nagata K, Adesnik M, Reiss A, Lapenson DP, Gillette J, Gelboin HV, Waxman DJ and Gonzalez FJ** 1989 Sequence requirements for cytochrome P4502B1 catalytic activity: Alterations of the stereospecificity and regionselectivity of steroid hydroxylation by a simultaneous change of two hydrophobic amino acid residues to phenylalanine. J. Biol. Chem. 264:21327-21333

286. **Halbert JR and He Y** 1993 Engineering of cytochrome P450 2B1 specificity. Conversion of an androgen 16 beta-hydroxylase to a 15 alpha-hydroxylase. J. Biol. Chem. 268:4453-4457

287. **Kronbach T and Johnson EF** 1991 An inhibitory monoclonal antibody binds in close proximity to a determinant for substrate binding in cytochrome P4502C5. J. Biol. Chem. 266:6215-6220

288. **Kronbach T, Keper B and Johnson EF** 1991 A hypervariable region of P4502C5 confers progesterone 21-hydroxylase activity to P4502C1. Biochemistry. 30:6097-6102

289. **Lindberg RPL and Negishi M** 1989 Alterations of mouse cytochrome P450coh substrate specificity by mutation of a single amino acid residue. Nature. 339:632-634

290. **Negishi M, Lindberg R, Lang M, Wong G, Itakura T and Yoshioka H** 1990 in: Drug Metabolizing Enzymes: Genetics, regulation and toxicology. Proceedings of the VIIIth International Symposium on Microsomes and Drug Oxidations (Ingelman-Sundberg, M., Gustafsson, J.-A., & Orrenius, S., Eds.) p 15, Karolinska Institutet, Stockholm, Sweden

APPENDIX A

Primer sequences used in baboon CYP11A1 amplification, sequencing and site-directed mutagenesis reactions. A *Xho*1 restriction site (underlined) was incorporated into the RT-PCR sense primer. The codons for the changed amino acid residues in the site-directed mutagenesis primers are represented in bold characters.

Primer name	Primer sequence	Target area
RT-PCR primers		
LP	5'-CTCGAGCTGTGGGGACAGC-3'	Upstream of CYP11A1 start site (-20)
RP	5'-AGTGACGACCCAACGAAG-3'	Downstream of CYP11A1 stop site (1569)
sequence primers		
LP	5'-CTCGAGCTGTGGGGACAGC-3'	First sense primer: 5' terminal (-20)
KS2 (530)	5'-ACTTCGTCAGTGTCCTGCAC-3'	Second sense primer: middle segment
KS4	5'-TACCTACTTCCGGAACTTGG-3'	Third sense primer: 3' terminal (1341)
KS1	5'-TTCTGGACATGGTGAAGGTG-3'	First anti-sense primer: 5' terminal (228)
KS3 (1017)	5'-CGTGCCATCTCATACAAGTG-3'	Second anti-sense primer: middle segment
RP	5'-AGTGACGACCCAACGAAG-3'	Third anti-sense primer: 3' terminal (1569)
Site-directed mutagenesis primers		
K98I LP	5'-CCAATATTACCAGAGACCC**ATA**GGAGTCCTG-3'	
K98I RP	5'-TGGGTCTCTGGTAATATTGGTGATAGGCG-3'	
I98Q LP	5'-CCAATATTACCAGAGACCC**CAA**GGAGTCCTG-3'	
I98Q RP	5'-TGGGTCTCTGGTAATATTGGTGATAGGCG –3'	
K103A LP	5'-ACCCATAGGAGTCCTGTT**GGC**GAAGTCAGC-3'	
K103A RP	5'-AACAGGACTCCTATGGGTCTCTGGTAATATTG-3'	
T291A LP	5'-GGCAGGAGGGGTGGAC**GCG**ACGTCCAT-3'	
T291A RP	5'-GTCCACCCCTCCTGCCAGCATCTCTGTG-3'	

LP – Left Primer

RP – Right Primer

All primers used were dissolved in water

APPENDIX B

Nucleotide and deduced amino acid sequences of baboon and human CYP11A1 cDNA and the constructs CYP11A1a, CYP11A1b and CYP11A1c. The nucleotide bases and amino acid residues which differ from the baboon CYP11A1 cDNA are indicated in coloured bold letters for human CYP11A1 (**purple**), CYP11A1a (**blue**), CYP11A1b (**red**) and CYP11A1c (**green**). The putative 39 amino acid residue presequence is indicated in bold **orange** letters.

```
Const.
Human                                                    C
cDNA    1    ATG CTG GCC AAG GGT CTT CCC CCA CGC TCA GTC TTG GTC AAA GGC   45
cDNA    1    Met Leu Ala Lys Gly Leu Pro Pro Arg Ser Val Leu Val Lys Gly   15
Human
Constr.

Const.
Human         A                                 G      G           G
cDNA   46    TGC CAG ACC TTT CTG AGT GCC CCC AAG GAG AGG CTG GGG CAT CTC   90
cDNA   16    Cys Gln Thr Phe Leu Ser Ala Pro Lys Glu Arg Leu Gly His Leu   30
Human        Tyr                             Arg     Gly         Arg
Const.

Const.
Human                     T G C     G                    C
cDNA   91    AGG GTG CCC ACC AGT GAG AGA GCT GGC ATC TCC ACT CGC AGT CCT   135
cDNA   31    Arg Val Pro Thr Ser Glu Arg Ala Gly Ile Ser Thr Arg Ser Pro   45
Human                     Gly     Gly
Const.

Const.
Human
cDNA  136    CGC CCC TTC AAT GAG ATC CCC TCT CCT GGT GAC AAT GGC TGG CTA   180
cDNA   46    Arg Pro Phe Asn Glu Ile Pro Ser Pro Gly Asp Asn Gly Trp Leu   60
Human
Const.

Const.
Human                                       G
cDNA  181    AAC CTG TAC CAT TTC TGG AGG GAG ACA GGC ACA CAC AAA GTC CAC   225
cDNA   61    Asn Leu Tyr His Phe Trp Arg Glu Thr Gly Thr His Lys Val His   75
Human
Const.

Const.
Human
cDNA  226    CTT CAC CAT GTC CAG AAT TTC CAG AAG TAT GGC CCG ATT TAC AGG   270
cDNA   76    Leu His His Val Gln Asn Phe Gln Lys Tyr Gly Pro Ile Tyr Arg   90
Human
Const.

Const.                                          C   T
Human
cDNA  271    GAG AAG CTC GGC AAC GTG GAG TCG GTT TAT GTC ATC GAC CCT GAA   315
cDNA   91    Glu Lys Leu Gly Asn Val Glu Ser Val Tyr Val Ile Asp Pro Glu   105
Human
Const
```

```
Const.
Human
cDNA  316   GAT GTG GCC CTT CTC TTT AAG TCC GAG GGC CCC AAC CCA GAA CGA   360
cDNA  106   Asp Val Ala Leu Leu Phe Lys Ser Glu Gly Pro Asn Pro Glu Arg   120
Human
Const.

Const.
Human                                                 G
cDNA  361   TTC CTC ATC CCG CCC TGG GTC GCC TAT CAC CAA TAT TAC CAG AGA   405
cDNA  121   Phe Leu Ile Pro Pro Trp Val Ala Tyr His Gln Tyr Tyr Gln Arg   135
Human
Const.

Const.          A
Human                                     G
cDNA  406   CCC ATA GGA GTC CTG TTG AAG AAG TCA GCA GCC TGG AAG AAA GAC   450
cDNA  136   Pro Ile Gly Val Leu Leu Lys Lys Ser Ala Ala Trp Lys Lys Asp   150
Human
Const.         Lys

Const.
Human                                                       G
cDNA  451   CGG GTG GCC CTG AAC CAG GAG GTG ATG GCT CCA GAG ACC ACC AAG   495
cDNA  151   Arg Val Ala Leu Asn Gln Glu Val Met Ala Pro Glu Thr Thr Lys   165
Human                                                     Ala
Const.

Const.                                                             A
Human
cDNA  496   AAC TTT TTG CCC CTG TTG GAT GCA GTG TCT CGG GAC TTC GTC AGT   540
cDNA  166   Asn Phe Leu Pro Leu Leu Asp Ala Val Ser Arg Asp Phe Val Ser   180
Human
Const.                                                            Asn

Const.
Human                                     G   G                 A    G
cDNA  541   GTC CTG CAC AGG CGC ATC AAG AAA GCA GGC TCC GGA AAT TTC TCA   585
cDNA  181   Val Leu His Arg Arg Ile Lys Lys Ala Gly Ser Gly Asn Phe Ser   195
Human                                                       Tyr
Const.

Const.      T
Human
cDNA  586   GGG GAC ATC AGT GAT GAC CTG TTC CGC TTT GCC TTT GAG TCC ATC   630
cDNA  196   Gly Asp Ile Ser Asp Asp Leu Phe Arg Phe Ala Phe Glu Ser Ile   210
Human
Const.      Trp

Const.
Human
cDNA  631   ACT AAC GTC ATT TTT GGG GAG CGC CAG GGG ATG CTG GAG GAA GTA   675
cDNA  211   Thr Asn Val Ile Phe Gly Glu Arg Gln Gly Met Leu Glu Glu Val   225
Human
Const.
```

```
Const.                                                          C
Human                                  A                C
cDNA  676   GTG AAC CCC GAG GCC CAG CGG TTC ATT GAT GCT ATC TAC CAG ATG   720
cDNA  226   Val Asn Pro Glu Ala Gln Arg Phe Ile Asp Ala Ile Tyr Gln Met   240
Human
Const.                                                          His

Const.
Human                                                                G
cDNA  721   TTC CAC ACC AGC GTC CCC ATG CTC AAC CTT CCC CCA GAC CTA TTC   765
cDNA  241   Phe His Thr Ser Val Pro Met Leu Asn Leu Pro Pro Asp Leu Phe   255
Human
Const.

Const.
Human                                                              T
cDNA  766   CGT CTG TTC AGG ACC AAG ACC TGG AAG GAC CAT GTG GCC GCA TGG   810
cDNA  256   Arg Leu Phe Arg Thr Lys Thr Trp Lys Asp His Val Ala Ala Trp   270
Human
Const.

Const.                                 A     G
Human         C                T             A         C
cDNA  811   GAT GTG ATT TTC AGC AAA GCT GAC ATG TAC ACC GAG AAC TTC TAC   855
cDNA  271   Asp Val Ile Phe Ser Lys Ala Asp Met Tyr Thr Glu Asn Phe Tyr   285
Human                                  Ile         Gln
Const.                                 Val

Const.
Human                                  G                C
cDNA  856   TGG GAA TTG AGA CAG AAA GGA AAT GTT CAC CAT GAT TAC CGT GGC   900
cDNA  286   Trp Glu Leu Arg Gln Lys Gly Asn Val His His Asp Tyr Arg Gly   300
Human                                  Ser
Const.

Const.
Human         G
cDNA  901   ATC CTC TAC AGA CTC CTG GGA GAC AGC AAG ATG TCC TTC GAG GAC   945
cDNA  301   Ile Leu Tyr Arg Leu Leu Gly Asp Ser Lys Met Ser Phe Glu Asp   315
Human       Met
Const.

Const.                                                             T
Human
cDNA  946   ATC AAG GCC AAC GTC ACA GAG ATG CTG GCA GGA GGG GTG GAC ACG   990
cDNA  316   Ile Lys Ala Asn Val Thr Glu Met Leu Ala Gly Gly Val Asp Thr   330
Human
Const.                                                             Ser

Const.
Human
cDNA  991   ACG TCC ATG ACC CTG CAG TGG CAC TTG TAT GAG ATG GCA CGC AAC
1035
cDNA  331   Thr Ser Met Thr Leu Gln Trp His Leu Tyr Glu Met Ala Arg Asn   345
Human
Const.
```

```
Const.
Human
cDNA  1036  CTG AAG GTG CAG GAT ATG CTG CGG GCA GAG GTC TTG GCT GCG CGG
1080
cDNA  346   Leu Lys Val Gln Asp Met Leu Arg Ala Glu Val Leu Ala Ala Arg   360
Human
Const.

Const.                                        G
Human        A                                G       A
cDNA  1081  CGC CAG GCC CAG GGA GAC ATG GCC ACA ATG CTG CAG CTG GTC CCC
1125
cDNA  361   Arg Gln Ala Gln Gly Asp Met Ala Thr Met Leu Gln Leu Val Pro   375
Human       His
Const.

Const.
Human                                            A
cDNA  1126  CTC CTC AAA GCC AGC ATC AAG GAG ACA CTG AGA CTT CAC CCC ATC
1170
cDNA  376   Leu Leu Lys Ala Ser Ile Lys Glu Thr Leu Arg Leu His Pro Ile   390
Human
Const.

Const.
Human                                     T
cDNA  1171  TCC GTG ACC CTG CAG AGA TAT CTC GTA AAT GAC TTG GTT CTT CGA
1215
cDNA  391   Ser Val Thr Leu Gln Arg Tyr Leu Val Asn Asp Leu Val Leu Arg   405
Human
Const.

Const.
Human        A                                           A
cDNA  1216  GGT TAC ATG ATT CCT GCC AAG ACA CTG GTG CAG GTG GCC ATC TAT
1260
cDNA  406   Gly Tyr Met Ile Pro Ala Lys Thr Leu Val Gln Val Ala Ile Tyr   420
Human       Asp
Const.

Const.              C
Human               C              C
cDNA  1261  GCT CTG GGT CGA GAG CCC ACT TTC TTC TTC GAC CCG GAA AAT TTT
1305
cDNA  421   Ala Leu Gly Arg Glu Pro Thr Phe Phe Phe Asp Pro Glu Asn Phe   435
Human
Const.

Const.
Human                                                 C
cDNA  1306  GAC CCA ACC CGA TGG CTG AGC AAA GAC AAG AAC ATT ACC TAC TTC
1350
cDNA  436   Asp Pro Thr Arg Trp Leu Ser Lys Asp Lys Asn Ile Thr Tyr Phe   450
Human
Const.
```

```
Const.
Human
cDNA  1351  CGG AAC TTG GGC TTT GGC TGG GGT GTG CGG CAG TGT CTG GGA CGG
1395
cDNA  451   Arg Asn Leu Gly Phe Gly Trp Gly Val Arg Gln Cys Leu Gly Arg   465
Human
Const.

Const.                    T
Human                  T
cDNA  1396  CGG ATC GCC GAG CTA GAG ATG ACC ATC TTC CTC ATC AAT ATG CTG
1440
cDNA  466   Arg Ile Ala Glu Leu Glu Met Thr Ile Phe Leu Ile Asn Met Leu   480
Human
Const.

Const.           G
Human                                      C
cDNA  1441  GAG AAC TTC AGA GTT GAA ATC CAA CAT CTC AGC GAT GTG GGC ACC
1485
cDNA  481   Glu Asn Phe Arg Val Glu Ile Gln His Leu Ser Asp Val Gly Thr   495
Human
Const.          Ser

Const.                                          A
Human                          T
cDNA  1486  ACA TTC AAC CTC ATC CTG ATG CCT GAA AAG CCC ATC TCC TTC ACC
1530
cDNA  496   Thr Phe Asn Leu Ile Leu Met Pro Glu Lys Pro Ile Ser Phe Thr   510
Human
Const.

Const.
Human
cDNA  1531  TTC TGG CCC TTT AAC CAG GAA GCA ACC CAG CAG TGA   1566
cDNA  511   Phe Trp Pro Phe Asn Gln Glu Ala Thr Gln Gln End
Human
Const.
```